ABSTRACT

Title of Document:              IMPROVING RESILIENCE OF RAIL-BASED
                                INTERMODAL FREIGHT
                                TRANSPORTATION SYSTEMS

                                Xiaodong Zhang, Doctor of Philosophy, 2013

Directed By:                    Professor Elise Miller-Hooks, Department of
                                Civil & Environmental Engineering


With the increasing natural and human-made disasters, the risk of an event with potential

to cause major disruption to our transportation systems and their components also

increases.  It is of paramount importance that transportation systems could be effectively

recovered, thus economic loss due to the disasters can be minimized.  This dissertation

addresses the optimization problems for transportation system performance measurement,

decision-making on pre-disaster preparedness and post-event recovery actions planning

and scheduling to achieve the maximum network resilience level.

In assessing a network's potential performance given possible future disruptions,

one must recognize the contributions of the network's inherent ability to cope with

disruption via its topological and operational attributes and potential actions that can be

taken in the immediate aftermath of such an event.  A two-stage stochastic program is

formulated to solve the problem of measuring a network's maximum resilience level and

simultaneously determining the optimal set of preparedness and recovery actions

necessary to achieve this level under budget and level-of-service constraints.  An exact

methodology, employing the integer L-shaped method and Monte Carlo simulation, is proposed for its solution.

In this dissertation, a nonlinear, stochastic, time-dependent integer program is proposed, from operational perspective, to schedule short-term recovery activities to maximize transportation network resilience. Two solution methods are proposed, both employing a decomposition approach to eliminate nonlinearities of the formulation. The first is an exact decomposition with branch-and-cut methodology, and the second is a hybrid genetic algorithm that evaluates each chromosome's fitness based on optimal objective values to the time-dependent maximum flow subproblem. Algorithm performance is also assessed on a test network.

Finally, this dissertation studies the role of network topology in resilience. 17 specific network topologies were selected for network resilience analysis. Simple graph structures with 9~10 nodes and larger network with 100 nodes are assessed. Resilience is measured in terms of throughput and connectivity and average reciprocal distance. The integer L-shaped method is applied again to study the performance of the network structure with respect to all three resilience measures. The relationships between resilience and average degree, diameter, and cyclicity are also investigated.

Improving Resilience of Rail-Based Intermodal Freight Transportation Systems

By

Xiaodong Zhang

Dissertation submitted to the Faculty of the Graduate School of the
University of Maryland, College Park, in partial fulfillment
of the requirements for the degree of
Doctor of Philosophy
2013

Advisory Committee:
Professor  Elise Miller-Hooks, Chair/Advisor
Professor  Paul Schonfeld
Professor  Lei Zhang
Professor  Chengri Ding
Professor  Qingbin Cui

# Acknowledgements

I would like to express my deepest gratitude to my advisor, Dr. Elise Miller-Hooks, for her tremendous inspiration, guidance, encouragement and patience during my study at the University of Maryland. Her passionate attitude to the scientific research and life has strong influenced on my future career path. Whenever I face the challenges and hesitate to move forward, she is always there to direct me toward the right road. Without her persistent guidance and knowledgeable insight, this dissertation cannot be complete.

My special thanks go to my committee members, Dr. Paul Schonfeld, Dr. Lei Zhang, Dr. Chengri Ding and Dr. Qingbin Cui, for their participation and help. Their insightful comments and constructive criticisms have been valuable inputs to my research and dissertation, and make this dissertation more solid and sound.

I acknowledge National Science Foundation to support this research. Thanks to all the fellow students working in the resilience project: Lichun Chen, Reza Faturechi, Kevin Denny, and Mariana Salinas. I also thank Zichuan Li, Yue Liu, Lichun Chen, Chih-Sheng Chou for their help and friendship during my study in Maryland.

I would like to thank my parents for their unconditional encouragement and support in my life. Finally, I owe my deepest thanks to my wife, Yuqiong Bai. Her immeasurable support, patience, encouragement and love are undeniably the cornerstones that allow me to succeed in this long journey. I dedicate this dissertation to them.

# Table of Contents

# List of Figures

# List of Tables

# Chapter 1: Introduction

## 1.1 *Motivation and Objectives*

Disasters, of any kind, can create a wide range of challenges. Examples of recent disasters include: the 9/11 terrorist attacks, the Nisqually Earthquake of 2001, Hurricanes Katrina and Rita in 2005, Minneapolis' bridge collapse of August 2007, 2010 Haiti earthquake, and 2011 Tohoku earthquake and subsequent tsunami. These disasters, both natural and human-made, have resulted in massive fatalities, property and/or environmental damage, significant economic losses, and displacement of population. The estimated economic loss in Louisiana and Mississippi due to Hurricane Katrina is nearly $150 billion, for example. Further, Hurricane Katrina forced the relocation of over one million people from the central Gulf Coast.

Under a natural (e.g. earthquake, flood) or human-made disaster (e.g. terrorist attack) it is of paramount importance that transportation systems remain operational or their functionality be repaired quickly to provide effective transport services in the disaster's aftermath (Nicholson and Du, 1997). Using empirical data from the 1995 Kobe earthquake, Chang (2000) showed the significance of a functioning transportation system in disaster recovery and the long-term economic impact of continued substandard operations. Past data has shown that damage to road network components (e.g., bridges, tunnels, highway, etc.) can severely disrupt traffic flow and negatively impact the economic activity of a region as well as post-disaster emergency response and recovery activities (Franchin and al., 2006a; Franchin and al., 2006b; Lupoi and al., 2006; Schotanus and al., 2004). For example, Hurricane Katrina damaged over 45 bridges and

1

most highways in Alabama, Louisiana, and Mississippi. These losses to the transportation infrastructure significantly obstructed emergency response activities, caused loss of lives, and hampered the movement of needed suppliers to the region.

This dissertation provides tools to support the creation of resilient intermodal freight transportation systems. Performance measures, such as system resiliency, can provide indication of the system's ability to withstand or cope with a disaster, and thus, can offer insights for disaster management. Resilience in the context of transportation networks is quantified herein as the ability of a transportation network to withstand and quickly recover from disruption. This measure considers the network's inherent ability to cope with negative consequences of disruptions as a result of the network's topological and operational attributes. To achieve the maximum network resilience level, pre-disaster preparedness and post-disaster recovery actions and investments are planned and scheduled given the possibility of a host of disaster scenarios that might arise. That is, a multi-hazard approach is taken.

This dissertation work has arisen from increasing concerns, both nationally and internationally, for securing existing transportation systems. Details of the specific problems to be addressed are described next, followed by general contributions derived from this dissertation.

## 1.2 *Specific Problems Addressed*

An overview of the three main problems addressed within this dissertation is given in this section. These problems are discussed in terms of conceptual framework, problem modeling and analytical methodologies developed for their solution.

1.2.1 Resilience with preparedness options (RPO),

Preparedness and recovery are key components to support efficient disaster management and mitigate the impacts to our society due to disaster. From the perspective of planning, preparedness should be considered for the provision of equipment and personnel ahead of time to facilitate and enhance potential recovery actions. The recovery phase emphasizes the evacuation of traffic demand, mobilization of the preparedness resources and restoration of transportation system capacity that was lost during the disaster.

Although interest by researchers and practitioners has grown in past decades, the extent to which transportation network resilience analysis is systematically investigated is still insufficient. Most studies on this topic focus on either disaster management following events or develop methods to support pre-disaster preparedness. For example, models have been proposed to identify essential activities in transportation system planning under emergencies by analysis and modeling of capacity in transportation networks (Chen et al., 1999; Chen et al., 2002; Wong, 1996; Yang and Bell, 1998; Yang et al., 2000). These models aimed to determine the maximum level of demand that can be served by a transportation network and provided useful information for managing mobility demand and identifying efficient strategies for controlling traffic demand under emergencies. Barbarosoglu and Arda (2004) further investigated post-disaster transportation network management to consider uncertainties in available supplies, demand and network arc capacities through consideration of a set of potential disaster scenarios. Chen and Miller-Hooks (2012) provide a means for quantifying the resilience measure conceptualized in (Rose, 2004) that chooses the optimal set of recovery actions to take for each disaster scenario.

Few works consider preparedness and recovery actions that can be taken to maximize resilience. Several advocate for resilience measures that account for recovery capability, but provide only qualitative discussions. The work by Chen and Miller-Hooks (2012) from which concepts of this thesis are built introduces a quantitative measure of resilience that explicitly accounts for recovery options. It only implicitly considers preparedness options. Johnstone et al. (2004) used pre-positioning strategies for equipment and ammunition to facilitate rapid and effective response to conflicts from a military view. Again, the developed model focuses on planning of necessity, but does not consider the evacuation of the traffic demand from origins to destinations.

Additionally, few existing models account for uncertainty in demand or damage to the network. The possibility of adverse outcome and uncertainty over the occurrence, timing or magnitude of the adverse outcome from a disaster must be considered (Covello and Merkhofer 1994). Such uncertainty makes the establishment of a comprehensive and directly relevant disaster management plan difficult and leads to a complex stochastic decision problem.

Few works study the synergies between preparedness and recovery. These works are discussed in succeeding chapters. This dissertation expands on the conceptualization of resilience by incorporating preparedness decisions and exploits synergies between preparedness activities and recovery options. A two-stage stochastic integer program is proposed in which preparedness decisions are taken in the first stage and recovery actions are suggested for each disaster scenario in the second stage. Incorporating risk mitigation through preparedness investment within a framework that accounts for the inherent network coping capacity along with immediate post-disaster recovery options, the

4

developed model aims to provide tactical support for improving pre-disaster preparedness and post-disaster recovery and, as a result, achieving an optimal balance between preparedness and recovery investment under budget and level-of-service constraints.

Two-stage stochastic integer programs are difficult to solve because they are generally non-convex and discontinuous. An exact methodology, employing with some adaptation of the integer L-shaped method of Laporte and Louveaux (1993) and Monte Carlo simulation, is proposed for its solution. Optimal allocation of a limited budget between preparedness and recovery activities is explored on an illustrative problem instance involving a network abstraction of a rail-based intermodal container network in United States.

This resilience concept that accounts for pre-disaster preparedness and post-disaster recovery activities is presented in Chapter 2.

1.2.2 Resilience with optimal recovery scheduling (RORS)

Decision-making in post-disaster activities in (Chen and Miller-Hooks 2012)) and Chapter 2 is conducted at a planning level. While choosing the optimal set of recovery actions to take for each disaster scenario, details of the recovery action implementation are handled in an aggregate way. That is, candidate recovery activities chosen for implementation are assumed to begin immediately after the event. That resources are limited and all activities cannot be implemented simultaneously is not addressed.

A time-dependent modeling approach is required to incorporate the effects of scheduling decisions that can be used to prioritize the implementation of recovery actions over the response period. Prioritization is also necessary to take advantage of efficiencies

that can be gained as a result of synergies between actions and the timing of their implementations.

This work studies the resilience of a transportation system from a practical operational perspective. A stochastic, time-dependent, nonlinear, integer program that accounts for both scheduling recovery activities under various disaster scenarios and managing dynamic flow to maximize the network resilience level, is proposed. This model aims to (1) select what recovery activities are to be taken, (2) identify where the recovery activities should be implemented, (3) determine when each of the recovery activities should get started and, (4) determine how fast the recovery activities should be completed, that is how much resources to supply for each action.

In this dissertation, two solution methodologies are presented. The first method is exact; it employs decomposition with branch-and-cut. The exact solution method requires extraordinary computational effort. An efficient solution algorithm is required that can quickly generate optimal or near-optimal solutions. Thus, the second method, a heuristic approach that relies on the concept of genetic algorithm, is proposed to speed up the process of finding a satisfactory solution.

Chapter 3 presents the proposed method for scheduling of recovery actions in a time-dependent network is formulated, and the formulation and its solution are demonstrated on an illustrative case study.

## 1.2.3 Assessing the role of network topology

Network topology can impact a network's ability to withstand the impact of disaster. This dissertation further studies the role of network topology in resilience. Different network

topologies demonstrate different inherent capacity to cope with potential disaster. In this chapter, systematically designed numerical experiments were conducted to assess a host of known network structures with the goal of gaining insight into the role of a network's topology in its resilience.

17 specific network topologies were selected for network resilience analysis. Simple graph structures with 9~10 nodes are first assessed. These were tiled together or expanded to produce larger instances (100 nodes each) with similar structure. These larger networks were also tested. Resilience is measured in terms of throughput and connectivity and average reciprocal distance. The integer L-shaped method is applied again to study the performance of the network structure with respect to all three resilience measures.

This portion of dissertation further studies the relationship between overall system health and component-level resilience. The relationships between network resilience and average degree, diameter, and cyclicity were also investigated. The impact of damage at the component-level on overall system health and the recovery capability was also assessed.

Details of the experimental design, numerical results and insights learned from the results are presented in Chapter 4.

## 1.3 _Contributions_

The primary goal of this dissertation is to formulate models and develop associated solution methodologies to support transportation system performance measurement, optimal decision-making on pre-disaster preparedness and post-event recovery actions

planning and scheduling to achieve the maximum network resilience level. This dissertation also studies the role that transportation network topology, including specific network structures, plays in resilience.

Synergies between preparedness activities and recovery activities were systematically studied. A two-stage stochastic integer model is developed to support the decisions associated with pre-disaster preparedness and the selection of post-event recovery activities. The model yields (1) optimal pre-disaster preparedness activities (types of equipment and personnel) and (2) post-event optimal recovery activities (locations for implementation, types of activities). Solution of the proposed two-stage stochastic integer program remains challenging and requires significant computational time. An integer L-shaped method that takes advantage of the existence of binary first-stage decision variables derived by Laporte and Louveaux (1993) is employed for transportation network resilience analysis. The integer L-shaped method decomposes the original model into many deterministic sub-problems. This decomposition eliminates intractable nonlinearity terms.

A stochastic, time-dependent, nonlinear integer model is formulated to account for scheduling recovery activities. Two solution methods are proposed, both employing a decomposition approach to eliminate nonlinearities of the formulation. The first is an exact decomposition with branch-and-cut methodology, and the second is a hybrid genetic algorithm that evaluates each chromosome's fitness based on optimal objective values to the time-dependent maximum flow subproblems. A novel chromosome representation for the scheduling of post-disaster recovery action is proposed to reduce the computational effort of the standard genetic algorithm procedure.

Decision support enabled through the research effort of this dissertation takes into account society's need for a stable transportation system in the event of an accident, natural hazard or act of terrorism resulting in large-scale disruption. It enables prejudice-free decisions and can offer transparency in the decision-making process. Moreover, decision-makers will be better informed and prepared to make logical and systematic decisions in an emergency.

General conclusions and future extensions are discussed in Chapter 5.

# Chapter 2: Measuring and Maximizing Resilience of Freight Transportation Networks

## 2.1 *Introduction and Motivation*

Freight transportation infrastructure and related transport elements (trains, ships, planes and trucks) comprise a crucial lifeline for society. In the United States (U.S.), for example, an extensive freight transportation system, with a network of 4 million miles of roadway, nearly 140,000 miles of rail, approximately 25,000 miles of waterways, more than 350,000 intermodal terminals, almost 10,000 coastal and inland waterway facilities, and over 5,000 public-use airports (USDOT RITA BTS 2010), enables the expedient movement of raw materials, other resources, and end-products between suppliers, manufacturers, wholesalers, retailers and customers. Its expediency and efficiency are in large part due to an open, accessible design. This design, that supports mobility objectives, leaves the system vulnerable to malicious and random acts with the aim or unintended consequence of disrupting operations. Even minor disruptions can have effects that ripple through the network, resulting in major reductions in system efficiency with nation-wide or even global impact (as discussed in Miller Hooks et al., 2009).

This chapter proposes a method for assessing and maximizing the resilience of an intermodal freight transport network. Resilience involves both the network's inherent ability to cope with disruption via its topological and operational attributes and potential actions that can be taken in the immediate aftermath of a disruption or disaster event. This conceptualization of resilience in terms of both inherent and adaptive components is discussed in (Rose, 2004) and was quantified in (Chen and Miller-Hooks, 2012). See also

(Nair et al., 2010) in which the concept was applied in a component-based application involving the intermodal port of Świnoujście in Poland.

Chen and Miller-Hooks (2012) formulated the problem of measuring resilience, defined as the expected system throughput given a fixed budget for recovery action and fixed system demand, in an intermodal freight transportation application. The problem was posed as a stochastic, mixed integer program. The program includes no first-stage variables. All decisions are taken once the outcome of the random disaster event is known. Thus, the problem can be decomposed into a set of independent, scenario-specific, deterministic (albeit NP-hard) problems and the focus of their solution approach is on the sampling methodology and exact solution of each independent deterministic problem that results for a given network state. They presented a solution framework employing Benders decomposition (Benders, 1962), column generation and Monte Carlo simulation. A secondary outcome from solving the mathematical program is the optimal set of recovery actions that can be taken to obtain the maximum attainable throughput for each potential network state.

This conceptualization of resilience that includes not only the network's inherent coping capacity, but also the potential impact of immediate recovery action within a limited budget is illustrated in Figure 2.1.
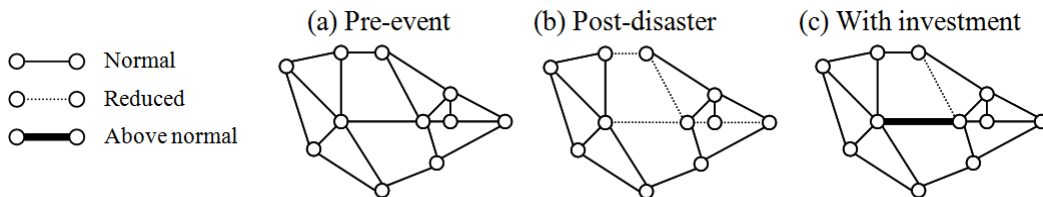


Figure 2.1: Illustrative example showing impact of recovery activities on system performance

11

As depicted in the figure, post-disaster arc capacities may be significantly reduced for affected arcs (Figure 2.1(b)), resulting in a poorly performing network. However, if recovery actions can be taken in the immediate aftermath of disaster to restore and even improve at least a subset of the affected arcs (Figure 2.1(c)), and such restoration can be accomplished quickly and within an acceptable budget, one may view the network *a priori* as highly performing, i.e. resilient.

This chapter expands on this conceptualization of resilience by incorporating preparedness decisions and capturing synergies between preparedness activities and recovery options. The concept of resilience as defined by Chen and Miller-Hooks (2012) was developed as a strategic tool. It permits the measurement of a network's resilience level given a set of possible, future network states and potential remedial actions. Remedial actions that may be taken pre-event (e.g. adding additional arcs to the network, ordering spare parts or backup equipment, prepositioning resources in anticipation of potential recovery activities, implementation of advanced technologies, training, and other pre-event actions that can reduce the time or budget required to complete potential recovery activities should they be required post-event) were not considered in their work. Thus, their formulation does not include pre-event, i.e. first-stage, decision variables and their approach does not incorporate decisions concerning actions that can be taken pre-disaster.

In determining resilience within this research, a budget is available for both preparedness and recovery options. A two-stage stochastic, integer program is presented in which preparedness decisions are taken in the first stage and recovery actions are suggested for each disaster scenario in the second stage. The incorporation of first-stage

12

decisions precludes the problem's decomposition into a set of independent, deterministic problems as was possible when only recovery options were considered (i.e. as in (Chen and Miller-Hooks, 2012)). An integer L-shaped method is proposed herein for solution of the resilience problem with preparedness options.

By incorporating risk mitigation through preparedness investment within a framework that accounts for the inherent network coping capacity along with immediate post-disaster recovery options, the developed solution methodology will provide tactical support for improving pre-disaster preparedness and post-disaster response, thus, achieving an optimal balance between preparedness and recovery investment. While this research focuses on intermodal freight transport networks, general concepts developed herein have wider applicability.

In the next section, related works in the literature are reviewed. In Section 3, the concept of resilience with preparedness options is defined. A two-stage stochastic integer program is presented for obtaining the allocation of funds to preparedness and recovery activities such that resilience, measured in terms of expected system throughput, is maximized. The formulation accounts for the inherent coping capacity of the network, along with the impact of cost-effective preparedness and recovery actions that can be taken to preserve or restore the system's ability to perform its intended function in a disaster's aftermath. The integer L-shaped method proposed for its solution is presented in Section 4. Solution of the program results in a measure of maximum resilience in terms of expected throughput for a given budget level, as well as the preparedness and post-disaster actions that are needed to achieve the maximum resilience value. Finally, these concepts and the effectiveness of the proposed solution methodology are illustrated on

the Double-Stack Container Network (Morlok and Chang, 2004; Sun et al., 2006) under disaster scenarios involving a terrorist attack, flooding or earthquake. Results of the numerical study show the additional benefits in terms of increased resilience level that are derived from taking preparedness actions. In addition, the optimal allotment of the budget between preparedness and recovery options for the case study is investigated.

## 2.2 *Literature Review*

Numerous works in the literature address network vulnerability, reliability and flexibility. These concepts are not always well defined and their meaning often varies from one work to another. It is only in rare cases, however, that consideration is given to actions that can be taken in the immediate aftermath of the disaster to improve system performance. An overview of the concepts of vulnerability, reliability, flexibility and resilience in the literature is given in (Chen and Miller-Hooks, forthcoming). Prior to (Chen and Miller-Hooks, forthcoming) and (Nair et al., 2010), a few works have considered compatible notions. Havidán et al. (2006) developed qualitative measures of resilience related to business contingency planning that account for actions taken to mitigate event impact. Srinivasan (2002) and Chatterjee (2002) espouse the need for recovery planning in the context of intermodal freight systems. Srinivasan (2002) advocates for a comprehensive and quantitative vulnerability index that can account for recovery potential, but does not provide such an index. A number of additional works recognize the importance of having resilient systems. Bruneau et al. (2003) emphasize that resilient systems reduce the probability of failure and its consequences, as well as the time for recovery. Other works consider recovery actions in the wake of natural and human-induced disasters (Juhl 1993,

Daryl 1998, Williams et al. 2000 and), but do not consider a network performance measurement.

Ip and Wang (2009) define network resilience as a function of the number of reliable paths between all node pairs. Such a concept is consistent with other notions of network reliability. Ta et al. (2009) developed a qualitative definition of resilience in the context of freight transport as a tool for visualizing disruption consequences. Their definition captures the interactions between managing organizations, the infrastructure, and its users. Murray-Tuite (2006) introduced a quantitative measure of resilience designed to consider network performance under disruption. The measure involves 10 dimensions: redundancy, diversity, efficiency, autonomous components, strength, collaboration, adaptability, mobility, safety and the ability to recover quickly. She considered both system optimal and user equilibrium traffic assignment modeling approaches and examined and compared the network performance based on the last four dimensions of the resilience measure. Zhang et al. (2009) also evaluate resilience as a function of change in system mobility, accessibility and reliability from pre-disruption levels for intermodal transportation systems.

Numerous works address disaster operations management, which can affect network performance in a disaster's aftermath. A review of many of these works can be found in (Altay and Green, 2006). Altay and Green (2006) categorized these works based on the phases of the disaster management lifecycle phases addressed or type of disaster considered. Examples of works addressing disaster operations management include (Feng and Wen 2005, Kondaveti et al. 2009 and Chen and Miller-Hooks 2012). These works seek an optimal post-disaster allocation of resources and optimal recovery actions that

15

can be taken in a disaster's immediate aftermath, but do not attempt to assess network performance *a priori.*

In this research, not only are short-term recovery options incorporated within a quantitative pre-disaster measure of resilience, but preparedness actions that can affect recovery capacity are considered. To address the preparedness phase, numerous works study network fortification by pre-positioning resources (Huang et al. 2007, Rawls and Turnquist 2010 and Zhu et al. 2010) and reinforcing network components (Holmgren et al. 2007, Liu et al. 2009, Fan and Liu 2010, Peeta et al. 2010, Cappanera and Scaparra 2011) to reduce disruption consequences and probability of failure. Huang et al. (2007) seek the optimal locations for fire stations and number of emergency vehicles to position at each station such that coverage of critical transportation infrastructure components is maximized in preparation for a major disaster. Zhu et al. (2010) determine optimal storage locations and capacities to meet post-disaster demand that is known in advance only with uncertainty. Holmgren et al. (2007) present a game-theoretic approach to optimally allocating resources for reinforcement in the context of the electric grid. Such reinforcement actions have implications for the total system recovery time. Peeta et al. (2010) addressed pre-disaster planning as an investment problem with the aim of strengthening the highway network and enhancing its ability to cope with disaster. Cappanera and Scaparra (2011) developed a methodology that seeks a network fortification plan to minimize the length of the shortest path between O-D pairs in response to a worst-case disruption scenario.

Liu et al. (2009) and Fan and Liu (2010) examine the allocation of limited resources (i.e. a fixed budget) for retrofitting and repairing bridges within a region. It was

assumed that if a bridge were retrofitted, it would withstand all disaster forces. They further assume that non-retrofitted bridges will be damaged and impassable in the event of disaster and all damaged bridges will require repair. They model the problem of optimal investment in either pre-disaster retrofitting or post-disaster repair as a two-stage stochastic program in which a fixed budget is available for retrofitting the bridges. The objective is to minimize a function of travel and repair costs. Liu et al. (2009) compute travel costs from total travel time incurred by all vehicles in the system. Fan and Liu (2009) compute travel costs assuming an user equilibrium is reached. In both works, travel times are based on conditions in the immediate aftermath of the disaster. Liu et al. (2009) require that all demand be met in each disruption scenario, while Fan and Liu (2010) only penalize solutions containing unsatisfied demand. Neither work considers the impact of repair on system performance.

Liu et al. (2009)'s two-stage stochastic program involves a nonlinear recourse function in the second stage. They propose a modified L-shaped method to solve the problem using a convex and piecewise linear approximation of the second stage objective function. The formulation given in Fan and Liu (2010) can be categorized as a mathematical program with complementarity constraints due to the traffic flow equilibrium constraints. As the L-shaped method relies on an assumption of convexity, an alternative solution approach is required. Thus, they propose a progressive hedging (PH) method due to (Rockafellar and Wets 1991) that decomposes the problem into multiple independent subproblems based on scenarios. Within this solution framework, the subproblems are further reformulated into a series of mixed integer nonlinear programs in which the complementarity constraints are relaxed. Each such program is solved using a

commercial solver. One can view the techniques proposed herein as extending the capabilities proposed in Liu et al.'s work to include recovery actions in the second stage as proposed in Chen and Miller-Hooks (forthcoming), as well as retrofit and repair options with intermediate, as opposed to all-or-nothing, impact. This work also provides a network performance measurement tool, which was not the goal of these earlier works.

Stochastic programming has been applied in numerous arenas, including, for example, production management, financial modeling, logistics, energy, pollution control, and healthcare. See (Wallace and Ziemba, 2005) for a review of stochastic programming applications. This approach is particularly well suited to the problem posed herein, as generally two-stage stochastic programs can be seen as having a preparedness stage, i.e. a stage in which decisions must be taken prior to the realization of a random event, and a recovery stage, referred to as recourse, in which changes to earlier decisions can be made to improve the solution once the random values are actualized.

It appears that no prior work in the literature provides a network resilience measurement tool incorporating both preparedness and post-disaster recovery actions, as well as the potential impact of those actions.

## 2.3 *Problem Definition*

In this section, the problem of measuring resilience given preparedness options is defined. To the extent possible, for consistency, notation and definitions presented in (Chen and Miller-Hooks, forthcoming) are used.

As in the previous work, network resilience is defined as the expected fraction of demand that can be satisfied post-disaster:

$$\alpha = E\left(\sum_{w \in W} d_w \Big/ \sum_{w \in W} D_w\right) = \left(1 \Big/ \sum_{w \in W} D_w\right) \cdot E\left(\sum_{w \in W} d_w\right) \tag{2.1}$$

where $D_w$ is the original pre-disaster demand for O-D pair w. $d_w$ is the post-disaster maximum demand that can be satisfied for O-D pair $w$. Demand that can be satisfied depends on the inherent coping capacity of the network and post-disaster recovery actions taken to restore or enhance network capacity. The network's inherent ability to cope with disaster can be enhanced through preparedness efforts. Moreover, new options for actions that can be taken in the immediate aftermath of disaster may exist if certain preparedness actions are taken. That is, preparedness actions can affect recovery capacity.

The problem of measuring resilience given preparedness options, referred to herein as Resilience with Preparedness Options (RPO), is formulated as a two-stage stochastic program. The first stage includes decisions on pre-disaster preparedness actions, actions that would be taken prior to disaster realization. The second stage, the recourse stage, involves the selection of post-disaster recovery actions to take in the aftermath of disruption, once the impact of the disaster on network performance, specifically on arc capacities and traversal times, is known.

A network representation of the intermodal system is exploited in the formulation and solution framework. Let $G=(N,A)$, where $N$ is the set of nodes and $A$ is the set of arcs. To address intermodal movements within the system, a representation employing intermodal connections between modal arcs would ordinarily be employed. For simplicity, intermodal movements are considered only in recovery options, and thus, in the following problem definition, modal arcs are indistinguishable. This is acceptable here, because decision variables represent the movement of shipments in the form of

containers that can be transported along any modal arc in the network. Had the decision variables produced vehicular-movements, such as rail car or truck movements, the intermodal network representation would need to be explicit. Notations employed in the problem formulation are synopsized as follows.

| $W$ | set of O-D pairs |
|---|---|
| $K_w$ | set of paths $k$ connecting O-D pair $w$ |
| $D_w$ | original demand between O-D pair $w$ |
| $R$ | Set of available recovery actions |
| $b_{ar}$ | cost of implementing recovery activity $r \in R$ on arc a |
| $P$ | Set of available preparedness actions |
| $b_{ap}$ | cost of implementing preparedness activity $p \in P$ on arc a |
| $b_{ar}^p$ | cost of implementing recovery activity $r$ on arc $a$ if preparedness action $p$ is taken |
| $B$ | given budget |
| $c_a(\xi)$ | post-disaster capacity of arc $a$ for disruption scenario $\xi$ |
| $\Delta c_{ap}$ | augmented capacity of arc $a$ given preparedness action $p$ is taken |
| $\Delta c_{ar}(\xi)$ | augmented capacity of arc $a$ due to implementing recovery activity $r$ for disruption scenario $\xi$ |
| $t_a(\xi)$ | Traversal time of arc $a$ under disruption scenario $\xi$ |
| $t_{ar}$ | Traversal time of arc $a$ if recovery activity $r$ is implemented |

| | |
|---|---|
| $q_{ar}$ | Implementation time of recovery activity $r$ on arc $a$ |
| $q_{ar}^{p}$ | Traversal time of arc $a$ if related preparedness action $p$ and recovery action $r$ is implemented |
| $Q_{k}^{w}(\xi)$ | Maximum implementation time of recovery actions on path $k$ between O-D pair $w$ |
| $T_{max}^{w}$ | Maximum allowed traversal between O-D pair $w$ |
| $\lambda$ | Preparedness-recovery action relationship matrix in which each element $\lambda_{pr}$ is set to 1 if recovery action r is affected by preparedness action p and 0 otherwise. |
| $\delta_{ak}^{w}$ | path-arc incidence (=1 if path $k$ uses arc $a$, and =0 otherwise) |

Decision variables

| | |
|---|---|
| $\beta_{ap}$ | binary variable indicating whether or not preparedness activity $p$ is undertaken on arc $a$ (=1 if preparedness action p is taken on arc a and =0 otherwise) |
| $y_{k}^{w}(\xi)$ | binary variable indicating whether or not shipments use path $k$ (=1 if path $k$ is used and =0 otherwise) between O-D pair $w$ |
| $f_{k}^{w}(\xi)$ | post-disaster flow of shipments along path $k$ between O-D pair $w$ under scenario $\xi$ |
| $\gamma_{ar}(\xi)$ | binary variable indicating whether or not recovery activity $r$ is undertaken on arc $a$ in the aftermath of disruption scenario $\xi$ (=1 if recovery action $r$ is taken on arc $a$ and =0 otherwise) |

Based on this notation, resilience with preparedness options (RPO) is formulated

as the following two-stage stochastic program:

(*RPO*)

First stage:

$$\max \quad E_{\tilde{\xi}}\left[Z(\xi)\right] \tag{2.2}$$

s.t.

$$\sum_p \beta_{ap} \le 1, \forall a \in A \tag{2.3}$$

$$\beta_{ap} \in \{0,1\}, \qquad \forall a \in A, p \in P \tag{2.4}$$

Second stage:

$$Z(\xi) = \max \sum_{w \in W} \sum_{k \in K_w} f_k^w(\xi) \tag{2.5}$$

s.t.

$$\sum_{k \in K_w} f_k^w(\xi) \le D_w, \qquad \forall w \in W \tag{2.6}$$

$$\sum_a \sum_p b_{ap} \cdot \beta_{ap} + \sum_a \sum_r b_{ar} \cdot \gamma_{ar}(\xi) + \sum_a \sum_r \sum_p (b_{ar}^p - b_{ar}) \cdot \lambda_{pr} \cdot \beta_{ap} \cdot \gamma_{ar}(\xi) \le B, \tag{2.7}$$

$$\sum_{w \in W} \sum_{k \in K_w} \delta_{ak}^w \cdot f_k^w(\xi) \le c_a(\xi) + \sum_r \Delta c_{ap} \cdot \beta_{ap} + \sum_r \Delta c_{ar}(\xi) \cdot \gamma_{ar}(\xi), \qquad \forall a \in A \tag{2.8}$$

$$\sum_{a \in k} t_a(\xi) + \sum_{a \in k} \sum_r (t_{ar} - t_a(\xi)) \cdot \gamma_{ar}(\xi) + Q_k^w(\xi) \le T_{\max}^w + M \cdot (1 - y_k^w(\xi)), \qquad \forall k \in K_w, w \in W \tag{2.9}$$

$$f_k^w(\xi) \le My_k^w(\xi), \qquad \forall k \in K_w, w \in W \tag{2.10}$$

$$Q_k^w(\xi) - q_{ar} \cdot \gamma_{ar}(\xi) - \sum_p (q_{ar}^p - q_{ar}) \cdot \lambda_{pr} \cdot \beta_{ap} \cdot \gamma_{ar}(\xi) \ge 0, \quad \forall a \in k, k \in K_w, w \in W \tag{2.11}$$

$$\sum_r \gamma_{ar}(\xi) \le 1, \forall a \in A, r \in R \tag{2.12}$$

$$\gamma_{ar}(\xi) \in \{0,1\} \qquad \forall a \in A, r \in R \tag{2.13}$$

$$y_k^w(\xi) \in \{0,1\}, f_k^w(\xi) \text{ integer}, \qquad \forall k \in K_w, w \in W \tag{2.14}$$

The objective function (2.2) in the first stage seeks to maximize the expectation of

$Z(\xi)$ over disruption realizations $\xi$ for a given decision on preparedness actions, where

$Z(\xi)$ is the maximum total post-disaster number of shipments, $f_k^w(\xi)$, that can be made

between all O-D pairs for a given disruption scenario $\xi$. Thus, objective function (2.2)

gives the maximum expected total throughput. First-stage constraint (2.3) specifies that at

most one set of preparedness actions can be taken for each arc and (2.4) restricts the

preparedness variable $\beta_{ap}$ to be binary. Demand constraints (2.6) guarantee that the total

number of shipments pushed along all paths between a particular O-D pair $w$ will not

exceed the original pre-disaster demand for the O-D pair. Constraint (2.7) requires that

the total cost of all chosen pre-disaster preparedness action and post-disaster recovery

actions not exceed available budget $B$. The monetary interaction between pre-disaster

preparedness and post-disaster recovery actions is accounted for by preparedness-

recovery action relationship matrix $\lambda$. This matrix consists of predetermined binary

elements that specify whether the preparedness action $p$ impacts recovery action $r$ in

terms of its implementation cost. That is, the cost of implementing recovery action $r$ on a

arc $a$, $b_{ar}^P$, given that a relevant preparedness action $p$ is taken pre-disaster, i.e. $\lambda_{pr} = 1$,

can decrease the implementation cost of recovery activity $r$ when taken alone. Note that

constraint (2.7) is nonlinear.

Constraints (2.8) account for the impact of preparedness actions on network

capacity enhancement. An augmented capacity $\Delta c_{ap}$ can be achieved by taking

preparedness action $p$ in arc $a$. The post-disaster capacity of the arc, thus, is the sum of

the post-disaster reduced capacity for the given disruption scenario and the augmentation

in capacity obtained by implementing preparedness and recovery actions. Note that $\Delta c_{ar}$

is a function of the disaster scenario realization. This permits the modeling of situations

where the impact of a recovery action may be minimal under certain scenarios. For example, pumping water from a roadway arc will provide added capacity in a flooding scenario, but will provide little aid in mitigating the effects of an earthquake.

The fact that taking preparedness actions in advance can reduce the implementation time of recovery actions is taken into account through level-of-service (LOS) constraints (2.9) through (2.11). These constraints limit the total traversal time, including arc travel time and recovery action implementation time, between each O-D pair $w$ for a pre-defined threshold $T_{max}^w$. This restriction holds only for paths along which flow is ultimately sent. $y_k^w(\xi)$ specifies whether path $k$ is used for sending shipments between O-D pair $w$. If it is not, the limitation is not imposed. If for a given shipment the total traversal time exceeds the threshold, the shipment is considered unserved and is not included in the throughput computation. The implementation time of recovery actions depend on whether or not certain preparedness actions have been taken, as described in constraints (2.11). Recovery action implementation times are accounted for in LOS computations.

At most one set of recovery actions can be taken along each arc as specified through constraints (2.12). Constraints (2.13) restricts recovery action variables, $\gamma_{ar}$, to be binary and constraints (2.14) impose integrality and non-negativity restrictions for second stage variables.

Note that for simplicity of notation, as written, all preparedness and recovery actions are presumed to be available for every arc. This need not be the case.

*2.4 <u>Solution Methodology</u>*

2.4.1 Overview of solution methodology

The aim of the solution methodology is to determine the optimal portion of the budget to spend on preparedness and amount of the budget to save for post-disaster recovery given future network states that could result from one of many possible disaster scenarios. The probability of each disaster scenario is assumed to be known *a priori* and it is possible that no such disaster scenario will be realized. The optimal investment plan will result in the maximum expected resilience index for the network.

*(RPO)* is a non-linear, two-stage stochastic program with binary first-stage decision variables and binary, as well as integer, second stage decision variables. The nonlinearity arises in second stage constraints, where first- and second-stage variables are multiplied. A primal decomposition method that decomposes the problem by stage will eliminate this nonlinearity by fixing the value of the first-stage variables when considering the second stage problem at each iteration. An L-shaped method, a type of primal decomposition method, is proposed herein for solution of *(RPO)*. Alternatively, one could apply the dual decomposition approach, designed to address integer stochastic programs, proposed by Caroe and Schultz (1998); however, such an application would require solution of a nonlinear, deterministic program for each scenario, i.e. at each iteration of the algorithm.

The L-shaped method of Van and Wets (1969), a variant of Benders' decomposition, is typically applied in solving two-stage stochastic programs. Within this approach, a single variable, $\theta$, is used to approximate the expected value of the second-

stage recourse function. The technique seeks the solution corresponding with the optimal $\theta$, and $\theta$ is determined iteratively by using LP duality to construct a convex piecewise linear approximation of the objective function. Because this approach requires that dual variables be obtained in each iteration, it cannot be applied in solving stochastic programs with integer decision variables. Instead, an integer L-shaped method for problems with binary first-stage variables and arbitrary second stage variables developed by Laporte and Louveaux (1993) and applied successfully to a vehicle routing problem (Laporte and Louveaux, 1998) is employed. Laporte and Louveaux's technique extends earlier work by Wollmer (1980) for two-stage stochastic programs with binary first-stage and continuous second-stage decision variables.

Like the standard L-shaped method, the integer L-shaped method applied herein begins with the decomposition of the two-stage stochastic program into a master problem (MP) in which integrality constraints are relaxed and a set of subproblems (SPs), one subproblem for each network state. A branch-and-bound tree structure is imposed. Nodes, referred to as pendant nodes, are added to the tree during the procedure. The initial problem, in which no variables are fixed, is solved at the root of the tree.

At any step $v$, solution of the master problem results in an approximation of $E_{\tilde{\xi}}[Z(\xi)]$ (from first stage objective function (2)), denoted $\theta^v$. If solution of the master problem is not integer, two new branches are created from the current node to two new pendant nodes, fixing the value of a chosen variable, and the process continues by branching.

26

If the solution is integer, decision variables from the master problem are fixed

within the subproblems and the subproblems are solved. An expectation, which in step $v$

is denoted as $\psi(\beta^v)$, $\beta^v = \{\beta_{ap}^v\}_{a \in A, p \in P}$, is taken over the resulting subproblem

objective function values weighted by network state probabilities. If $\psi(\beta^v)$ is no less

than $\theta^v$, an optimality cut is generated from the solutions of the subproblems and an

absolute lower bound associated with the subproblems. This cut is added back to the

master problem starting the next step $v+1$. The master problem is resolved. Otherwise, if

$\psi(\beta^v) < \theta^v$, the current node is fathomed and the process continues at the next pendant

node.

When no pendant nodes of the tree that have not yet been considered remain, the

entire procedure terminates. As optimality cuts are added to the master problem, the

master problem becomes increasingly constrained. This integer L-shaped algorithm is

guaranteed to converge in a finite number of steps.

To generate network states with properties related to a chosen set of scenario

classes (e.g. earthquake, flooding,...), Monte Carlo simulation is employed. Through

Monte Carlo simulation, arc capacities for a set of network states are set through repeated

sampling so as to approximate pre-specified probability distribution functions and to

preserve a given correlation structure among the random variables. The greater the

number of samples (i.e. network states), the more accurate the approximation. The

approach developed by Chang et al. (1994) and employed by Chen and Miller-Hooks

(forthcoming) in a similar context is applied herein to generate multivariate correlated

random variates of arc capacities. This approach transforms the original arc capacity

probability distributions with correlation matrix to standard normal space. By taking the orthogonal transformation of the correlation matrix to produce its eigenvector matrix, correlated normal random variates can be generated, which can be transformed back to the original probability space. Different correlation matrices are used for each distinct scenario. These sample network states are generated during initialization.

The general framework for the integer L-shaped method employed herein is illustrated in Figure 2.2. The Monte Carlo simulation technique embedded with the framework generates scenarios based on assumed probability distribution functions for event occurrence and consequence. These probability distribution functions can be estimated using one of several methodologies that have been introduced to obtain realistic probability distributions related to disaster events. Many of these techniques use historical data of past disasters and estimate the probability and damage potentials of disasters based on the geographical and geologic characteristics of a targeted network. For floods and storm events, hydrologic models, such as the Precipitation-Runoff Modeling System (Chang et al 2010) and CoreLogic Flood Model (Jeffery et al. 2011), can be applied to estimate the probability and severity of a flooding event. The Precipitation-Runoff Models, for example, are calibrated based on historical data. The calibrated model is employed within a simulation framework to determine the probability of future flooding for new situations. Seismologists apply methodologies to predict the probabilities of earthquakes in different locations. The U.S. Geological Survey (USGS) is known as a reliable resource of national seismic hazard data, which can be used to estimate the probability of earthquake and its severity in terms of measures of Peak Ground Acceleration (PGA) and Spectral Acceleration (FEMA 2006). These measures

provide information that can be used to predict potential damage to different types of buildings. After the attack of September 11, 2001, numerous studies have focused on quantitative approaches to measure the risk of terrorism (Willis et al. 2005, Rosoff and John 2009). These studies primarily employ physical attributes of potential targets in predicting the attractiveness of a particular structure and risk of terrorist attack on that structure. Risk models, e.g. the Risk Management Solution (RMS) model (Willis et al. 2005) and Proxy Utility Model (Rosoff and John 2009), have been proposed for estimating the likelihood of terrorist attack on a particular structure. These models further predict the probability distribution of consequence to a structure for a given event.
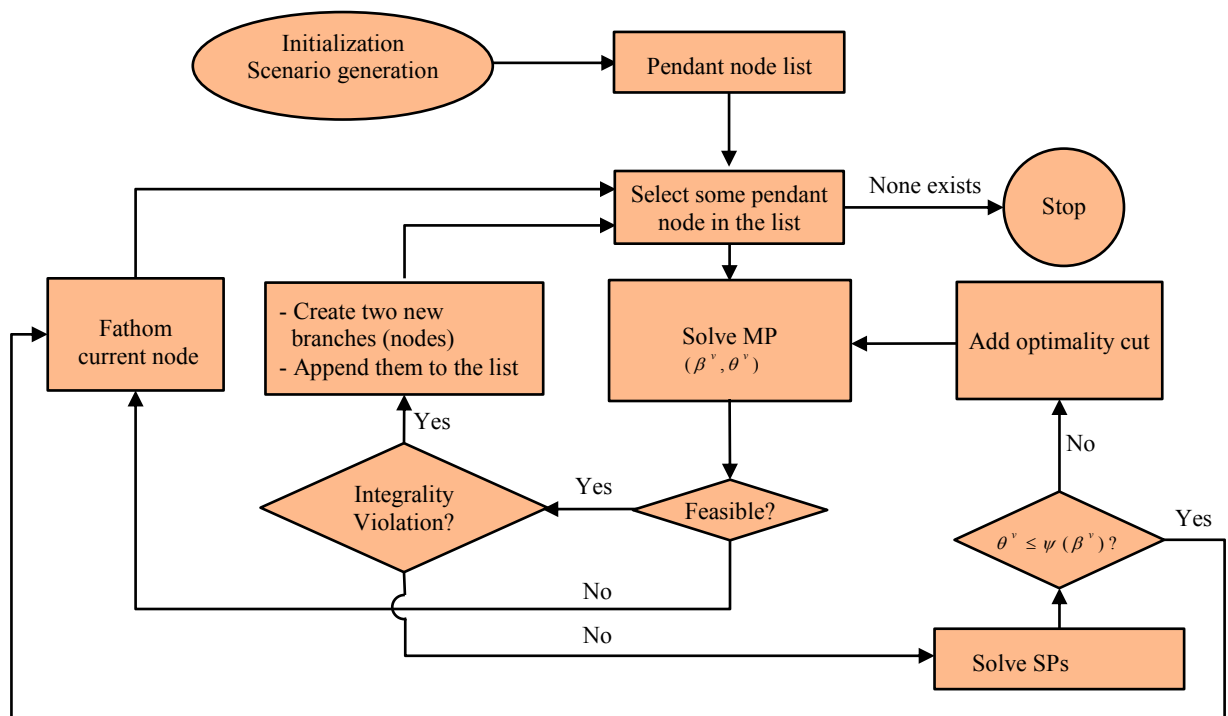
Figure 2.2: Flowchart for integer L-shaped method

2.4.2 Applying the integer L-shaped method for solution of (RPO)

To implement the integer L-shaped method for solution of the (*RPO*), the problem is treated as one of minimization, i.e. (2.2) is replaced by (2.15), and the problem is decomposed into a master problem (MP) and subproblems (SPs) as follows.

$$\min \quad E_{\tilde{\xi}} \left[ \min\{- \sum_{w \in W} \sum_{k \in K_w} f_k^w(\xi)\} \right] \tag{2.15}$$

$$(MP) \quad \min \quad \theta \tag{2.16}$$

$$s.t. \quad \sum_p \beta_{ap} \leq 1 \tag{2.3}$$

$$\sum_a \sum_p b_{ap} \beta_{ap} \leq B, \tag{2.17}$$

$$f(\theta, \beta) \geq 0, 0 \leq \beta_{ap} \leq 1, \tag{2.18}$$

where $\theta$ is the approximation of expected second-stage objective function value, $\beta = \{\beta_{ap}\}_{a \in A, p \in P}$, and $f(\theta, \beta) \geq 0$ is the set of linear optimality cuts generated during the algorithm. A valid constraint (2.17) that requires that the cost of preparedness actions not exceed the total budget is also added to the master problem.

$$(SPs) \quad E_{\tilde{\xi}} \left[ \min \left( - \sum_{w \in W} \sum_{k \in K_w} f_k^w(\xi) \right) \right] \tag{2.19}$$

$$s.t. \quad \text{constraint} \quad s \ (2.6 \sim 2.14).$$

For $|P|$ available preparedness activities and $|A|$ arcs, the number of elements in $\beta = |P| \cdot |A|$, denoted here by $n$. Let the $i^{th}$ element in vector $\beta$ be given as $\beta_{ap}(i)$. Then, $\{\beta_{ap}(1), \beta_{ap}(2),..., \beta_{ap}(n)\} \subset \{0,1\}^n$. Index set $I = \{i : \beta_{ap}(i) = 1\}$. Optimality cuts are obtained through equation (2.20).

$$\theta \geq [\psi(\beta) - L] \left[ \sum_{i \in I} \beta_{ap}(i) - \sum_{i \notin I} \beta_{ap}(i) \right] - [\psi(\beta) - L](|I| - 1) + L, \tag{2.20}$$

where $L$ is a finite absolute lower bound on (19). Since the total throughput cannot exceed the total pre-disaster demand, we can set the negative of the total demand as a valid absolute lower bound. Thus, $L = -\sum_w D_w$. The validity of the optimality cuts (2.20) is

a consequence of the fact that $\sum_{i \in I} \beta_{ap}(i) - \sum_{i \notin I} \beta_{ap}(i) \leq |I|$.

In implementing the procedure, branching is based on the most fractional variable. Addition of the optimality cuts to the master problem is implemented following the scheme proposed by Listes (2004), which was shown to reduce computation times. Unlike the original implementation of the integer L-shaped method in which any cuts added to the master problem are applied until termination, this scheme employs a dynamic list of optimality cuts. Optimality cuts generated at an ancestor node in the branch-and-bound tree are imposed on only descendant nodes in the tree.

Constraint (7) includes the nonlinear term $\beta_{ap} \cdot \gamma_{ar}(\xi)$. Since the elements of $\beta$ are set in the first stage, they can be treated as constants in the second stage where the constraint is enforced. Thus, the structure of the solution approach is exploited to eliminate concerns with nonlinearities in the formulation.

## 2.5 *Illustrative Case Study*

To assess the impact of preparedness on resilience level, the integer L-shaped method was applied on the Double-Stack Container Network introduced by (Morlok and Chang, 2004; Sun et al., 2006) and considered in (Chen and Miller-Hooks, forthcoming). The

solution methodology was implemented in C++ and run in the Microsoft Visual Studio C++ 2005 environment, employing IlOG's CPLEX 10.1 and the Concert Library. The computations were carried out on a personal workstation with a Pentium 4 3.20 GHz processor with 2.00 GB RAM running Windows XP Professional Edition.

## 2.5.1 Illustration on the double-stack container network

The Double-Stack Container Network depicted in Figure 2.3 provides a simplified representation of the intermodal freight network in the Western U.S. It contains 8 nodes, representing major cities, 24 rail one-way arcs and 22 bi-directional virtual highway arcs. It is assumed that highway arcs have sufficient capacity to support all freight transport demand for the region. Travel time estimates for the virtual highway arcs were obtained from Google Maps. Intermodal arcs exist at every node (i.e. at every city), connecting each rail terminal with the highway network. 17 O-D pairs are considered.
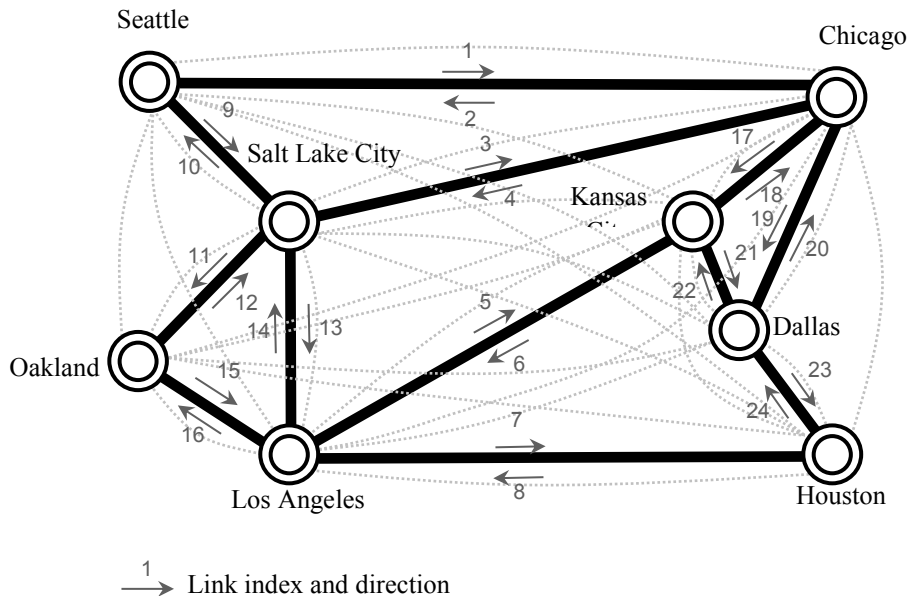


Figure 2.3: Western U.S. Double-Stack Container Network

2.5.2 Disaster scenarios, preparedness and recovery activities

Consistent with (Chen and Miller-Hooks, 2012), five scenario classifications designed for replicating five general disaster event types (bombing (1), terrorist attack (2), flood (3), earthquake (4) and intermodal terminal attack (5)) were considered in the experimental runs. Each scenario realization corresponds with a setting of the random arc attributes. A bombing scenario was replicated by reducing arc capacities on randomly selected arcs within the network. In the case of a terrorist attack, a few pre-specified arcs were assumed to incur significant damage, and thus, significant reduction in capacity. The attack is assumed to impact not only the chosen arcs, but also arcs directly connected to these chosen arcs. The capacity reduction of the directly connected arcs is presumed to be smaller than that incurred by the chosen arcs. For the impact of flood scenario, the capacities of multiple connected arcs (i.e. a single randomly chosen arc and all arcs incident on an end node of this arc) were reduced. To replicate an earthquake, arcs were randomly selected over a large area and their capacities were randomly reduced. In the last disaster event type, rail service is assumed to be inoperable into and out of the terminals in Chicago and Los Angeles.

Monte Carlo simulation was used to generate each network state under different disaster scenarios. Due to the dependency of random capacity of adjacent arcs under various disasters, network attributes for each state are characterized through correlation matrices. In the experiments, the arc capacities are assumed to have a uniform distribution $U[0, C_a(\xi)]$, and travel times increase in proportion to capacity decrease. For one unit decrease in capacity, an increase of 10% is incurred in travel time. Since a virtual highway network is employed, and alternative roadway paths may exist that

connect the same O-D pair, it is assumed that only rail arcs will be impacted by a disaster. This study assumes that the impacts to arcs and links in disaster scenarios will not evolve over time, and no further changes on capacity and travel time are considered.

As the computational effort required to solve a stochastic program is significant, and that effort increases linearly with each realization, only 100 realizations from each disaster classification, or a total of 500 realizations, were generated in this experiment. A larger number of realizations will reduce the sampling error. For simplicity, we assume the probability of each of the five disaster scenarios to equal 0.2.

One might also consider a case in which the probability of any disaster arising is quite small, thus adding an additional scenario in which no changes to the network occur. Because the budget is fixed, there will be no change in solution as a result of considering a no disaster scenario when disaster scenarios are considered proportionately identical in both cases. If an objective of minimizing expenses were considered, however, solution in the case involving a positive probability of no disaster will result in reduced spending in the preparedness stage and greater spending in the response stage.

To compare the resilience level when preparedness activities are implemented, the same six recovery activities defined by Chen and Miller-Hooks (2012) are available. The duration time, cost of implementation, impact to the arc capacity, and candidate arc for application of each recovery activity are listed in Table 2.1.

Table 2.1: Characteristics of recovery activities

| Recovery activities | Recovery activity duration (units) | Cost (units) | (% increase in link capacity) | Candidate links |
|---|---|---|---|---|
| R1 | 2 | 6 | 10 | 1-12 |
| R2 | 1 | 10 | 10 | 1-6 |
| R3 | 6 | 1 | 5 | 7-12 |
| R4 | 4 | 4 | 10 | 1,3,5,7,9,11 |
| R5 | 3 | 8 | 15 | 2,4,6,8,10,12 |
| R6 | 3 | 10 | Return to original capacity | 1-12 |

Two preparedness options that might be taken in preparation for a disaster event are available for implementation in this study: special training of personnel along specific routes to enhance recovery (P1) and prepositioning of water pumps (P2). These actions are coupled with a level of retrofit that provides additional enhancement to the capacities of arcs to which these actions are applied. Additional information pertaining to the preparedness actions are given in Table 2.2.

Table 2.2: Characteristics of preparedness activities

| Preparedness activities | Cost (units) | (% increase in link capacity) | Candidate link | Applicable for disaster scenarios |
|---|---|---|---|---|
| P1 | 3 | 10 | 1-6 | 1-5 |
| P2 | 2 | 8 | 1-6 | 3 |

The implementation time and cost of all six recovery actions on a given arc will be reduced if P1 is taken on that arc. It is assumed that the reduction is 20% for both travel time and cost. The benefits of P2 will only be realized if recovery action 4 (e.g. pumping water) is implemented. If P2 is chosen for application between two cities, its

benefits will be received in both directions. The preparedness-recovery relation matrix is shown in Table 2.3.

Table 2.3: Preparedness-recovery activity relationship matrix, $\lambda$

|     | R1 | R2 | R3 | R4 | R5 | R6 |
| --- | --- | --- | --- | --- | --- | --- |
| P1  | 1  | 1  | 1  | 1  | 1  | 1  |
| P2  | 0  | 1  | 1  | 0  | 0  | 0  |

A budget of 30 units and an unlimited budget are considered. The maximum allowable travel time for each O-D pair is assumed to be 1.5 times the travel time of the shortest path between the O-D pair in the original network. That is, an increase of as much as 50% in travel time is assumed to produce an acceptable level of service given the disaster occurrence.

2.5.3 Experimental results

Results of the numerical experiments in terms of obtained resilience level are given in Figure 2.4. Note that all obtained solutions are optimal. Because equal probability of each type of scenario was presumed, one can obtain the total resilience for the network over all scenario classes by simply adding the conditional resilience values and dividing by five. To judge the impact of preparedness actions on the network's resilience level, three additional runs were completed. The runs are synopsized in Table 2.4, along with overall resilience level (i.e. expected throughput over all scenarios). Results are shown for each disaster category. The first of the additional runs considers the case where no recovery or preparedness activities are available, a measure comparable to some notions of reliability. The second set of additional runs permits only preparedness actions, while the third

considers only recovery options. Results from these additional runs are provided for comparison in Figure 2.4.
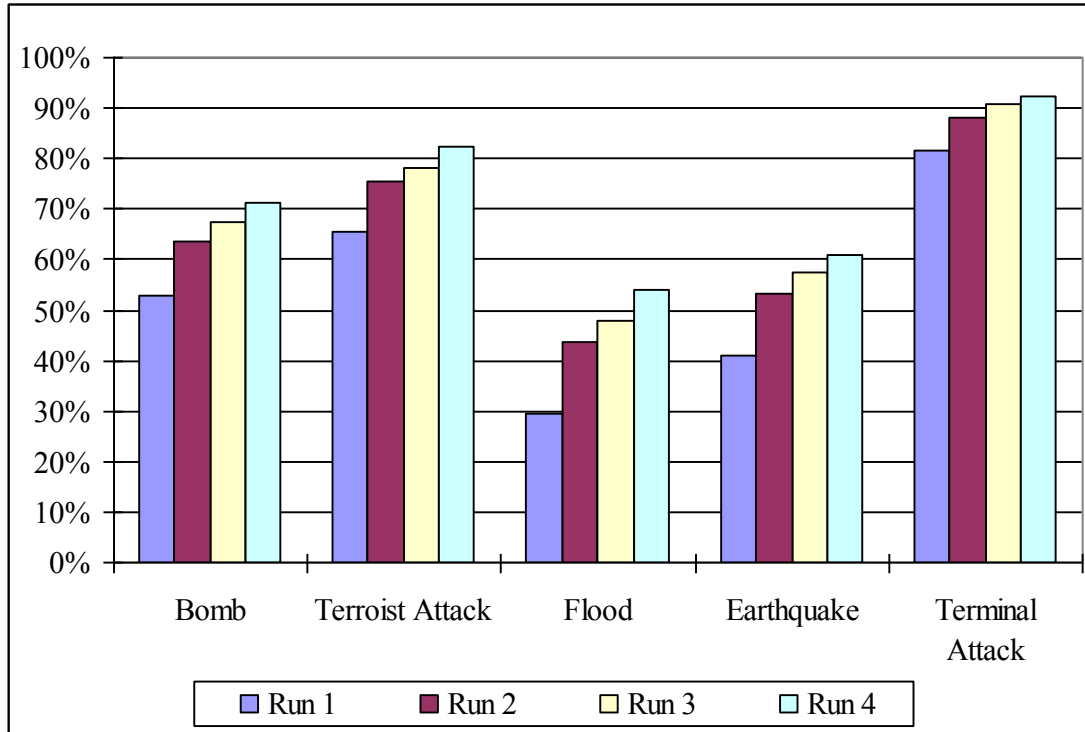


Figure 2.4: Resilience level by disaster scenario (budget=30)

Table 2.4: Description of implementations of resilience measure

| Run | Description | Overall Resilience, $\alpha$ |
|---|---|---|
| 1 | no recovery and preparedness activities taken | 0.54 |
| 2 | only preparedness activities are implemented | 0.65 |
| 3 | only recovery activities are implemented | 0.68 |
| 4 | both preparedness and recovery activities can be undertaken | 0.72 |

The results indicate that both preparedness and recovery activities can significantly improve network resilience level. When taken alone, the recovery actions

have greater impact than the preparedness actions. Moreover, the implementation of both preparedness and recovery activities provides a higher resilience level than either can reach alone. As evidence of this, note that on their own recovery activities led to a 14% improvement in the overall resilience level, while just under an 11% increase was obtained through preparedness activities alone. An 18% increase was obtained when both types of activities were available.

The average portion of the budget allocated to preparedness and recovery activities, as well as the maximum and minimum cost incurred over the set of disaster scenarios, are provided in Table 2.5.

Table 2.5: Cost of activities (budget=30)

| Scenario | Runs | | | | | | | |
|----------|------|----|----|----|----|----|----|----|
| | Run 1 | | Run 2 | | Run 3 | | Run 4 | |
| | CP | CR | CP | CR | CP | CR | CP | CR |
| Bomb | 0 | 0 | 18 | 0 | 0 | 26.7 | 16 | 12.6 |
| Terrorist Attack | 0 | 0 | 18 | 0 | 0 | 28.2 | 16 | 12.5 |
| Flood | 0 | 0 | 18 | 0 | 0 | 29.6 | 16 | 13.4 |
| Earthquake | 0 | 0 | 18 | 0 | 0 | 29.3 | 16 | 13.3 |
| Terminal Attack | 0 | 0 | 18 | 0 | 0 | 26.6 | 16 | 11.8 |
| M | 0 | | 18 | | 30 | | 30 | |
| m | 0 | | 18 | | 10 | | 18 | |

CP- Average cost of preparedness activities

CR- Average cost of recovery activities

M- Maximum cost of actions on tested disaster realizations

m- Minimum cost of actions on tested disaster realizations

The budget was not restrictive in Run 2. That not all the budget is used in each scenario may be a function of the discrete nature of activity costs. Results of Run 4 indicate that more funds were spent on preparedness actions than on recovery actions in the optimal solution. If a scenario involving no disaster were considered and this scenario

were given a relatively high probability, one would expect that much more of the budget would be spent on recovery actions than on preparedness. It may also be particular to this example.

To further investigate the allocation of the budget between preparedness and recovery options, Runs 3 and 4 were repeated with an unlimited budget. Runs 1 and 2 need not be reconsidered since the maximum budget used in any realization was less than the original budget permitted. Results from these runs are provided in Figure 2.5. The associated allocation of the budget across activity types is given in Table 2.6.
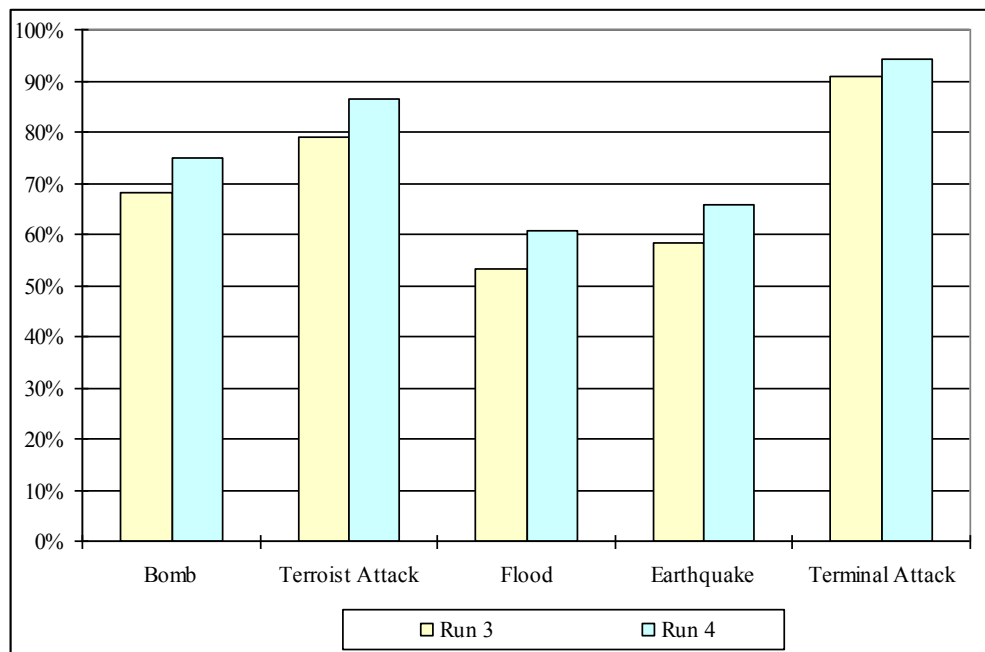


Figure 2.5: Resilience level by disaster scenario (unlimited budget)

With increased budget, the resilience level for Runs 3 and 4 are 0.70 and 0.76, respectively, leading to an increase in resilience by 2% and 4%, respectively. The maximum cost of actions taken in any disaster realization was 79 units. It was found that

for many disaster realizations, no additional improvement in resilience could be obtained from increasing the budget.

Table 2.6: Cost of activities (unlimited budget)

| Scenario | Runs | | | |
|---|---|---|---|---|
| | Run 3 | | Run 4 | |
| | CP | CR | CP | CR |
| Bomb | 0 | 38.7 | 18 | 27.9 |
| Terrorist Attack | 0 | 41.9 | 18 | 32.6 |
| Flood | 0 | 62.6 | 18 | 48.1 |
| Earthquake | 0 | 47.5 | 18 | 33.8 |
| Terminal Attack | 0 | 40.4 | 18 | 30 |
| M | 76 | | 79 | |
| m | 12 | | 16 | |

CP---Average cost of preparedness activities

CR--- Average cost of recovery activities

M---Maximum cost of actions on tested disaster realizations

m---Minimum cost of actions on tested disaster realizations

## 2.5.4 Additional study of computational time requirements

Several factors affect the required computational time required for running the L-shaped method: network size in terms of number of nodes and arcs, and number of preparedness activities, recovery activities, and instances of disaster scenarios. The network size and number of preparedness activities, i.e. factors affecting first stage decisions, play a more significant role in the required computational effort of the procedure, because these factors directly impact the size of the branch-and-bound tree. Additionally, computation time grows exponentially with the number of recovery activities considered in the second stage and linearly with the number of disaster instances.

Additional runs were conducted to assess the impact of these problem characteristics on computation time. The Double-Stack Container Network was modified

to create three additional networks for consideration. Problem characteristics and required CPU time are provided in Table 2.7. Results obtained for the unmodified Double-Stack Container Network are listed under network 2 in the table. These results indicate that the computational requirements of the proposed methodology increase substantially with increasing problem size. Note that while a feasible solution was obtained, no guarantee of optimality was received after several days of running on the largest network.

Table 2.7: Descriptions and computation time of tested experiments

| Network | Size of network | | # of preparedness activities | # of recovery activities | Disaster instances | | CPU time (seconds) |
| | # of nodes | # of arcs | | | # of scenarios | Instances per scenario | |
| --- | --- | --- | --- | --- | --- | --- | --- |
| 1 | 5 | 10 | 2 | 3 | 5 | 20 | 1136 |
| 2 | 8 | 24 | 2 | 6 | 5 | 100 | 31304 |
| 3 | 12 | 38 | 2 | 6 | 5 | 150 | 317526 |
| 4 | 15 | 52 | 4 | 6 | 5 | 200 | N/A |

## 2.6 *Conclusions*

This chapter revisits the notion of resilience proposed by Chen and Miller Hooks (forthcoming), which accounts for recovery actions that can be taken post-disaster within a limited time frame and budget. Herein, this notion is extended to include preparedness actions that can provide increased recovery capability, in addition to increased coping capacity. The concept is applied in the context of an intermodal rail application, but its relevance extends beyond transportation. The inclusion of preparedness decisions in determining a network's resilience level provides an extra level of decision support; however, this addition increases the problem difficulty. Whereas omission of

41

preparedness options permits the problem's decomposition into a set of deterministic subproblems, its inclusion prevents it. In this work, the problem of measuring a network's resilience level and determining the optimal set of preparedness and recovery actions needed to achieve this level given budget and level of service constraints is formulated as a two-stage stochastic program. An integer L-shaped method accredited to Laporte and Louveaux (1993) is proposed for its solution. The solution method decomposes the problem into a master problem and set of subproblems, each associated with a different disaster realization. Monte Carlo simulation is employed for the generation of the disaster realizations. This decomposition eliminates concerns associated with nonlinearities in the budget constraint of the formulation. The solution approach was applied on the Double-Stack Container network abstracting the intermodal rail system of the Western U.S. Optimal allocation of a limited budget between preparedness and recovery options is studied and the proposed expanded notion of resilience is compared with resilience without optimizing preparatory actions and a comparable notion of reliability.

Results of the numerical experiments provide some insight into optimal investment allocation of a fixed budget between preparedness and recovery stages. While improvements in resilience level are obtained from taking preparedness or recovery actions alone, the highest resilience level is attained when both preparedness and recovery options are available. In general, whether the budget or the available preparedness and recovery options were the limiting factors, greater benefit was derived through greater allocation of funds to the preparatory actions. If a scenario involving no disaster were introduced; however, one should expect that a greater portion of the budget would be reserved for the recovery stage.

42

The techniques presented herein will substantively increase our ability to aid in pre-disruption network vulnerability assessment and making pre-disaster vulnerability-reduction investment decisions. Quick identification of the appropriate actions to take can play a crucial role in lessening post-disaster economic and societal loss. Competing measures, such as reliability and flexibility, that do not consider quick and inexpensive recovery actions that may be taken post-disaster may underestimate the network's ability to cope with unexpected events and may lead to unnecessary or misdirected investment.

The problem instance studied within this research is rather small. To represent a real-world transport network with greater fidelity, the problem size will grow substantially. Exact solution of such large problem instances will be difficult to obtain as indicated by numerical experimentation. The conceptualization of the problem as a two-stage stochastic program and suggested solution approach provide a methodology for solving small benchmark problems against which the performance of a developed heuristic can be measured. Development of heuristics for assessing and maximizing network resilience is the subject of future work by the authors.

Alternatives to the (RPO) formulation might be considered. For example, one might envision a version of the problem with an objective of minimizing the required budget needed to obtain a specific resilience level. Other formulations might incorporate details for alternative applications. The authors are currently conceiving of a similar notion of resilience for passenger traffic, where no load can be left unserved.

Also discussed in (Liu et al., 2009), added realism may be obtained by considering decision-dependent network state probabilities (addressed by Jonsbraten et

al. (1998) in the context of generic discrete decision problems through an implicit enumeration method). This is because the probability of a specific realization of a disaster scenario may be impacted by the taking of a preparedness action. That is, if a component of the infrastructure is hardened, the probability that its capacity would be substantially reduced may be decreased as a result of the action. Such consideration, however, greatly reduces the problem's tractability.

# Chapter 3: Scheduling Short-Term Recovery Activities to Maximize Transportation Network Resilience

## 3.1 *Introduction and Motivation*

Freight transportation plays an important role in U.S. economic growth and international competitiveness. The U.S. freight transportation network handled more than $3.4 trillion in international merchandise trade in 2008 and 4.6 trillion ton-miles of domestic traffic (RITA 2008). Investment in the transportation network, through capacity expansion, infrastructure improvement, and application of advanced intelligent technologies nonetheless does not keep pace with increasing freight transport demand. Consequently, this growth in demand places escalating pressure on an already congested transportation system. Disruptions and other emergencies have further negative impact on system capacity. Recent disasters, including those caused by for example the 9/11 terrorist attacks, Hurricanes Katrina and Rita in 2005, 2007 Minneapolis 35W bridge collapse, and the 2011 Tohoku, Japan earthquake with ensuing tsunami, have brought to bear the need for transportation management agencies to prepare for the impact of potential future disaster events. A sustainable and well-functioning freight transportation system is able to satisfy the demand for fast, safe and efficient movement of goods, commodities, equipment and other materials even in the presence of disruptions. Thus, preparation for disaster is needed to reduce the impact of such events and the potential negative economic consequences.

Optimal allocation of available resources (e.g. equipment, materials and personnel) and post-disaster scheduling of recovery actions by responsible agencies can

aid in successful recovery from disaster. Recovery actions in this context might include, for example, repair of a roadway stretch or railway track, re-establishment of major transport linkages, removal of large debris, pumping of water from a flooded area, and utilities and communications restoration. The longer the recovery, the greater and longer lasting the economic consequences. Thus, it is of paramount importance to get the freight transport system back up and running quickly.

This research proposes a methodology for quantifying and maximizing resilience of rail-based freight transportation systems. 41% of the U.S. domestic freight market is handled by rail as measured in ton-miles (BTS 2009). Resilience in this context is a measure of how much throughput the system is expected to be able to handle post-disaster compared to demand handled pre-disaster. Building on a definition of resilience posed in (Chen and Miller-Hooks, 2012), resilience as discussed herein involves both the network's inherent coping capacity via its topological and operational attributes and potential actions that can be taken post-disruption or disaster event.

A multi-hazard approach is used, where any number of disaster scenarios is possible, and the scenarios can be drawn from a host of different disaster event types, such as naturally-induced events like hurricanes or earthquakes, or accidental/malicious events. To achieve the maximum resilience level, an efficient allocation of limited resources in the immediate aftermath of a disaster event to a chosen subset of potential short-term recovery actions is required. As only limited resources will be available to support recovery activities, simultaneous implementation of all needed repair actions may not be possible and the order in which recovery actions are taken can greatly affect gains achieved in capacity recovery over time. The need for sequencing these actions was

ignored in the prior work. Instead, it was assumed that all chosen actions could be taken simultaneously, beginning immediately post-disaster, and that the entire path was inoperable until the time at which all constituent damaged arcs were repaired. In this chapter, a stochastic integer mathematical program is proposed that, given a fixed budget and duration of time to undertake recovery activities, will (1) select what recovery activities are to be taken, (2) identify where the recovery activities should be implemented, (3) determine when each of the recovery activities should begin, and (4) determine how much resources should be supplied for each action, affecting time for completion. This time-dependent formulation permits flow across undamaged arcs and across repaired arcs at the time the repairs are complete.

Although a significant number of works in the literature have proposed models to support emergency recovery, these works are primarily strategic in nature; few consider operational details as will be described in the following section. Notation definition and problem formulation are also given in the next section. Two solution methodologies are proposed in section 4. The first is an exact solution method that uses decomposition with branch-and-cut (*D-BAC*). An alternative hybrid genetic algorithm (*GA*) is presented for solution of larger problem instances for which exact solution may be difficult to obtain. Both methods rely on decomposition for separating the decision variables related to recovery activities from the variables associated with flow. This separation eliminates nonlinear terms that exist in the model, and simultaneously guarantees an optimal solution to the original problem. Within the hybrid method, the fitness of each chromosome is taken as the objective value for a time-dependent maximum flow subproblem, which is solved exactly through CPLEX. In section 5, application of these

methodologies on a numerical example is presented. Performance of the *hybrid GA* is compared with that of the exact solution methodology. The benefits derived from scheduling the activities as compared with the more simplistic planning model that presumes all recovery activities begin simultaneously are evaluated. In section 6, the contributions are summarized and limitations are discussed.

*3.2 Literature Review*

Resilience has been defined in a variety of ways in the literature beginning decades ago with Hollings' seminal work on the persistence of natural systems to the changes in ecosystem variables (Hollings, 1973). Hollings defined resilience as the time required for an ecosystem to return to an equilibrium following a perturbation. Alternative resilience measures have been given in, for example, (Berkes and Folke 1998, Srinivasan, 2002, Gunderson and Holling 2002, Bruneau et al. 2003, Rose, 2004, Havidán et al. 2006, Murray-Tuite 2006, Ta et al. 2009, Chen and Miller-Hooks 2012, Gooding 2012). Chen and Miller-Hooks (2012) provide a means for quantifying the resilience measure conceptualized in (Rose, 2004) in which not only is the inherent coping capacity of a system to be included, but the effects of adaptive actions that can be taken to mitigate the effects of the disaster are accounted for. Nair et al. (2010) applied this methodology to evaluate intermodal (IM) freight operations of a port. Miller-Hooks et al. (2012) and Faturechi et al. (forthcoming) further study resilience of freight transportation networks also incorporating pre-disaster preparedness and post-disaster recovery actions in rail (in press) and airport pavement (in review) networks, respectively. A recent review of works on risk, reliability, vulnerability, robustness, survivability, flexibility and resilience in the context of transportation systems is given in (Faturechi and Miller-Hooks, under review).

Very few works consider recovery actions in pre-disaster system evaluation, and none consider the optimal sequencing of these actions in this context.

This work builds on the work of Chen and Miller-Hooks (2012) in which an indicator of network resilience and technique for its maximization are proposed for quantifying the expected performance of a rail-based IM freight transport network faced with numerous potential future disaster scenarios and accounting for the potential impact of post-disaster recovery actions that can be taken quickly and at a low cost. Their technique employs concepts of stochastic mixed integer programming and takes a planning perspective. While choosing the optimal set of recovery actions to take for each disaster scenario, details of the recovery action implementation are handled in an aggregate way. That is, candidate recovery activities chosen for implementation are assumed to begin immediately after the event. That resources are limited and all activities cannot be implemented simultaneously is not addressed. With only limited resources, a sequencing, and thus prioritization, of these activities will be necessary, and computation of the effects of the chosen sequence will be required. Further, it is presumed that no flow is permitted along any path that requires repair until the last of the repair actions on that path is complete. For example, consider a rail line from city A to B to C with demand from city A to city B that is awaiting clearance to depart. If both arcs (A,B) and (B,C) require repair, and arc (A,B) is chosen for repair first, the time for the shipments to arrive at C will be earlier than if repairs are made to arc (B,C) first. The potential impact of treating recovery activities from this operational, as opposed to planning, perspective is investigated herein.

Many works in the literature address emergency management decision-making for post-disaster applications. Brown and Vassiliou (1993) introduced a real-time operational and tactical decision support system named ARES to determine the optimal assignment of units for required tasks. Tamura et al. (1994) used a genetic algorithm to prioritize improvements to roadway segments for use in an urban area post-disaster. Fiedrich et al. (2000) suggest a resource allocation decision support system for post-earthquake search-and-rescue missions. Both simulation and analytical modeling techniques are employed in the system. Özdamar et al. (2004) proposed an emergency logistics planning model for natural disasters. Their model was formulated as a dynamic, time-dependent problem. Yi and Özdamar (2007) proposed a dynamic logistics coordination model for both evacuation and support in disaster relief operations. Examples of other works that address optimal allocation of resources for post-disaster repair include Knott (1988), Rathi et al. (1992), Barbarosoglu et al. (2002), Sheu (2006), and Chen and Miller-Hooks (2012). While these works investigate emergency recovery and associated resource allocation strategies, none of these works accounts for improvements obtained through the scheduling of recovery actions. Also, measuring system performance is not a goal of these works.

Management of debris is a concern after many major disasters. There are several studies in the literature focusing on post-disaster debris management. Concerns related to disaster debris removal after Hurricane Katrina are discussed in (Luther 2006, Stephenson 2008, Roper 2008). Relatively few quantitative studies on debris cleanup exist. Yan and Shih (2009) proposed a model that simultaneously considers emergency road repair and relief distribution. Fetter and Rakes (2011) use prospective statistical

process control methods to achieve equity in allocating debris disposal resources. Carbajal et al. (2009) discussed debris management operations in the both pre- and post-disaster phases. Additional literature exists in the form of government issued guidelines. USEPA (2008) and FEMA (2007) give a range of general technical and management options for disaster waste. These documents can inform models designed to predict debris quantities and may be helpful in organizing short-term clean-up efforts post-disaster.

Numerous additional works consider the ordering of infrastructure repair operations and assignment of tasks to crews for civil infrastructure maintenance (e.g. Carnahan et al. (1987), Madanat and Ben-Akiva (1994), Chen and Tzeng (1999), Childress and Durango-Cohen (2005), and Durango-Cohen and Sarutipand (2009)). Optimal maintenance policies are derived given deterioration estimates arising from natural causes. These works offer insights into the optimal scheduling of repair actions for infrastructure systems; however, network attributes are assumed to be known with certainty, and the emphasis of these works is on long-term system performance in which disrepair is limited and arises gradually and deterministically over time. Thus, techniques developed for this application cannot be directly applied for post-disaster resilience analysis in which one of a host of potential disaster scenarios might arise, the impact of which is likely to be sudden and severe and cannot be known *a priori* with certainty.

In the next section, a framework that explicitly considers scheduling of activities in the measurement and maximization of system resilience in the context of rail-based goods movement is provided.

## 3.3 _Definitions, Preliminaries and Problem Formulation_

### 3.3.1 Network resilience indicator

A mathematical formulation that exploits a network representation of a rail freight transportation system is presented. This formulation seeks to maximize resilience through a selection of a subset of recovery actions and the scheduling of their implementation, along with the optimal movement of traffic flow through the network. This problem of selecting and scheduling these actions is referred to herein as the Resilience with Optimal Recovery Scheduling (RORS) problem. The formulation considers that improvements in component and/or network performance due to implementation of recovery actions are obtained over time, as the actions are completed. Thus, time-dependent network attributes are considered. Travel times may increase and capacities may decrease post-disaster; their values depend on the disaster realization, which cannot be known _a priori_ with certainty.

### 3.3.2 Network definition

Network $N = (G, u, t, \xi)$ is a digraph $G = (V, A)$, where $G$ is defined by a set of nodes $V$ and $A$ is the set of directed arcs. Time is discretized into small increments of equal duration, i.e. $t = \{0, 1, \dots T\}$. A potential distribution of traffic is assessed under a variety of possible network states $\xi$, each of which is defined by a set of non-negative arc capacities given by $c_{ij}(\xi, t)$ and travel times given by $\tau_{ij}(\xi, t)$ for each arc $(i, j) \in A$. Arc capacities bound the amount of total flow that can be shipped along an arc departing the arc's origin node $i$ at time $t$. Capacities are recaptured over time as flow moves through the arcs. That is, as introduced by Ford and Fulkerson (1958 and 1962), dynamic

properties of flow are captured. Concepts from the first of these two papers are employed in the problem formulation in the following subsection. For a given state $\xi$, the distributions of post-disaster arc capacities and travel times are assumed to be known. Details associated with overtaking due to nonFIFO travel times are not considered. It is assumed that where overtaking is possible a train will pull onto the side rail to permit passing behavior. Arc travel times are taken as multiples of the time increment employed in time discretization and are assumed to be frozen from the time of entry (Orda and Rom, 1991).

Multiple source nodes, $O_w$, and sink nodes, $l_w$, at which flow originates and terminates, respectively, are included. For each origin-destination (O-D) pair $w$, there is a set of paths $P_w$ connecting $O_w$ with $l_w$. Let $y_{ij}^p(\xi, t)$ denote the flow that leaves node $i$ at time $t$ along path $p$ and reaches node $j$ at time $t + \tau_{ij}(\xi, t)$. Flow can be held in storage at intermediate nodes along a path before being shipped onward. The holdover capacity for an arc $(i, i)$ is determined by the node capacity at $i$, representing the amount of flow that can stay in the node at a given time. For simplicity, an infinite capacity is assumed to exist at all nodes. The travel time for a path is computed from the summation of travel and waiting times of a path's constituent arcs and nodes, respectively.

A time-expanded network is employed in the formulation of the RORS problem. Such a network expansion is depicted Figure 3.1.

**Time-dependent arc travel time**

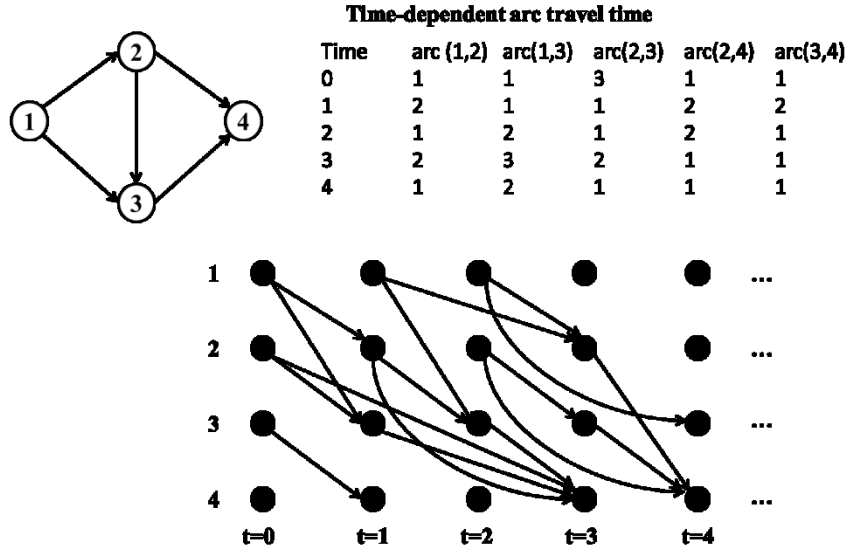| Time | arc (1,2) | arc(1,3) | arc(2,3) | arc(2,4) | arc(3,4) |
|------|-----------|----------|----------|----------|----------|
| 0 | 1 | 1 | 3 | 1 | 1 |
| 1 | 2 | 1 | 1 | 2 | 2 |
| 2 | 1 | 2 | 1 | 2 | 1 |
| 3 | 2 | 3 | 2 | 1 | 1 |
| 4 | 1 | 2 | 1 | 1 | 1 |

Figure 3.1: Example of dynamic and time-dependent network and its time-expansion

Notation employed in the problem formulation is summarized as follows.

| | |
|---|---|
| $W$ | set of O-D pairs |
| $P_w$ | set of paths, $p$, connecting O-D pair $w$, $w \in W$ |
| $D_w$ | pre-disaster demand between O-D pair $w$, $w \in W$ |
| $K$ | set of available recovery actions, $k$ |
| $o_p$ | origin node of path $p$ |
| $l_p$ | destination node of path $p$ |
| $T$ | timeframe of interest |
| $T_{\max}^w$ | maximum allowed travel time for O-D pair $w$ |
| $\tau_{ij}(\xi,t)$ | travel time along arc $(i,j)$ at departure time $t$ for disruption scenario $\xi$ |
| $T_i^p(\xi,t)$ | time that a unit of flow will have spent traveling from the origin $o_p$ departing at time $t$ and heading toward node $i$ along path $p$ under disruption scenario $\xi$ |
| $B$ | budget |
| $U(k)$ | maximum number of allowable recovery activities, $k$, that can be simultaneously undertaken |

| $c_{ij}(\xi)$ | post-disaster capacity of arc $(i,j)$ for disruption scenario $\xi$ |
|---|---|
| $\Delta c_{ijk}(\xi)$ | augmented capacity of arc $(i,j)$ due to implementing recovery activity $k$ for disruption scenario $\xi$ |
| $b_{ijk}$ | cost of implementing recovery activity $k \in K$ on arc $(i,j)$ |
| $q_{ijk}$ | required implementation time of recovery activity $k$ on arc $(i,j)$ |
| $\delta_{ijp}$ | path-arc incidence (=1 if path $p$ uses arc $(i,j)$, and =0 otherwise) |

Decision variables

| $y_{ij}^{p}(\xi,t)$ | flow of shipments on arc $(i,j)$ along path $p$ at departure time $t$ from node $i$ under disruption scenario $\xi$ |
|---|---|
| $z_{p}^{w}(\xi)$ | binary variable indicating whether or not shipments use path $p$ (=1 if path $p$ is used and =0 otherwise) between O-D pair $w$ for disruption scenario $\xi$ |
| $\alpha_{ijk}(\xi)$ | binary variable indicating whether or not recovery activity $k$ is undertaken on arc $(i,j)$ for disruption scenario $\xi$ |
| $\gamma_{ijk}(\xi,t)$ | binary variable indicating whether or not recovery activity $k$ is undertaken on arc $(i,j)$ at time $t$ for disruption scenario $\xi$ |
| $\theta_{ijk}(\xi,t)$ | binary variable indicating whether or not recovery activity $k$ is completed on arc $(i,j)$ at time $t$ for disruption scenario $\xi$ |

### 3.3.3 Problem formulation

The RORS problem can be formulated as ($P$): (2)-(17).

$$(P) \quad \max \; E_{\xi}\left[ \max \sum_{\{t'|t'+\tau_{ij}(t')=t\},\, t\in\{0,...,T\}} \sum_{(i,l_p)\in p} \sum_{p\in P_w} \sum_{w\in W} y_{il_p}^{p}(\xi,t') \right] \tag{3.2}$$

$$y_{ij}^{p}(\xi,t) = y_{o_p h}^{p} \cdot [\xi, t - T_i^{p}(\xi,t)] \qquad \forall t \in \{0,...,T\},\, (i,j)\in p,\, (o_p,h)\in p,\, p\in P_w,\, w\in W \tag{3.3}$$

$$T_i^{p}(\xi,t) = T_j^{p}(\xi,t) + \tau_{ji} \cdot [\xi, t + T_j^{p}(t)] \qquad \forall t \in \{0,...,T\},\, (j,i)\in p,\, p\in P_w,\, w\in W \tag{3.4}$$

$$T_{o_p}^{p}(\xi,t) = 0 \qquad\qquad \forall\, t \in \{0,..., T\},\ p \in P_w,\ w \in W \qquad (3.5)$$

$$\sum_{w \in W} \sum_{p \in P_w} \delta_{ijp} \cdot y_{ij}^{p}(\xi,t) \le c_{ij}(\xi) + \sum_{k} \Delta c_{ijk}(\xi) \cdot \theta_{ijk}(\xi,t) \qquad \forall\, t \in \{0,..., T\},\ (i,j) \in A \qquad (3.6)$$

$$\tau_{ij}(\xi,t) = \tau_{ij}(\xi,0) - \sum_{k} \Delta\tau_{ijk}(\xi) \cdot \theta_{ijk}(\xi,t) \qquad \forall\, t \in \{0,..., T\},\ (i,j) \in A \qquad (3.7)$$

$$\sum_{(i,j)\in A} \sum_{k} b_{ijk} \cdot \alpha_{ijk}(\xi) \le B \qquad\qquad (3.8)$$

$$\sum_{t=0}^{T} \gamma_{ijk}(\xi,t) = q_{ijk} \cdot \alpha_{ijk}(\xi) \qquad \forall\, (i,j) \in A,\ k \in K \qquad (3.9)$$

$$q_{ijk} \cdot \theta_{ijk}(\xi,t) \le \sum_{h=0}^{t} \gamma_{ijk}(\xi,h) \qquad \forall\, t \in \{0,..., T\},\ (i,j) \in A,\ k \in K \qquad (3.10)$$

$$q_{ijk} + \theta_{ijk}(\xi,t) - \sum_{h=0}^{t} \gamma_{ijk}(\xi,h) \ge 1 \qquad \forall\, t \in \{0,..., T\},\ (i,j) \in A,\ k \in K \qquad (3.11)$$

$$T_{i}^{p}(\xi,t) \le T_{\max}^{w} + M\,[1 - z_{p}^{w}(\xi)] \qquad \forall\, t \in \{0,..., T\},\ i = l_p,\ p \in P_w,\ w \in W \qquad (3.12)$$

$$\sum_{t\in\{0,...,T\}} \sum_{(o_p,j)\in p} \sum_{p \in P_w} y_{ij}^{p} \cdot (\xi,t) \le D_w \cdot z_{p}^{w}(\xi) \qquad \forall\, w \in W \qquad (3.13)$$

$$\sum_{k} \alpha_{ijk}(\xi) \le 1 \qquad \forall\, (i,j) \in A \qquad (3.14)$$

$$\sum_{(i,j)\in A} \alpha_{ijk}(\xi) \le U(k) \qquad k \in K \qquad (3.15)$$

$$\alpha_{ijk}(\xi),\gamma_{ijk}(\xi,t),\theta_{ijk}(\xi,t),z_{p}^{w}(\xi) \in \{0,1\} \qquad \forall\, t \in \{0,..., T\},\ (i,j) \in A,\ k \in K,\ p \in P_w,\ w \in W \qquad (3.16)$$

$$y_{ij}^{p}(\xi,t) \ge 0 \qquad \forall\, t \in \{0,..., T\},\ (i,j) \in A,\ p \in P_w,\ w \in W \qquad (3.17)$$

Objective (3.2) seeks the maximum expected total throughput over a set of possible disruption realizations. Throughput is measured by the total flow into the destination nodes of all O-D pairs $w \in W$. For each scenario, the maximum throughput in terms of number of shipments that can reach their destination before the end of the chosen time horizon and within $T_{max}^{w}$ for each $w \in W$ is sought, and the maximum expectation over all scenarios is taken. The network's resilience level can be assessed by dividing the maximum expected throughput provided through the objective function

value by the throughput that was accommodated prior to the disaster (i.e. the pre-disaster demand).

For each path of a given O-D pair $w$, constraints (3.3) ensure flow conservation accounting for time-dependent flows. Constraints (3.4) are recursive equations needed to compute $T_i^p(\xi, t)$, the total time that the flow travels from origin node $O_p$ at departure time $t$ to node $i$ along path $p$. This computation employs the travel time taken to arrive at the predecessor node $j$, $T_j^p(\xi, t)|(j, i) \in p$, plus the travel time on arc $(j, i)$ at time $t + T_j^p(\xi, t)$, $\tau_{ji}[\xi, t + T_j^p(\xi, t)]$. Boundary conditions restricting travel time to the origin of the path to be zero are given in constraints (3.5). Waiting at the path's origin is captured in the departure time index, $t$. Capacity constraints (3.6) restrict the flow on each arc to be less than the arc's capacity. The capacity depends on the impact of the disaster and recovery activities that are taken. Augmented capacity $\Delta c_{ijk}$ is included when recovery activity $k$ is completed.

Several constraints are used to model recovery activities. Constraints (3.7) are used to compute the arc travel times, which depend on the post-disaster travel time and improvements in travel times due to recovery activities. That is, the arc travel time along arc $(i, j)$ can be reduced by $\Delta\tau_{ijk}$ if recovery activity $k$ is completed. That total cost of selected recovery actions should not exceed a given budget is accounted for in constraint (3.8). Constraints (3.9) require that all recovery actions be completed by time $T$; otherwise, their impact in terms of enhancing arc capacities is not included. That only one recovery action can be implemented for each arc is enforced through constraints (3.14), and the number of activities that can be undertaken over the entire network at any point in

time is limited to $U(k)$ in constraints (3.15), reflecting limitations in equipment and personnel. Constraints (3.16) and (3.17) enforce non-negativity and integrality requirements.

Constraints (10) and (11) are transformations of desired if-then constraints (3.18).

$$\text{if} \quad \sum_{\lambda=0}^{t} \gamma_{ijk}(\xi, \lambda) = q_{ijk}, \quad \text{then} \quad \theta_{ijk}(\xi, t) = 1; \quad \text{otherwise} \quad \theta_{ijk}(\xi, t) = 0. \quad (3.18)$$

That is, if $\sum_{\lambda=0}^{t} \gamma_{ijk}(\xi, \lambda) = q_{ijk}$, from constraints (11) we have $\theta_{ijk}(\xi, t) = 1$. likely, if

$\sum_{\lambda=0}^{t} \gamma_{ijk}(\xi, \lambda) < q_{ijk}$, from constraints (3.10) we have $\theta_{ijk}(\xi, t) = 0$. If the total amount of time assigned to implementation of a recovery action equals the required amount of time for its implementation, implementation of the action is considered complete and its benefits derived.

In constraints (3.12) and (3.13), $Z_p^w(\xi)$, for each $\xi$, specifies whether or not path $p$ $\in P_w$ is used for sending shipments between O-D pair $w$. Level of service (LOS) constraints (3.12) require that the time that each shipment spends traversing a path $p \in P_w$ not exceed a pre-defined threshold $T_{max}^w$ if the path is active. Demand restrictions that limit flow leaving the origin of each O-D pair to its pre-disaster demand are given in constraints (3.13). The use of such an indicator variable, $Z_p^w(\xi)$, removes nonlinearities that would exist through the introduction of complementarity constraints in which decision variables associated with flows are multiplied by LOS constraints. Such an approach to addressing complementarity constraints through the introduction of such binary variables is known as a disjunctive constraints approach. This approach was originally prosed in (Fortuny-Amat and McCarl, 1981) and was adopted in (Chen and

Miller-Hooks, 2012), where constraints similar to (3.6) - (3.9) and (3.12) - (3.14) were also included.

Some concepts used in this mathematical program, such as the indexing for the sum in the objective function, were adapted from formulations of the time-dependent dynamic minimum cost and maximum flow problems of Miller-Hooks and Stock Patterson (2004) and Cai et al. (2001), respectively. ($P$) is a stochastic, time-dependent, integer, nonlinear program with nonlinear terms in both objective function and constraints. This nonlinearity arises from interactions between flows and travel times, as well recovery action variables.

## 3.4 *Solution Methodology*

The RORS problem is an integer nonlinear program with binary and integer decision variables. The nonlinearity arises in both objective function and constraints 3.3 and 3.4. In the objective function, decision variable $y_{ij}^{p}(\xi, t)$ is a function of arc travel time, and the arc travel times depend on the selection of recovery actions. Furthermore, the number of nonlinear terms will increase exponentially with increasing network size, number of time intervals and options for recovery activities. Though integer nonlinear programs (INLPs) or mixed-integer nonlinear programs (MINLPs) have been widely studied for decades, they remain challenging from both theoretical and computational perspectives. Available methods for addressing INLPs are still rather limited and some methods are problem specified. *D-BAC* and *Hybrid GA* solution methods are presented next. Both methods rely on decomposition for separating the decision variables related to recovery activities from the variables associated with flow.

3.4.1 Exact solution method

Given the block-separable characteristics of the RORS problem, a solution approach employing decomposition with branch-and-cut (*D-BAC*) is applied. *D-BAC* was first introduced in (Sen and Sherali 2006) for solving stochastic mixed integer programs. The framework of *D-BAC* is outlined in Figure 3.2. Briefly, this approach decomposes a problem into a master problem (*MP*) and set of subproblems (*SPs*), one for each scenario. The *MP* and *SPs* are solved iteratively. For each iteration, cuts are generated from solutions of the *SPs* and are added to the *MP* in the form of constraints, narrowing the solution space. The generation of these cuts is key to the success of *D-BAC*. A valid cut ensures convergence to the optimal solution for the original problem, and also determines how fast the algorithm converges. Each SP is deterministic, and its solution can be readily obtained through application of a commercial software product like CPLEX. In the context of the RORS problem, the *MP* seeks a schedule of recovery activities that maximizes expected throughput over all scenarios, and each SP is a time-dependent maximum flow problem given tentative scheduling decisions taken in the *MP*.
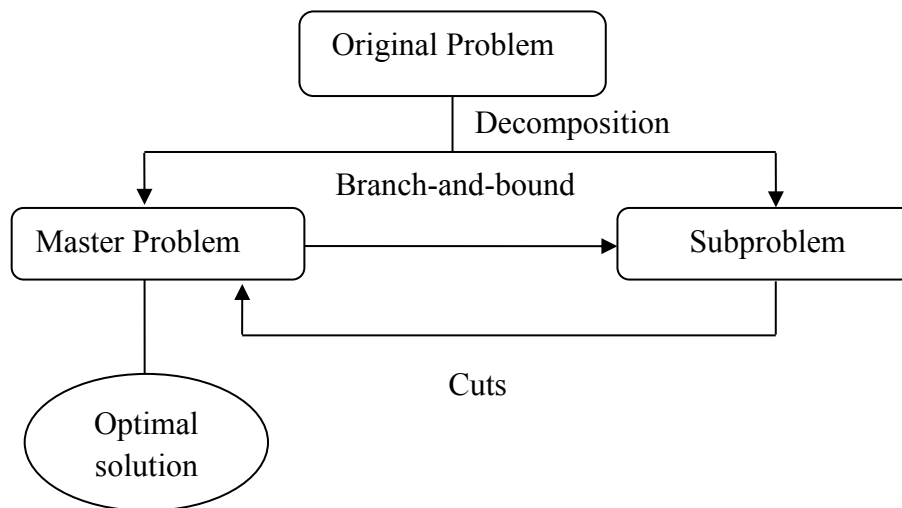


Figure 3.2: *D-BAC* solution methodology framework

Specification of the *MP* and *SPs*, along with an absolute lower bound and valid cuts as required by the procedure, are given in the context of the RORS problem following requirements outlined in (Sen and Sherali 2006). The decomposition with branch-and-cut approach is outlined next:

1. Initialization: Denote the initial problem by $P$ and decompose it to a master problem ($MP$) and a subproblem ($SP$). Set the active nodes of $MP$ to be $N = \{NMP^0\}$. Set the upper bound of the original problem to be $\bar{Z} = +\infty$, and $\eta$ is set to $-\infty$ or to an appropriate lowest value of $SP$. Set $v = 0$.

2. Termination: If $N$ is empty, the solution which yields the incumbent objective value $\bar{Z}$ is optimal, and stop.

3. Selection: Select a node $NMP^l$ from $N$.

4. Solve $MP$: Set $v = v + 1$, solve $MP$ and obtain the optimal solution $(x^v, \eta^v)$, $x$ is decision variable in $MP$. If $MP$ is infeasible, fathom the node $NMP^l$ and go to Step 3. If $(x^v, \eta^v)$ is not integer, two new branches are created from $NMP^l$ to generate two new nodes and add the nodes to $N$ and branch and bound process continues. If $(x^v, \eta^v)$ is integer, go to Step 5.

5. Solve $SP$: Solve the $SP$ by fixing $x^v$, and compute $\psi(x^v)$ as the objective value of $SP$. Update $\bar{Z} = \psi(x^v)$ if $\bar{Z} < \psi(x^v)$.

6. Generating cuts: If $\eta^v \geq \psi(x^v)$, then fathom $NMP^l$ and go to Step 3. Otherwise, generate a cut and append it to $MP$. Go to Step 4.

To implement the solution method for the RORS problem (3.2) is replaced by (3.19).

61

$$\min\{ \ - \sum_{\{t'|t'+\tau_{ij}(t')=t\},\, t\in\{0,\dots,T\}} \ \sum_{(i,l_p)\in p} \sum_{p\in P_w} \sum_{w\in W} y^p_{il_p}(\xi,t')\} \tag{3.19}$$

The *MP* is specified as follows. (3.20)

$(MP)$     min     $\eta$

s.t. constraints (8)-(11), (14) and (15)

$$f[\eta, \alpha_{ijk}(\xi), \theta_{ijk}(\xi,t), \gamma_{ijk}(\xi,t)] \geq 0 \tag{3.21}$$

$$0 \leq \alpha_{ijk}(\xi), \gamma_{ijk}(\xi,t), \theta_{ijk}(\xi,t) \leq 1 \quad\quad \forall t \in \{0,\dots,T\}, (i,j) \in A, k \in K \tag{3.22}$$

$$\eta \in \mathfrak{R}^1 \tag{3.23}$$

$\eta$ is an approximation of the objective value of the *SPs*, and constraints (3.21) are linear cuts generated in solving the *SPs*. Constraints (3.8) - (3.11), (3.14) and (3.15) involve decision variables of recovery activity scheduling. The remaining functional constraints of (*P*) are included in the *SPs* as follows.

$(SP)$     $\min\{ \ - \sum_{\{t'|t'+\tau_{ij}(t')=t\},\, t\in\{0,\dots,T\}} \ \sum_{(i,l_p)\in p} \sum_{p\in P_w} \sum_{w\in W} y^p_{il_p}(\xi,t')\}$ (3.24)

s.t. constraints (3)-(7), (12), (13) and (17)

    Let $\alpha = \cup \alpha_{ijk}$, $\gamma = \cup \gamma_{ijk}$, $\theta = \cup \theta_{ijk}$, and $\chi = \alpha \cup \gamma \cup \theta$. For $|R|$ candidate recovery activities applied to $|A|$ arcs within $|T|$ time intervals, the number of elements of $\chi$ is $(2|T|+1)|R|\cdot|A|$. Let $\chi(i)$ denote the $i^{th}$ element of $\chi$, $\chi$ is a binary variable. In each iteration, $S = \{i|\chi(i) = 1\}$ and $\overline{S} = \{i|\chi(i) = 0\}$. Constraints (21) can be computed by eq. (3.25).

$$\eta \geq \psi(\chi) - [|S| - \sum_{i\in S}\chi(i) + \sum_{i\in \overline{S}}\chi(i)][\psi(\chi) - L], \tag{3.25}$$

where $L$ is a finite absolute lower bound on (3.25). The maximum throughput is restricted by the total pre-disaster demand. Therefore, $L$ is set as the negative of the total demand. $L = -\sum_w D_w$.

3.4.2 Heuristic solution

*GAs* are search heuristics that belong to the larger class of evolutionary algorithms that generate solutions to optimization problems using techniques inspired by natural evolution. *GAs* have been demonstrated to be effective in applications related to a host of transportation problems. Different from many other metaheuristics that produce a single solution and seek improvements to this solution, *GAs* work with a set of potential solutions. Each solution is referred to as a chromosome. The representation of this chromosome can have significant impact on the performance of the algorithm. Mutation in a chromosome increases the diversity of solutions and reduces the likelihood that the *GA* will become trapped at a local minimum.

RORS consists two parts, first part is a scheduling plan that contains recovery activity-related decision variables ($\alpha_{ijk}$, $\gamma_{ijk}$, $\theta_{ijk}$) only, and second part is a time-dependent maximum flow problem (TDMFP) that is formed from the remaining flow-related decision variables and constraints. Initially, a population of chromosomes is generated to represent the scheduling of recovery activities. The quantity and length of chromosome do not change during iterations. Decision variable values set within each chromosome define link capacities and travel times over time, and thus, provide the parameters of a remaining TDMFP. The total maximum flow that can be achieved in this network provides the fitness value for each chromosome, which is employed in the *GA* for choosing chromosomes for crossover and survival to the next generation. The scheme used to represent each solution in a chromosome and details of the steps of the hybrid *GA* are provided next, an overview of which is given in Figure 3.3.
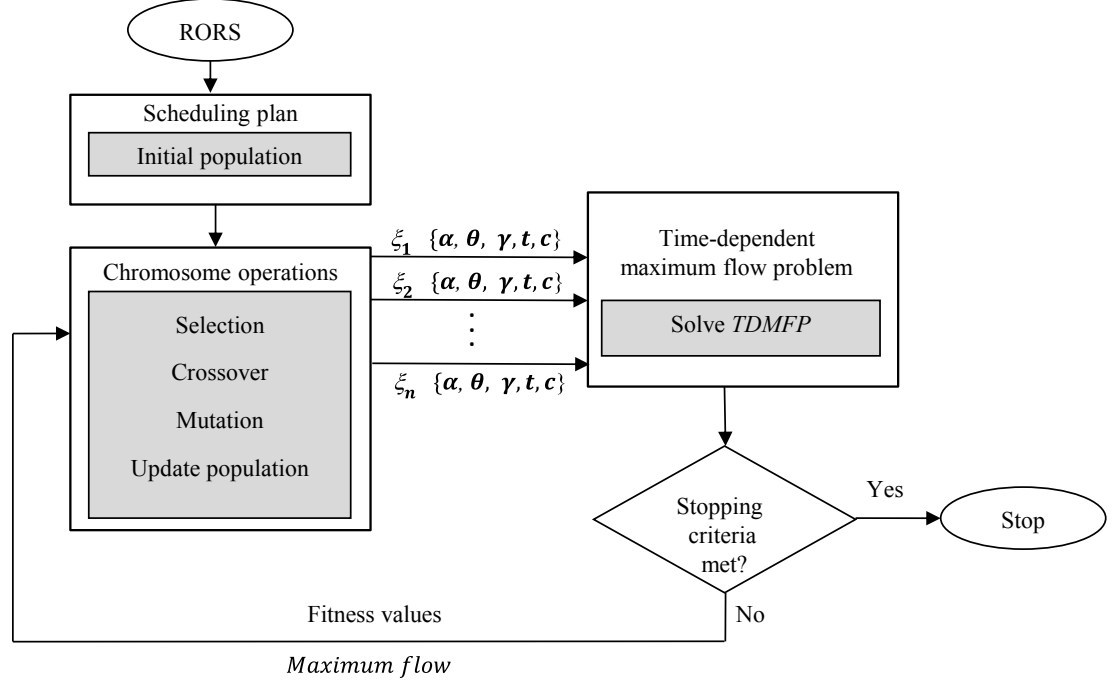
Figure 3.3: Overview of the *Hybrid GA*

*Solution representation*

The representation of a chromosome can have significant impact on the performance of the heuristic. For each arc $(i,j)$ and recovery activity $k$, $\alpha_{ijk}$ and $\theta_{ijk}(t)$ can be easily determined if $\gamma_{ijk}(t)$ is known; thus, the chromosome need only represent $\{\gamma_{ijk}(t)\}_{i,j,k,t}$ to form a candidate scheduling plan of recovery actions. A representation scheme that allows chromosomes to be created or heuristic operators to be applied so as to maintain feasibility is critical. An encoding scheme is proposed that is efficient in terms of its length, resulting solution search space, and convergence to a good solution.

The proposed encoding scheme for each chromosome involves an arc number represented by a string of bits, recovery activity options associated with that arc, and recovery action start times. Together, these provide a representation for the binary recovery activity implementation variables, $\gamma_{ijk}(t)$, and are referred to as an element, *e*,

of the chromosome. Define the set $C \subset A$ to be the set of arcs for which recovery activities are available. The constant number of elements to be included in a chromosome is computed by equation (3.26).

$$g = \min\left(|C|, \frac{B}{\min\{ b_{ijk} : (i, j) \in A, k \in K \}}\right). \tag{3.26}$$

Each element is unique in its association with an arc. This proposed encoding scheme is illustrated in Figure 3.4 and explained in detail next.
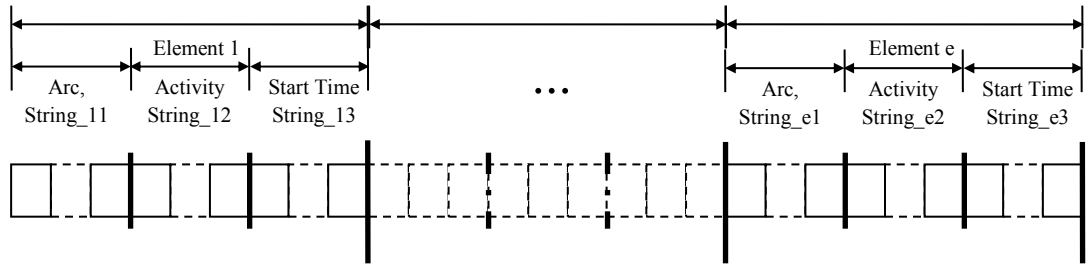


Figure 3.4: An encoding scheme for the RORS problem

*Step 1 (Arcs):* Assign each arc $(i,j) \in C$ an ID, $ARC_{ID}$, between 1 and $|C|$. This assignment of an $ARC_{ID}$ to arc $(i,j)$ is made through a string of bits ("Arc string_$ep$,") that form the first portion $p$ of the chromosome's element ($e$) associated with that arc. $n = \log_2 |C|$ is the number of required bits in this portion. To ensure a one-to-one mapping of element $e$ to a $ARC_{ID}$ using bits, the following strategy is proposed.

For each element $e$ taken in turn from $e=1$, the randomly generated binary ArcString_$e1$ is converted to a fraction of $n$ using equation (3.27). An index $e_i$ is assigned to each element by equation (3.28). This links the ArcString_$e1$ and $ARC_{ID}$.

$$f_i = \frac{\sum\limits_{k=1}^{n} g_k \, 2^{n-k}}{2^n} \tag{3.27}$$

$$e_i = \lceil 1 + (\,|\,C\,|\,-i-1)f_i \rceil \tag{3.28}$$

A simple example to illustrate this mapping strategy is provided in Figure 3.5 in which it is presumed that there are possible recovery actions that can be taken along all four arcs.
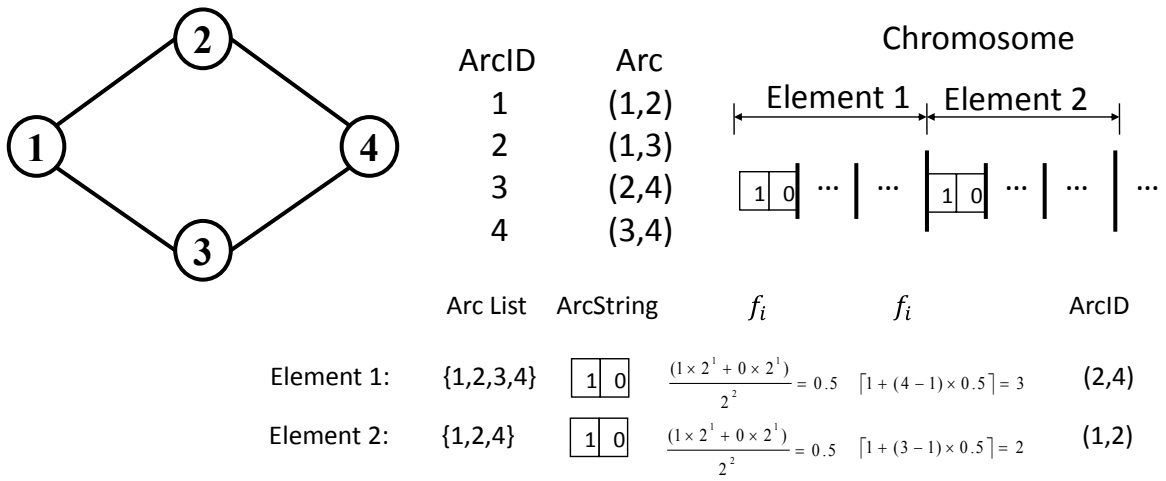


Figure 3.5: The mapping strategy

*Step 2 (Recovery activities):* Constraints (15) require that each activity $k$ be implemented only as many as $U(k)$ times throughout the network. Accordingly, each type of recovery activity in *String_e2* is assigned an ID, $R_{ID}$, between 1 and $|R|$, and a recovery activity list is generated: $\{1_1, 1_2, \dots 1_{U(1)}, 2_1, 2_2, \dots 2_{U(2)}, \dots, 1_{|R|}, 1_{|R|}, \dots 1_{U(|R|)}\}$. One recovery activity drawn (and not replaced) from the recovery activity list is assigned to each element of the chromosome. The assignment of $R_{ID}$ to each element $e$ is completed using a similar mapping strategy as is used in assigning each element with an $ARC_{ID}$.

66

*Step 3 (Start time of recovery activities):* The last portion to be encoded is

*string_e3*. Any given recovery activity $k = R_{ID}$ should be continuously implemented in

$q_{ijk}$ time intervals. Thus the start time of the recovery activity $R_{ID}$ should not exceed $T -$

$q_{ijk}$. As in steps 1 and 2, a mapping between a binary string and an integer number, in

this case a start time between 0 and $T - q_{ijk}$, is employed.

Using this proposed encoding scheme, all constraints of the RORS problem

except budget constraint (8) will be met throughout the steps of the algorithm. A

correction heuristic is employed after initialization and mutation to ensure feasibility in

constraint (3.8). In this heuristic operator, the sum of recovery activity costs, $\sum_e cost(e)$,

is computed. If this sum exceeds $B$, then the last $g$ in 1, 2, ..., $g$, for which (3.29) is

satisfied must be identified.

$$\sum_{e=1}^{g} cost\ (e) \le B \quad \text{and} \quad \sum_{e=1}^{g+1} cost\ (e) > B. \tag{3.29}$$

While each chromosome remains intact, only the first $g$ elements of the chromosome will

be decoded to obtain its interpretation in terms of the original decision variables. That is,

other elements (*g+1*, *g+2*...) are maintained and can be crossed over, but they are not

included in the fitness evaluation, because it is assumed they will not contribute to the

solution. Thus, only feasible solutions are generated.

*Creation of initial population*

A set of arcs, recovery actions and their start times, $\{\gamma_{ijk}(t)\}_{i,j,k,t}$ are randomly generated to form a candidate chromosome. A fixed number of chromosomes are generated, and the population size and length of each chromosome are fixed.

*Evaluation*

Each chromosome represents a scheduling plan. Given a chromosome, the travel time $t_{ij}(\xi, t)$ and capacity $C_{ij}(\xi, t)$ of each arc are known, thus the remaining TDMFP become deterministic. CPLEX is used to solve the resulting TDMFP and maximum flow of TDMFP is recorded. Chromosomes are evaluated in terms of the maximum flow achievable for the TDMFP, Fitness values of chromosomes are sent back for further chromosome operations.

*Crossover*

Pairs of chromosomes are selected for crossover, each crossover action producing two offspring. Single-point crossover is applied in which a point of exchange is set at a random location in the selected chromosomes.

*Mutation*

After crossover, the chromosomes are subjected to mutation. Mutation is applied by flipping a bit and can be implemented in any position belonging to the arc, recovery activity and start time of the recovery activity. Mutation in a chromosome increases the diversity of solutions and reduces the likelihood that the *GA* will become trapped at a local minimum.

*Selection for next generation*

A fixed population size is maintained. A linear ranking selection method is employed to select the individuals to continue into the next generation. This method first ranks the individuals of the population according to their fitness values. The individuals are selected with a probability in linear proportion to their rank. An elitist selection strategy is employed to ensure that the best individual solution in a generation continues to the next generation.

The *GA* is terminated when stopping criterion, i.e. the maximum number of generation have been produced, is met.

### 3.4.3 Addressing networks with waiting

The proposed *D-BAC* and *GA* assume that no waiting is permitted at the nodes. However, in the TDMFP solution, it may be beneficial for flow units to wait at nodes, because arc travel times do not necessarily follow the first-in first-out (FIFO) property. Additionally, waiting may be required as arcs are repaired. In this section, a method for transforming a network that includes waiting is provided. With this transformation, the proposed mathematical model and solution techniques can be applied directly.

A threshold on the maximum waiting time at any node, $T_R$, a multiple of the discrete time interval, is given. For each node $i$, a copy node $i'$ is created and an arc $(i,i',t)$ with infinite capacity is introduced for each time increment $t$ from zero to $T_R$. $t$ is the time required to traverse the arc. At most one arc $(i,i',t)$ can be used on any path. Positive flow along arc $(i,i',0)$ infers that no waiting at node $i$ is incurred. Likewise, positive flow along arc $(i,i',3)$ infers a waiting time of 3 units. This is illustrated in Figure 3.6.
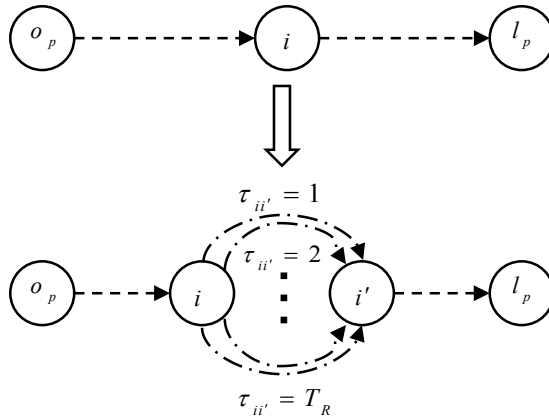
Figure 3.6: Network transformation example

## 3.5 *Illustrative Case Study*

The performance of the proposed solution methods are compared on the Double-Stack Container Network depicted in Figure 3.7. This network, originally described in (Morlok and Chang, 2004, Sun et al., 2006) contains 12 double-rail railways connecting 8 major western cities in the United States. Arc travel times were estimated from path lengths obtained from Google Maps. Demand between all 17 O-D pairs is considered. The *D-BAC* and *GA* were implemented in C++ interfacing with CPLEX Optimization Studio Academic Research Edition 12.3. Runs were conducted on a Pentium 4 desktop with 3.20 GHz processor and 2.00 GB RAM running Windows XP Professional Edition.

Figure 3.7:  Western U.S. Double-Stack Container Network

3.5.1 Experimental design

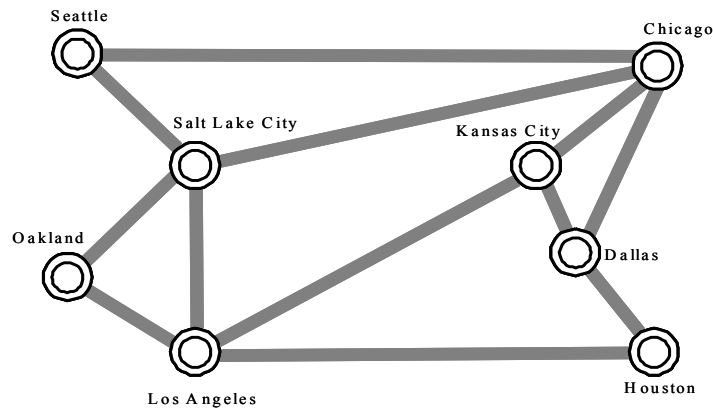Three disaster event categories were considered in the experiments from which scenarios were generated: (1) terrorist attack, (2) flood and (3) earthquake. For each terrorist attack scenario, damage in the form of capacity loss and performance degradation for a single randomly selected arc is incurred. While the arcs of this network span very large distances and a single attack would not take down the entirety of rail infrastructure between the cities, damage to any portion of the this infrastructure would have significant negative consequences for travel between the cities. Flooding scenarios are generated by capturing the consequences of an event occurring in one of the cities. Thus, in each scenario, a city is chosen randomly. All traffic entering and exiting the city is assumed to be impacted; thus, capacities and traversal times on incident links of the chosen node are affected. Finally, events involving an earthquake are replicated through changes to the capacities and travel times of randomly and independently chosen arcs.

300 disaster scenarios were generated through Monte Carlo simulation in equal proportion across scenario categories. For simplicity, the probability of each scenario is assumed to be equivalent. For each impacted arc, under any disaster scenario, the reduction in arc capacity due to the event is assumed to follow a uniform distribution on the interval from 0 to the arc's original capacity. Arc travel times are assumed to increase with decreasing capacity according to $\Delta\tau = \text{int}[\ t(1 - \Delta c / c)]$ , where int[$x$] returns the integer component of $x$, for $x$ a real number.

Three recovery activities were considered. The cost and duration of time required for their implementation, as well as the impact of the repair action on arc capacity, are provided in Table 3.1.

Table 3.1: Characteristics of recovery activities

| Recovery activities | Durations (units) | Cost (units) | Arc capacity increase (%) | Candidate arcs |
|---|---|---|---|---|
| Recovery-1 | 4 | 6 | 20 | 1-12 |
| Recovery-2 | 6 | 4 | 10 | 1-12 |
| Recovery-3 | 5 | 5 | 15 | 1-8 |

A budget of 30 units ($B$=30) and time horizon $T$=20 are considered. For each recovery activity, it is assumed that there are enough resources to implement each recovery activity in at most three locations simultaneously. The maximum allowable travel time $T_{max}^w$ for each O-D pair $w$ is 1.5 times the travel time along the O-D's shortest path in the pre-disaster network.

Finally, several combinations of crossover and mutation probabilities are tested. The probability of a chromosome being chosen for crossover ranged between 0.2 and 0.4 in increments of 0.05. Mutation probability varied between 0.15 and 0.3 in increments of 0.05. The best performance of the *GA* noted in preliminary experiments was obtained using the following parameter settings: 200 generations, population size of 30, crossover probability of 0.3, and mutation probability of 0.2.

3.5.2 Experimental results

The resilience level for each scenario is the expectation of resilience level of the 100 network realization. Run 1 is the case that no scheduling of recovery is considered, all the

72

actions will be implemented immediately in the aftermath of disaster, see details of solution methodology in Miller-Hooks and Zhang (2011). Run 2 and 3 show the results with recovery scheduling using *D-BAC* and *hybrid GA*. The network's resilience level under each disaster category obtained from numerical experiments is given in Table 3.2 and Figure 3.8.

Table 3.2: Description of designed resilience measurement runs for *T*=20, *B*=30

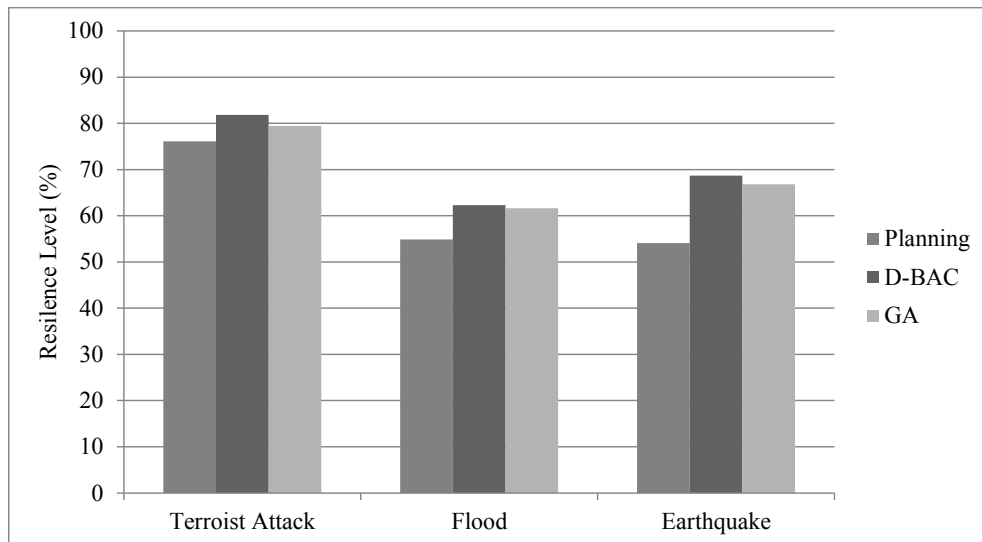| Run description | Resilience level |
|---|---|
| No scheduling, all actions start simultaneously after disaster, flow restricted, using a specialized version of *D-BAC* | 0.62 |
| With scheduling, flows permitted along open arcs from time zero, using *D-BAC* | 0.71 |
| With scheduling, flows permitted along open arcs from time zero, using *hybrid GA* | 0.70 |



Figure 3.8: Resilience level by disaster scenario

Under all three scenarios, an average of between 88 and 99% of the budget was utilized. Less than 100% utilization of the budget infers that other constraints, such as time for implementation and resource availability, were more limiting. Additional runs

were conducted to assess the impact of $T$ on resilience level. For $T$=15 time units, resilience is as low as 0.53. At $T$=25, it increases to 0.76.

The results of Table 2 also indicate that significant improvement in resilience level can be achieved from permitting flows along portions of the network when facilitated by the scheduling of recovery activities and flows. In fact, a nearly 15% improvement in resilience level is obtained through scheduling. Any benefits derived from assuming that enough resources are available to begin all recovery actions immediately after the disaster are dwarfed by losses due to restricting flows until the paths are open. Thus, the planning approach used in prior work results in significant underestimation of the network's resilience level. It also created a solution requiring a larger portion of the allowed budget (29.0 units) than did the solution of the RORS problem (requiring 27.4 units).

Convergence of the proposed $GA$ to an optimal solution using parameter settings as described in the prior subsection is displayed in Figure 3.9. A solution within 95% or 90% of optimal was obtained after 43 or 31 generations, respectively. These results were obtained in 361 and 335 seconds of CPU time, respectively, significantly lower than the time required to run $D$-$BAC$ (i.e. multiple days) for the same problem instance. The $GA$ was terminated once the solution value was within 1% of optimal; this solution was achieved after 105 generations and 992 seconds of CPU time. By comparison, exact results through $D$-$BAC$ required over 20 hours of computational time.
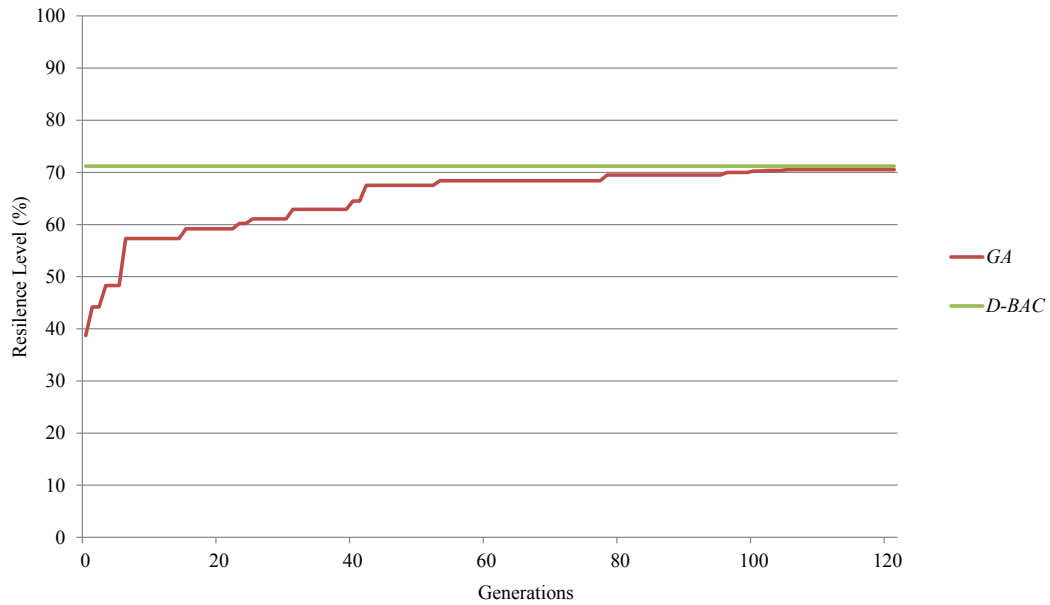
Figure 3.9: Evolution of resilience level over generations for proposed *hybrid GA*

## 3.6 *Conclusions*

In this chapter, the problem of assessing and maximizing network resilience is formulated

as a stochastic, time-dependent, nonlinear, integer program in which assignment of

resources to implement chosen recovery activities must be scheduled over time. This

extends prior work by Chen and Miller-Hooks (2012) in which a stochastic, static, linear,

integer program was proposed with the same goal. This earlier model did not capture the

limitations related to the availability of resources and thus presumed that all selected

actions could be taken simultaneously and immediately. It further restricted flows along

the paths while repairs are incomplete, despite that movements along significant portions

of the path may be possible while repairs are underway. To create the more realistic

version of the model introduces nonlinearities and time-dependencies. An exact solution

methodology that uses concepts of decomposition and branch-and-cut is proposed and

applied on a small case study. A specialized *hybrid GA* that exploits decomposition and

employs CPLEX to obtain exact fitness values at all generations is proposed for larger

networks and longer time periods; the *GA* performs well on the case study and requires comparatively minimal computation time.

A number of assumptions were made in the development of the proposed problem formulation or case study application. First, specific details related to rail operations are not included in this discussion. A directed representation of the arcs is assumed, which does not account for the potential use of track in both directions. Also, crossing of trains is not modeled. The solution method was applied on a test network with coarse granularity. Actual application of the tool to networks that include significantly more detail, and thus larger number of nodes and links, will be required. The *hybrid GA* is proposed with these larger problem instances in mind. Second, the arc capacity will not be restored until the entire arc is repaired, despite that a portion of the arc may be usable. For very long arcs, this may be unrealistic. The arc may need to be broken into smaller pieces. Finally, transfer of cargo to truck may warrant consideration as a recovery action if intermodality is permitted. The proposed methodologies can be applied directly in these cases.

# Chapter 4: Assessing the Role of Network Topology in Transportation Network Resilience

## 4.1 *Introduction*

The abstract representation of a transportation system as a network of nodes and interconnecting links, whether that system involves roadways, railways, sea links, airspace, or intermodal combinations, defines a network topology. Such topologies may have regular or irregular shape, and many topologies have been generically categorized. Among the most common in the context of transportation systems are the grid, ring, hub-and-spoke, complete, scale-free and small-world networks. Many arterial roadway networks have a grid or ring shape, networks of towns can be well-represented by small-world networks, while air systems are commonly shaped as hub-and-spoke networks. These networks can be characterized by various measures, and even networks with different topologies can have common characteristics. This paper investigates the role of network topology, and the topology's characteristics, in a transportation system's ability to cope with disaster. Specifically, the paper hypothesizes that the topological attributes of a transportation system significantly affect its resilience to disaster events.

In this study, a definition of resilience given in (Miller-Hooks et al., 2012) is adapted that explicitly considers the system's coping capacity, along with the effects of pre-disaster preparedness actions and adaptive response actions that can be quickly taken in the disaster's aftermath while adhering to a fixed budget. The system's coping capacity is measured through its capability to resist and absorb disaster impact through

redundancies and excess capacities. The pre- and post-disaster event actions are taken to prevent, reduce and ameliorate damage impact.

A quantitative approach developed in this earlier work that was originally posed for maximizing throughput in the context of freight movements is modified for the quantification of resilience measures relating also to connectivity and compactness. Specifically, two-stage integer stochastic programs designed for each considered resilience measure are described. This stochastic optimization approach provides a measure of system performance given pre- and post-event actions required for its maximization. Integer L-shaped decomposition is applied to obtain maximum performance measure values for each resilience interpretation.

Insights gleaned from results of systematically designed numerical experiments on 17 network structures employing this modeling framework and the appropriate adaptations provide a basis for the characterization of highly resilient network topologies and conversely identification of network attributes that might lead to poorly performing systems. In the assessment, the three resilience measures (based on throughput, connectivity and compactness) are considered with and without the benefits of preparedness and recovery actions.

Preliminary experiments involving four carefully designed 10-nodes complete, hub-based, grid and random networks were completed (Chen and Miller-Hooks, 2012). A concept of resilience in which recovery actions were possible was tested. However, no preparedness options that can improve a network's coping capacity and support recovery actions were considered in the study. Results of these runs indicated that topological

structures with limited redundancies faired worst when no recovery actions were supported; however, even with limited or modest budgets to support recovery options, improvements in resilience levels were achieved. It was also noted that improvements were greatest for networks with hubs. This is because exercising only a few options could restore connectivity between a large number of O-D pairs. Network structures that traditionally fair poorly when considering only the network's coping capacity (i.e. where no budget is available for response actions), perform well by focusing recovery actions on the most critical links. These experiments involved very small networks of only four topological classifications applying only one concept of resilience. A more comprehensive analysis from which significantly deeper and broader insights can be garnered is presented herein.

Network topologies that are studied herein are introduced in the next section. Measures for their characterization, such as diameter, betweeness centrality and the Shimbel index, are also discussed. This is followed by methods for measuring and maximizing resilience with respect to throughput, connectivity and average reciprocal distance (the measure of compactness). The experimental design, numerical results and analysis follow. Finally, conclusions and implications of the findings for transportation applications are discussed.

## 4.2 *Literature Review*

Many works have proposed measures to characterize networks and their performance for a range of applications, including physics, geography, the Internet, and biological and social systems. Early examples include (Kansky, 1963, Haggett and Chorley, 1967 and Garrison and Marble, 1974). Kansky (1963) considered nodal importance and network

complexity in the context of transportation network with three main indices: Alpha, Beta, and Gamma indices, all measures of connectivity. These measures and additional measures are defined in Table 4.1 of the next section. Their studies, however, were hampered by limited computational resources.

In random graphs, nodes are randomly linked with an equal probability of links between any pair of nodes. Two other types of random networks have been studied in the literature. Barabási and Albert (1999) defined a scale-free network as a network in which the distribution of degree between nodes follows a power law. In a scale-free network, some nodes have a degree that greatly exceeds the average. Wu et al. (2004) showed that scale-free type characteristics exist in urban transit networks in Beijing. Small-world networks, on the other hand, are densely connected in local regions, creating highly connected subgraphs with few crucial connections between distant neighbors. Watts and Strogatz (1998) studied the performance of neural and power grid networks in terms of shortest average path length and clustering. They found that some neural and power grid networks have the shape of small-world networks. They did not investigate the role of network topology in network performance, however. Latora and Marchiori (2002) suggested that the Boston subway system has a small-world network structure. Zhao and Gao (2003) studied the performance of small-world, scale-free and random networks in terms of their performance in terms of total travel time and traffic volumes in the context of a traffic network.

Some works have studied network topology in nature. Theraulaz et al. (1998) considered a nest network of interconnected chambers and galleries inside which the activities of insects take place. These networks are self-organized and emerge from the
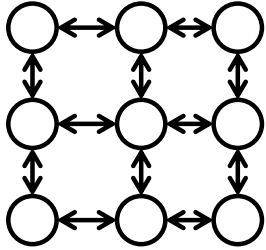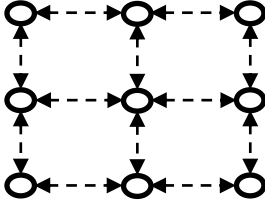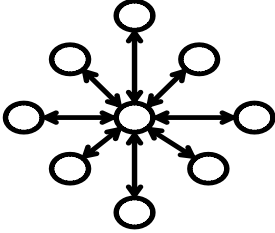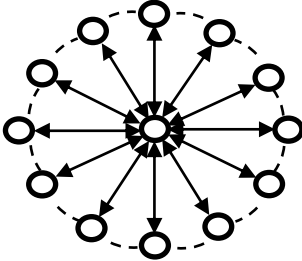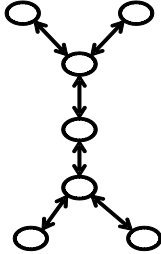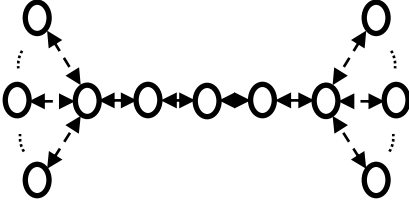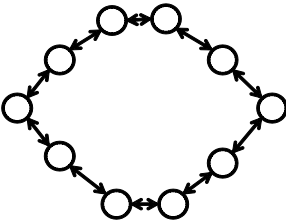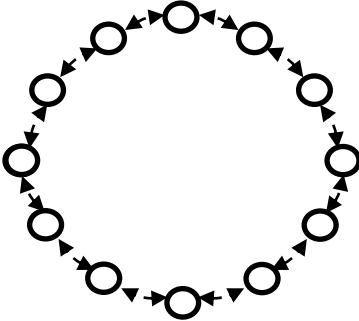
work of tens of thousands of insects. No model or results are provided. Perna et al. (2008) studied six 3-D networks of galleries found in nests built by termites. They measured communication efficiency within the network, using measures such as average path length, clustering coefficient, betweenness centrality, and local graph redundancy (also defined in Table 4.1 of the next section). These studies only focus on one specific network type; no comparison to other network types is made.
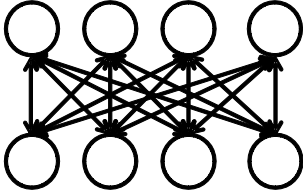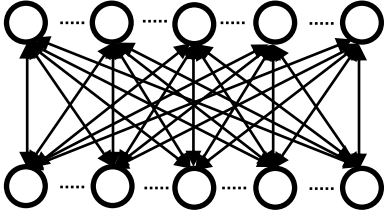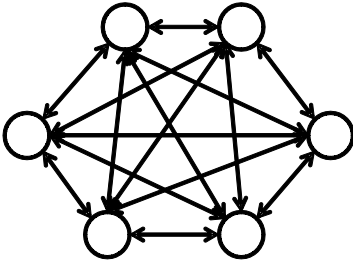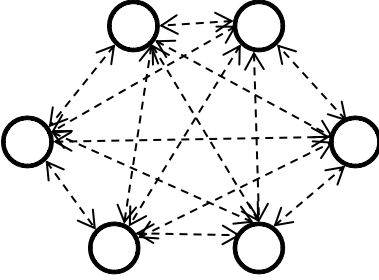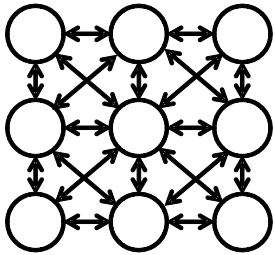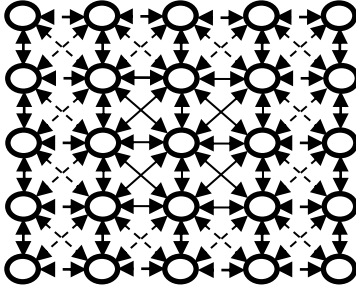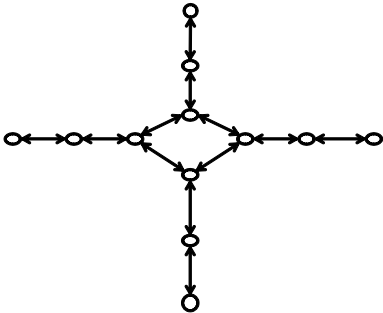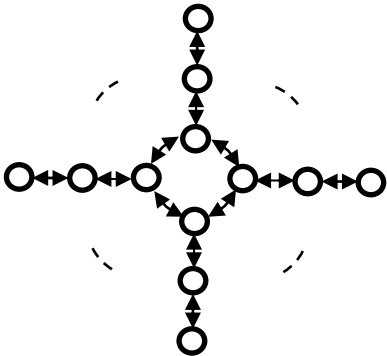
Studies that focus on the role of network topology in transportation or civil infrastructure application are limited.
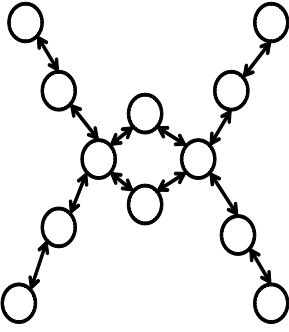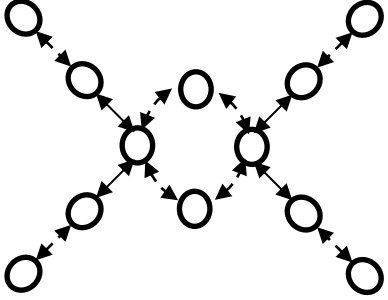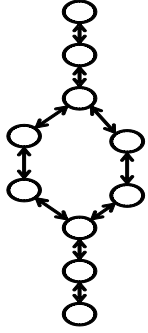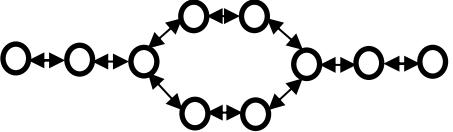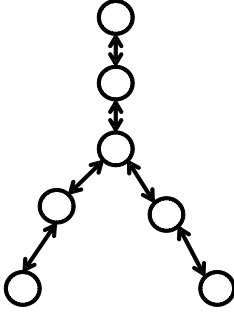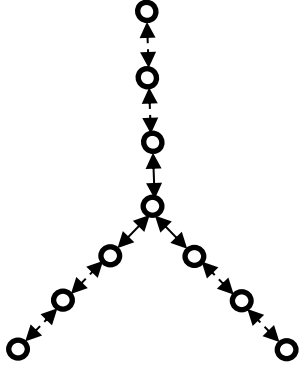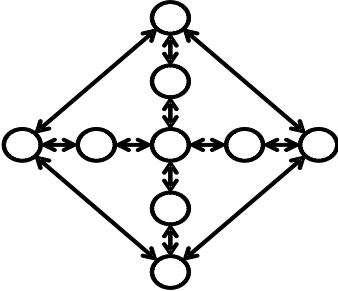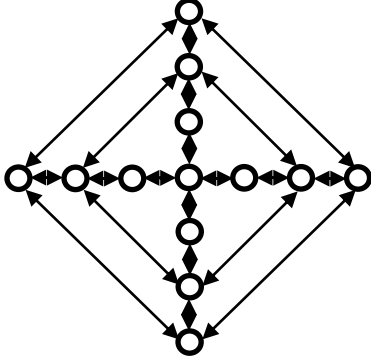
## 4.3 *Network Resilience Measurement*

### 4.3.1 Selection and characterization of network topologies

The 17 network topologies that were investigated were chosen from approximately 30 topologies discovered in a search of the literature covering many areas, including transportation, communications, the Internet, general graph theory and biological systems, among others. They were selected for their potential relationship with existing transportation system network representations. The basic structure of each of the chosen network classes is described in Figure 4.1. All networks were created with symmetry. These basic structures provide the fundamental elements for the construction of larger comparable networks. This extrapolation to larger network sizes (greater number of nodes and links) is also included in Figure 4.1. The resilience of each basic structure and structures constructed from these elements (used as tiles where logical to do so) is studied.

| Types | Basic elements | Extrapolations |
|---|---|---|
| Grid |  |  |
| Hub and spoke |  |  |
| Double tree |  |  |
| Ring network |  |  |

| | | |
|---|---|---|
| Matching pairs |  |  |
| Complete network |  |  |
| Complete grid network |  |  |
| Central ring |  |  |

| | | |
|---|---|---|
| Double-U |  |  |
| Converging tails |  |  |
| Diverging Tails |  |  |
| Diamond Network |  |  |

| | | |
|---|---|---|
| Single path | | |
| Crossing paths | | |
| Random | | |
| Scale-free | | |
| Small-world | | |
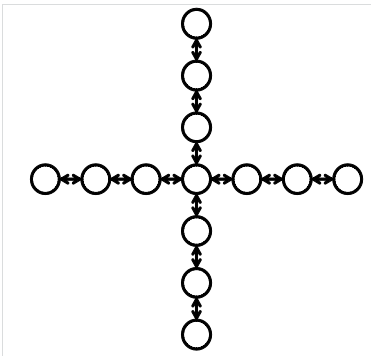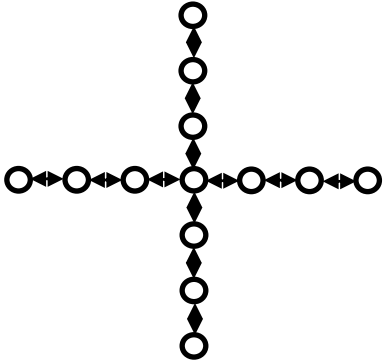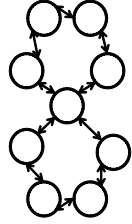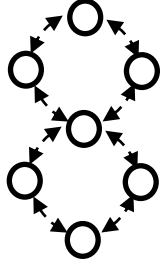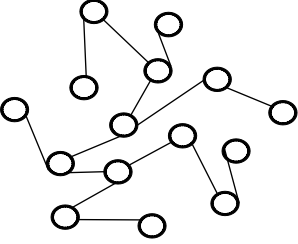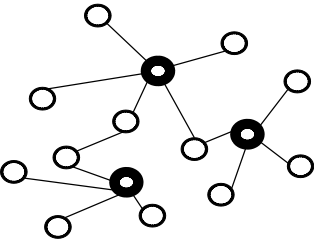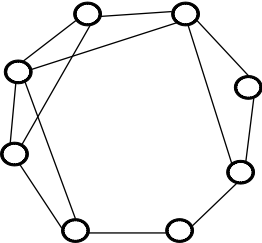
Figure 4.1: Network topology and extrapolation

Each network topology was characterized in terms of connectivity and accessibility measures. Connectivity measures are used to assess redundancies and other measures of connectedness, while accessibility measures are used to compare the relative position of nodes in the network. Commonly used measures in these categories are presented in Table 4.1. The aim of describing each studied topology by such measures is to provide consistency in comparisons and enable deeper insight and generalization of the findings.

Table 4.1: Typical graph-theoretic network measures

| *Connectivity* | | | |
|---|---|---|---|
| Index | Expression | Range | Note |
| Cyclomatic number | $\mu = e - v + G$ | $0 \leq \mu$ | Number of fundamental circuits in the network |
| Alpha index | $\alpha = \dfrac{\mu}{2v - 5}$ | $0 \leq \alpha \leq 1$ | Ratio of number of cycles to possible maximum number of cycles |
| Beta index | $\beta = \dfrac{e}{v}$ | $0 \leq \beta$ | Ratio between number of links and number of nodes, equivalent to average degree |
| Gamma index | $\gamma = \dfrac{e}{3(v - 2)}$ | $0 \leq \gamma \leq 1$ | Ratio of number of links to maximum possible number of links |
| Average degree | $\bar{d} = \dfrac{\sum_i n_i}{v}$ | $\bar{d} \geq 0$ | Average number of arcs incident on the nodes |
| Cyclicity | $\hat{c} = \dfrac{\sum_{j=1}^{n} Cycle_i}{|R|}$ | $0 \leq \hat{c} \leq 1$ | Number of times random walk led to a cycle back to a previously visited node/number of random walks |

| *Accessibility* | | |
|---|---|---|
| Index | Expression | Note |
| Diameter | $D = \max(d_{ij})$ | The maximum distance from all shortest distances between all O-D pair in the network |
| Average Shimbel index | $A_i = \dfrac{\sum_{j=1}^{n} d_{ij}}{v - 1}$ | Average of the sum of the lengths of all shortest paths connecting all pairs of nodes in the network |

| Betweenness centrality | $BC_i = \dfrac{\sigma_{jk(i)}}{\sigma_{jk}}$ | Number of times a node is crossed by shortest paths in the graph |
|---|---|---|

(Note: $e$- number of links in the graph, $v$-number of nodes in the graph, $G$-number of sub-graphs in the graph, $n_i$-number of arcs incident on node $i$, $d_{ij}$- distance of shortest path between O-D pair $(i,j)$, $Cycle_i$-number of times random walk cycled back to node $i$, $|R|$- number of random walks)

In this study, three measures are used to characterize a network: average degree $\bar{d}$, diameter $D$, and cyclicity $\hat{c}$. To obtain a value for cyclicity for a given network topology, a random walk is taken in a large number of randomly generated networks of the same topology and size. The random walk is terminated under one of three conditions: (1) n decisions corresponding to the traversal of links, where n = 1.5· D have been taken, (2) the walk returns to a node that was already visited, and (3) no further move is possible. In each random walk, a link may be traversed at most once. If that link has been used in one direction, it cannot be used again in that direction. For each network, the random walk is attempted 100,000 times. $\hat{c}$ = (number of runs on a network for which the walk returned to a node already visited) / (100,000 * number of nodes in the network).

4.3.2 Defining resilience

The term resilience has been used to mean many different things. Herein, the definition conceptualized in (Chen and Miller-Hooks, 2012) and expanded in (Miller-Hooks et al., 2012 and Faturechi and Miller-Hooks, 2013) is adopted. These works define resilience as a ratio of expected performance under a set of potential future disaster scenarios and possible preparedness and recourse (i.e. remedial) actions to pre-disaster achievable performance goals. In the context of transportation systems, Miller-Hooks et al. (2012) define resilience as the expected proportion of maximum throughput that can be

accommodated post-disaster given a required/achievable pre-disaster throughput level. Their concept differs from other previous approaches to measuring network performance in that it accounts for the possibility of taking preparedness and recovery actions *a priori* given a fixed, small budget and duration of time for implementing recovery options.

In these earlier work, the problem of measuring a network's resilience as an optimization problem was formulated as a two-state stochastic integer program, with first-stage preparedness and second-stage recovery decision variables. Thus, the problem of measuring resilience is also a problem of maximizing it. Herein, three interpretations of resilience are studied. The first is based on *throughput* using the earlier proposed definition from (Miller-Hooks et al., 2012). The second is based on a concept of connectivity between origin-destination pairs, termed *O-D connectivity*. The third is computed from the *average reciprocal distance* between all O-D pairs. These interpretations were chosen to incorporate some of the characteristics of classical graph theory measures described in the previous subsection. For example, classic connectivity and shortest distance forms the basic component of *O-D connectivity* and *average reciprocal distance*.

The original formulation from (Miller-Hooks et al., 2012) with resilience based on *throughput* and adaptations for *O-D connectivity* and *average reciprocal distance* are presented next. Notation used in these formulations are summarized in Table 4.2, and follow the notation given in Miller-Hooks et al. (2012) as closely as possible.

Table 4.2: Notation used for problem formulations

| Notation | Description` |
|---|---|
| $W$ | set of O-D pairs |
| $K_w$ | set of paths $k$ connecting O-D pair $w$ |
| $K_w^K$ | set of K shortest paths $k$ connecting O-D pair $w$ |
| $D_w$ | original demand between O-D pair $w$ |
| $\Gamma_w$ | original connectivity of O-D pair $w$ (=1 if connected, =0 otherwise) |
| $\Psi_w$ | original shortest distance of O-D pair w |
| $R$ | set of available recovery actions |
| $b_{ar}$ | cost of implementing recovery activity $r \in R$ on arc $a$ |
| $P$ | set of available preparedness actions |
| $b_{ap}$ | cost of implementing preparedness activity $p \in P$ on arc $a$ |
| $b_{ar}^p$ | cost of implementing recovery activity $r$ on arc $a$ if preparedness action $p$ is taken |
| $B$ | given budget |
| $c_a(\xi)$ | post-disaster capacity of arc $a$ for disruption scenario $\xi$ |
| $\Delta c_{ap}$ | augmented capacity of arc $a$ given preparedness action p is taken |
| $\Delta c_{ar}(\xi)$ | augmented capacity of arc $a$ due to implementing recovery activity $r$ for disruption scenario $\xi$ |
| $\Phi_a(\xi)$ | post-disaster connectivity of arc $a$ for disruption scenario $\xi$ |
| $\Delta\Phi_{ap}$ | augmented connectivity of arc $a$ given preparedness action $p$ is taken |
| $\Delta\Phi_{ar}(\xi)$ | augmented connectivity of arc $a$ due to implementing recovery activity $r$ for disruption scenario $\xi$ |
| $d_a$ | length of arc $a$ |
| $d^w(\xi)$ | shortest distance of O-D pair $w$ under disruption $\xi$ |
| $t_a(\xi)$ | traversal time of arc $a$ under disruption scenario $\xi$ |
| $t_{ar}$ | traversal time of arc $a$ if recovery activity $r$ is implemented |

| | |
|---|---|
| $q_{ar}$ | implementation time of recovery activity $r$ on arc $a$ |
| $q_{ar}^{p}$ | traversal time of arc $a$ if related preparedness action $p$ and recovery action $r$ is implemented |
| $Q_{k}^{w}(\xi)$ | maximum implementation time of recovery actions on path $k$ between O-D pair $w$ |
| $T_{\max}^{w}$ | maximum allowed traversal between O-D pair $w$ |
| $\lambda$ | preparedness-recovery action relationship matrix in which each element $\lambda_{pr}$ is set to 1 if recovery action $r$ is affected by preparedness action $p$ and 0 otherwise. |
| $\delta_{ak}^{w}$ | path-arc incidence (=1 if path $k$ uses arc $a$, and =0 otherwise) |
| $\beta_{ap}$ | binary variable indicating whether or not preparedness activity $p$ is undertaken on arc $a$ (=1 if preparedness action p is taken on arc a and =0 otherwise) |
| $\varphi^{w}(\xi)$ | binary variable indicating whether or not O-D pair $w$ (=1 if O-D pair $w$ is connected and =0, otherwise) under scenario $\xi$ |
| $\varphi_{k}^{w}(\xi)$ | binary variable indicating whether or not O-D pair $w$ is connected along path $k$ (=1 if path $k$ is connected and =0, otherwise) under scenario $\xi$ |
| $X_{a}^{w}(\xi)$ | binary variable indicating whether or not arc $a$ is used for O-D pair $w$ (=1 if link $a$ is used and =0, otherwise) under scenario $\xi$ |
| $y_{k}^{w}(\xi)$ | binary variable indicating whether or not shipments use path $k$ (=1 if path $k$ is used and =0 otherwise) between O-D pair $w$ under scenario $\xi$ |
| $f_{k}^{w}(\xi)$ | post-disaster flow of shipments along path $k$ between O-D pair $w$ under scenario $\xi$ |
| $\gamma_{ar}(\xi)$ | binary variable indicating whether or not recovery activity $r$ is undertaken on arc $a$ in the aftermath of disruption scenario $\xi$ (=1 if recovery action r is taken on arc $a$ and =0 otherwise) |

For completeness, the resilience formulation of RPO is presented next. Detailed explanation of the model is given in the earlier work. Modifications to this formulation

required for *O-D connectivity* and *average reciprocal distance* variants are provided thereafter.

*Resilience – Throughput* $(R^T)$

$$\max \quad E_{\tilde{\xi}} \left[ \max \sum_{w \in W} \sum_{k \in K_w} f_k^w(\xi) \right] \Big/ \sum_{w \in W} D_w \tag{4.1}$$

s.t.

$$\sum_p \beta_{ap} \le 1, \forall a \in A \tag{4.2}$$

$$\sum_{k \in K_w} f_k^w(\xi) \le D_w, \qquad \forall w \in W \tag{4.3}$$

$$\sum_a \sum_p b_{ap} \cdot \beta_{ap} + \sum_a \sum_r b_{ar} \cdot \gamma_{ar}(\xi) + \sum_a \sum_r \sum_p (b_{ar}^p - b_{ar}) \cdot \lambda_{pr} \cdot \beta_{ap} \cdot \gamma_{ar}(\xi) \le B, \tag{4.4}$$

$$\sum_{w \in W} \sum_{k \in K_w} \delta_{ak}^w \cdot f_k^w(\xi) \le c_a(\xi) + \sum_r \Delta c_{ap} \cdot \beta_{ap} + \sum_r \Delta c_{ar}(\xi) \cdot \gamma_{ar}(\xi), \qquad \forall a \in A \tag{4.5}$$

$$\sum_{a \in k} t_a(\xi) + \sum_{a \in k} \sum_r (t_{ar} - t_a(\xi)) \cdot \gamma_{ar}(\xi) + Q_k^w(\xi) \le T_{\max}^w + M \cdot (1 - y_k^w(\xi)), \qquad \forall k \in K_w, w \in W \tag{4.6}$$

$$f_k^w(\xi) \le M y_k^w(\xi), \qquad \forall k \in K_w, w \in W \tag{4.7}$$

$$Q_k^w(\xi) - q_{ar} \cdot \gamma_{ar}(\xi) - \sum_p (q_{ar}^p - q_{ar}) \cdot \lambda_{pr} \cdot \beta_{ap} \cdot \gamma_{ar}(\xi) \ge 0, \quad \forall a \in k, k \in K_w, w \in W \tag{4.8}$$

$$\sum_r \gamma_{ar}(\xi) \le 1, \forall a \in A, r \in R \tag{4.9}$$

$$\beta_{ap} \in \{0,1\}, \qquad \forall a \in A, p \in P \tag{4.10}$$

$$\gamma_{ar}(\xi) \in \{0,1\} \qquad \forall a \in A, r \in R \tag{4.11}$$

$$y_k^w(\xi) \in \{0,1\}, \qquad \forall k \in K_w, w \in W \tag{4.12}$$

$$f_k^w(\xi) \text{ integer}, \qquad \forall k \in K_w, w \in W \tag{4.13}$$

In classical connectivity analyses of digraphs, an O-D pair is said to be connected if there is a directed path with positive capacity between the path's origin and its destination. The network is strongly connected if such a path exists between every O-D pair. Consider a set of pre-disaster k-shortest paths for each O-D pair. In *O-D connectivity* considered herein, an O-D pair is considered connected if one of its pre-disaster k-shortest O-D paths exists, the total connectivity is set as the number of

connected O-D pairs. Alpha and Gamma indices described in Table 4.1 capture similar characteristics to this measure. Thus, interpret $K_w^K$ as the set of pre-disaster k-shortest, loopless paths between O-D pair $w$. Then, resilience with respect to *O-D connectivity* is formulated as follows.

*Resilience – O-D Connectivity* ($R^{OD}$)

$$\max \quad E_{\tilde{\xi}} \left[ \max \sum_{w \in W} \varphi^w(\xi) \right] \Big/ \sum_{w \in W} \Gamma_w \qquad (4.14)$$

s.t.

Constraints (4.2), (4.4), (4.9) ~ (4.11)

$$\varphi^w(\xi) \leq \sum_k \varphi_k^w(\xi), \qquad \forall k \in K_w^K, w \in W \qquad (4.15)$$

$$\varphi_k^w(\xi) \leq \Phi_a(\xi) + \sum_r \Delta\Phi_{ap} \cdot \beta_{ap} + \sum_r \Delta\Phi_{ar}(\xi) \cdot \gamma_{ar}(\xi), \qquad \forall a \in k, k \in K_w^K, w \in W \qquad (4.16)$$

$$\varphi^w(\xi), \varphi_k^w(\xi) \in \{0,1\}, \qquad \forall k \in K_w^K, w \in W \qquad (4.17)$$

Objective (4.14) seeks to maximize the expected number of O-D pairs that are connected divided by the total number of O-D pairs. Constraints (4.15) ensure that if an O-D path exists, then each arc along the path must either be in good working order, retrofitted so as to guarantee its operation in any disaster, or repaired post-disaster. Constraints (4.15) ensure O-D pair $w$ is connected as long as post-disaster there exists one path $k$ of the original k-shortest paths. The connectivity of path $k$ is assessed in constraints (4.16), where both the post-disaster state of each arc in the path and whether or not it is repaired if damaged are considered. $\varphi^w(\xi)$ and $\varphi_k^w(\xi)$ are restricted to be binary.

Finally, resilience in terms of *average reciprocal distance* is defined. *Average reciprocal distance* is similar to the Average Shimbel Index described in Table 4.1. It is

calculated by first computing one over the shortest post-disaster distance of existing paths between each O-D pair $w$. The *average reciprocal distance* is, thus, computed from the average of these reciprocal distances over all O-D pairs. If any O-D pair is disconnected, an exceptionally long distance is associated with that O-D pair. The resilience formulation is revised accordingly next.

*Resilience – Average Reciprocal Distance* ($R^{ARD}$)

$$\max \quad E_{\tilde{\xi}} \left[ \max \quad \sum_{w \in W} \frac{1}{d^w(\xi)} \right] \Big/ \sum_{w \in W} \frac{1}{\Psi_w} \tag{4.18}$$

s.t.

Constraint s (4.2), (4.4), (4.9) ~ (4.11)

$$\sum_{(i,j)=a} X_a^w(\xi) - \sum_{(j,i)=a} X_a^w(\xi) = \begin{cases} 1 & i = O_w \\ 0 & i \neq O_w, L_w \\ -1 & i = L_w \end{cases} \quad \forall a \in w, w \in W \tag{4.19}$$

$$d^w(\xi) \geq \sum_a d_a X_a^w(\xi) \qquad \forall a \in w, w \in W \tag{4.20}$$

$$0 \leq X_a^w(\xi) \leq \Phi_a(\xi) + \sum_r \Delta\Phi_{ap} \cdot \beta_{ap} + \sum_r \Delta\Phi_{ar}(\xi) \cdot \gamma_{ar}(\xi) \qquad \forall a \in w, w \in W \tag{4.21}$$

$$X_a^w(\xi) \in \{0,1\}, \ d^w(\xi) \ \text{integer}, \qquad \forall a \in w, w \in W \tag{4.22}$$

Constraints (4.19) are flow conservation constraints. They ensure that only one path is selected to connect O-D pair $w$. Constraints (4.20) compute the distance of the O-D path. The objective (4.18) aims for each such O-D path to be the shortest possible given a fixed budget for repairing damaged links post-disaster. Constraints (4.21) require that all arcs of each O-D shortest path is functional post-disaster. If an arc of a path does not function, that path will not exist. Binary and integer restrictions on $X_a^w(\xi)$ and $d^w(\xi)$ are indicated in constraints (4.22).

Three implementations of each resilience measure are considered corresponding to whether or not preparedness and/or recovery actions are enabled through a budget. If the budget is zero, the system's inherent coping capacity is measured. This is indicated by the addition of (CC) to the nomenclature, e.g. $R^T$(CC). Additions of (P), (R) and (P&R) indicate that a budget is available for only preparedness, only recovery or both preparedness and recovery actions, respectively. These implementations can be controlled by forcing the preparedness and recovery action decision variables to zero as appropriate.

*4.4 Obtaining Resilience Values: Solution Methodology*

An exact solution methodology based on integer L-shaped decomposition described in (Miller-Hooks et al., 2012) proposed for solution of formulation $R^T$ is employed herein and adapted for addressing formulations $R^{OD}$ and $R^{ARD}$. The Integer L-shaped method is a variant of Benders' decomposition. It was originally proposed in (Laporte and Louveaux 1993) for solving two-stage integer stochastic programs with binary first-stage decision variables. In this method, the two-stage stochastic program is decomposed into a master problem (MP) and set of subproblems (SPs), one for each scenario. In the MP, integrality constraints are relaxed. The MP and SPs are solved iteratively employing a pendant node list used to implement a type of branch-and-bound procedure. Solutions from the SPs provide valid optimality cuts that can be incorporated within the MP in the form of constraints, narrowing the solution space. The solution process terminates when the pendant node list is empty.

This procedure applies directly in solution of $R^{OD}$. It is, however, necessary to generate the set of k-shortest paths as a preprocessing step. There are several classical

94

algorithms presented in the literature for solving the k-shortest, loopless path problem. Yen's algorithm was adopted herein (Yen 1971). The integer L-shaped method is also used to solve $R^{ARD}$. To implement the integer L-shaped method for solution of $R^T$, $R^{OD}$ and $R^{ARD}$, the problem is treated as one of minimization. The reformulation for $R^T$, $R^{OD}$ and $R^{ARD}$ as a MP and set of SPs is given in Table 4.3.

Table 4.3: Decomposition for $R^T$, $R^{OD}$ and $R^{ARD}$

| | MP | SPs |
|---|---|---|
| $R^T$ | min $\theta^T$<br>s.t. Constraints (4.2)<br><br>$\sum_a \sum_p b_{ap} \beta_{ap} \leq B$,<br><br>$f(\theta^T, \beta) \geq 0$, $\quad 0 \leq \beta_{ap} \leq 1$ | $E_{\tilde{\xi}}\left[\min\left(-\sum_{w \in W}\sum_{k \in K_w} f_k^w(\xi)\right)\right]$<br><br>*s.t.* constraints (4.6 - 4.14) |
| $R^{OD}$ | min $\theta^{OD}$<br><br>s.t. Constraints (4.22)<br><br>$\sum_a \sum_p b_{ap} \beta_{ap} \leq B$,<br><br>$f(\theta^{OD}, \beta) \geq 0$, $\quad 0 \leq \beta_{ap} \leq 1$ | $E_{\tilde{\xi}}\left[\min\left(-\sum_{w \in W} \varphi^w(\xi)\right)\right]$<br><br>*s.t.* constraints (4.4, 4.9, 4.11, 4.15 - 4.17) |
| $R^{ARD}$ | min $\theta^{ARD}$<br>s.t. Constraints (4.22)<br><br>$\sum_a \sum_p b_{ap} \beta_{ap} \leq B$,<br><br>$f(\theta^{ARD}, \beta) \geq 0$, $\quad 0 \leq \beta_{ap} \leq 1$ | $E_{\tilde{\xi}}\left[\min\left(-\sum_{w \in W} \frac{1}{d^w(\xi)}\right)\right]$<br><br>*s.t.* constraints (4.4, 4.9, 4.11, 4.15 - 4.17) |

Note that each subproblem in the decomposition of $R^{ARD}$ is an all pairs shortest path problem. Floyd-Warshall's algorithm (1962) can be applied to solve each SP in this case. Also, $D_w$, $\Gamma_w$, $\Psi_w$ are constants and need not be considered in the steps of the solution method.

*4.5 Numerical Experiments*

Numerical experiments were conducted to assess resilience of the network topologies given in Figure 4.1 through solution of each of the three considered resilience problems. The experiments were completed first on the small (tile-size) networks and then again on their larger extrapolations. All arcs were assumed to have identical pre-disaster capacity. This capacity decreased by 50% or 100% if the arc is impacted in a disaster scenario. Arc travel times were assumed to increase 100% for a capacity drop of 50%. Arc lengths were set to 1 unit in all networks for all arcs with one exception. Diagonal arcs of the matching pair, complete and diamond networks have a length consistent with their Euclidean length. Regardless of network size, 100 network realizations were considered in scenario generation. In each scenario, the number of impacted arcs, *n*, follows a binomial distribution with parameter p=0.25. *n* arcs are chosen randomly from a uniform distribution. Half of the chosen arcs had a 50% drop in capacity and the remaining 50% had a 90% drop in capacity. The assignment of the capacity drop is made randomly.

Two preparedness (P1 and P2) and three recovery (R1, R2, and R3) actions are designed to mitigate the impact of disaster. For the $R^T$ analysis, the characteristics of these actions are summarized in Table 4.4. The implementation time and cost of all three recovery actions are reduced by 20% or 25% if action P1 or P2 is taken for that arc respectively.

Table 4.4: Characteristics of preparedness and recovery actions

| Actions | Recovery activity duration (units) | Cost (units) | Increase in arc capacity (units) | Reduction in arc traversal time (units) |
|---------|-----------------------------------|--------------|----------------------------------|------------------------------------------|
| P1 | N/A | 10 | 1 | N/A |
| P2 | N/A | 20 | 1 | N/A |
| R1 | 2 | 25 | 2 | 4 |
| R2 | 1 | 10 | 1 | 2 |
| R3 | 3 | 50 | 3 | 5 |

In the case of $R^{OD}$ and $R^{ARD}$, the three recovery activities restore arc connectivity but at different costs. Though preparedness actions do not directly improve the performance of target arcs in terms of connectivity, in the case of $R^{OD}$ and $R^{ARD}$, such actions can reduce the cost of recovery actions. The cost of recovery and the relationship between preparedness and recovery actions in $R^{OD}$ and $R^{ARD}$ are set to be the same as in $R^{T}$. A budget of 200 and 2,000 units is assumed for small and large networks, respectively.

For each resilience measure, four results are given in terms of: coping capacity (CC), preparedness only (P), recovery only (R), and preparedness and recovery (P & R). That is, in coping capacity, no preparedness or recovery actions are permitted, while in preparedness only and recovery only, the budget can be used for only preparedness or recovery actions, respectively. In the last category, the budget can be allocated across both types of actions.

Table 4.5: Resilience levels of network topologies (small networks)

| Type | $v$ | $e$ | $\bar{d}$ | $R^{T}$ | | | | $R^{OD}$ | | | | $R^{ARD}$ | | | |
|------|-----|-----|-----------|---------|---------|--------|----------|----------|---------|--------|----------|-----------|---------|--------|----------|
| | | | | CC | P only | R only | P& R | CC | P only | R only | P& R | CC | P only | R only | P& R |
| 1 | 9 | 12 | 2.6 | 70.6 | 76.2 | 87.3 | 92.2 | 70.4 | 73.2 | 92.4 | 97.3 | 52.1 | 53.3 | 55.2 | 61.7 |

| | | | | CC | P only | R only | P&R | CC | P only | R only | P&R | CC | P only | R only | P&R |
|---|---|---|---|---|---|---|---|---|---|---|---|---|---|---|---|
| 2 | 9 | 8 | 1.8 | 65.3 | 72.1 | 78.8 | 85.3 | 70.0 | 78.6 | 83.1 | 92.5 | 44.8 | 46.9 | 51.4 | 58.8 |
| 3 | 9 | 8 | 1.8 | 56.2 | 65.6 | 73.1 | 82.4 | 63.1 | 65.3 | 88.3 | 90.5 | 40.4 | 45.9 | 48.7 | 54.0 |
| 4 | 9 | 9 | 2 | 45.9 | 50.4 | 65.4 | 72.7 | 48.6 | 58.3 | 73.6 | 86.7 | 27.7 | 32.7 | 42.5 | 49.2 |
| 5 | 8 | 16 | 4 | 90.8 | 94.9 | 96.2 | 100 | 92.5 | 98.5 | 100 | 100 | 60.9 | 62.3 | 65.5 | 68.5 |
| 6 | 9 | 16 | 3.6 | 78.1 | 85.2 | 88.6 | 95.3 | 87.9 | 91.2 | 96.5 | 100 | 54.7 | 55.5 | 60.3 | 67.4 |
| 7 | 9 | 36 | 8 | 100 | 100 | 100 | 100 | 100 | 100 | 100 | 100 | 83.5 | 87.3 | 94.5 | 97.3 |
| 8 | 10 | 10 | 2 | 66.6 | 72.5 | 80.8 | 86.4 | 72.4 | 80.2 | 84.7 | 92.8 | 46.1 | 50.2 | 54.8 | 57.8 |
| 9 | 10 | 10 | 2 | 66.3 | 71.9 | 80.5 | 85.3 | 70.5 | 75 | 88.8 | 90.4 | 46.4 | 48.5 | 52.6 | 55.1 |
| 10 | 10 | 10 | 2 | 65.2 | 72.6 | 79.3 | 85.6 | 68.6 | 79.3 | 81.2 | 92.2 | 44.1 | 49.7 | 52.2 | 60.0 |
| 11 | 10 | 9 | 1.8 | 52.5 | 57.2 | 72.6 | 79.3 | 57.2 | 60.4 | 77.8 | 81.1 | 29.6 | 36.6 | 44.2 | 52.3 |
| 12 | 9 | 12 | 2.6 | 75.4 | 81.7 | 88.3 | 94.3 | 84.6 | 85.6 | 97.4 | 98.5 | 54.4 | 56.3 | 58.7 | 65.7 |
| 13 | 9 | 8 | 1.8 | 61.0 | 69.3 | 72.6 | 80.2 | 61.5 | 71.6 | 75.6 | 86.1 | 45.2 | 48.7 | 51.9 | 58.9 |
| 14 | 9 | 10 | 2.2 | 65.8 | 76.3 | 82.4 | 91.6 | 71.9 | 80 | 92.2 | 93.3 | 46 | 50.8 | 56.7 | 61.4 |
| 15 | 9 | 12 | 2.6 | 64.3 | 69.3 | 77.4 | 85.4 | 68.4 | 70.4 | 79.8 | 89.9 | 45.2 | 48.9 | 53.7 | 57.2 |
| 16 | 9 | 12 | 2.6 | 62.2 | 67.5 | 73.6 | 82.6 | 65.4 | 68.1 | 76.1 | 86.6 | 42.1 | 44.5 | 47.6 | 53.8 |
| 17 | 9 | 12 | 2.6 | 60.3 | 66.2 | 70.7 | 76.1 | 64.7 | 69.2 | 72.5 | 78.0 | 41.3 | 44.0 | 47.2 | 52.1 |

* 1 Grid, 2 Hub and Spoke, 3 Double Tree, 4 Ring Network, 5 Matching Pairs, 6 Complete grid network, 7 Complete network, 8 Central ring, 9 Double-U, 10 Converging tails, 11 Diverging tails, 12 Diamond Network,  13 Crossing paths networks, 14 single depot network, 15 Random network, 16 Scale Free, 17 Small world

* $\bar{d}$  Average degree of network

Table 4.6: Resilience levels of network topologies (large networks with 100 nodes)

| Type | $\bar{d}$ | D | $\bar{C}$ | $R^T$ | | | | $R^{OD}$ | | | | $R^{ARD}$ | | | |
|---|---|---|---|---|---|---|---|---|---|---|---|---|---|---|---|
| | | | | CC | P only | R only | P&R | CC | P only | R only | P&R | CC | P only | R only | P&R |
| 1 | 3.6 | 18 | 6.7 | 71.6 | 79.5 | 87.3 | 92.2 | 71.9 | 76.3 | 91 | 96.3 | 53.9 | 55.8 | 58.6 | 64.9 |
| 2 | 1.98 | 20 | 0.0 | 66.1 | 71.1 | 81.5 | 90.3 | 71.3 | 74.3 | 79.6 | 93.2 | 46.3 | 51.3 | 55.8 | 63.8 |
| 3 | 1.98 | 24 | 0.0 | 56.8 | 72.3 | 75.1 | 82.7 | 64.4 | 64.3 | 83.8 | 87.6 | 41.8 | 48.4 | 52.2 | 58.5 |
| 4 | 2 | 50 | 0.0 | 46.7 | 49.2 | 62.4 | 75.6 | 53.8 | 62.4 | 75.4 | 84.1 | 33.0 | 37.0 | 46.0 | 53.1 |
| 5 | 50 | 51 | 67.6 | 91.9 | 93.2 | 97.4 | 100 | 94.0 | 95.6 | 100 | 100 | 62.8 | 65.7 | 66.7 | 70.7 |
| 6 | 6.84 | 13 | 31.0 | 79.2 | 88.7 | 92.3 | 97.4 | 91.1 | 92.4 | 95.6 | 100 | 58.1 | 59.2 | 64.1 | 69.5 |
| 7 | 99 | 1 | 100 | 100 | 100 | 100 | 100 | 100 | 100 | 100 | 100 | 88.2 | 89.2 | 95.9 | 98.9 |
| 8 | 2 | 23 | 0.0 | 67.6 | 76.1 | 81.4 | 91.1 | 74.1 | 82.8 | 88.2 | 94.8 | 48.1 | 54.6 | 58.4 | 60.9 |
| 9 | 2 | 48 | 0.2 | 70.5 | 74.6 | 82.7 | 89.3 | 72.5 | 75.4 | 90.0 | 95.0 | 51.1 | 51.2 | 55.1 | 58.3 |
| 10 | 2 | 97 | 0.0 | 69.5 | 74.6 | 81.7 | 89.2 | 76.1 | 82.3 | 82.8 | 93.9 | 47.0 | 53.3 | 55.1 | 64.0 |
| 11 | 1.98 | 66 | 0.0 | 53.2 | 57.6 | 73.1 | 84.9 | 58.9 | 63.0 | 77.8 | 82.7 | 31.4 | 39.2 | 44.7 | 54.4 |
| 12 | 4 | 51 | 0.0 | 76.7 | 85.4 | 91.1 | 96.1 | 88.0 | 89.1 | 94.6 | 97.2 | 58.0 | 61.4 | 62.7 | 67.9 |

| | $\bar{d}$ | $D$ | $\hat{C}$ | | | | | | | | | | | | |
|---|---|---|---|---|---|---|---|---|---|---|---|---|---|---|---|
| 13 | 1.98 | 51 | 0.0 | 63.3 | 71.7 | 74.1 | 85.3 | 64.0 | 71.6 | 76.5 | 91.2 | 48.6 | 51.1 | 53.6 | 60.9 |
| 14 | 2.02 | 49 | 0.0 | 67.1 | 76.8 | 82.8 | 93.2 | 73.1 | 80.3 | 94.9 | 95.7 | 47.8 | 52.3 | 59.2 | 64.9 |
| 15 | 3.6 | 18 | 5.2 | 69.2 | 76.5 | 81.0 | 87.3 | 72.2 | 77.8 | 83.0 | 91.5 | 46.0 | 49.9 | 54.5 | 57.4 |
| 16 | 3.6 | 18 | 4.1 | 65.8 | 69.3 | 74.4 | 82.9 | 69.1 | 72.8 | 76.3 | 84.3 | 42.1 | 45.3 | 48.4 | 54.3 |
| 17 | 3.6 | 18 | 3.8 | 64.6 | 68.1 | 72.3 | 80.4 | 66.2 | 70.3 | 75.4 | 81.6 | 41.4 | 44.7 | 47.6 | 52.9 |

\* 1 Grid, 2 Hub and Spoke, 3 Double Tree, 4 Ring Network, 5 Matching Pairs, 6 Complete grid network, 7 Complete network, 8 Central ring, 9 Double-U, 10 Converging tails, 11 Diverging tails, 12 Diamond Network, 13 Crossing paths networks, 14 single depot network, 15 Random network, 16 Scale Free, 17 Small world

\*2 $\bar{d}$ - average degree, $D$ - diameter, and $\hat{C}$ - cyclicity.

The analysis directly applies to the system-level resilience concept that treats each transportation component as simple nodes with no properties or specific structure. These components, however, can be complex networks in their own right. Thus, it was assumed that an event that impacts a component's capacity will be realized through a reduction in capacity of incident links. Thus, additional experiments were conducted to explore the relationship between component health and system resilience. Sometimes, several components of a system have similar characteristics. In the experiments, those components generate a group or tile. When a tile is impacted by disaster, only the nodes and arc within the tile will have capacity reductions. The component-based application of the resilience measure in the proposed programs provided a quantitative assessment of a component's level of vulnerability. The ability to compute such a resilience index allows decision makers to assess the potential impact of greater investment levels for recovery actions on facility resilience, as well as the magnitude of the benefits that can be derived from the application of security measures, including technology implementations and changes to the physical infrastructure.

For small networks, damage to a single randomly selected arc or node (.5 probability of each) was simulated. 100 such simulations were run. In the runs with

damage to a node, capacity of all incident arcs (incident on or emanating from the node) was reduced by either 50% or 100% (.5 probability of each). A similar capacity reduction pattern was employed for damage to a single arc. In each simulation run on the large networks, damage was imposed on one randomly chosen "tile" used in creating the larger network structure. The capacity of all arcs within the damaged tile was reduced by between 50 and 100% (.5 probability of each). 100 such simulations ran in the experiment.

Resilience estimates from the runs are provided in Tables 4.7 and 4.8. Note that only the coping capacity (i.e. in which no preparedness or recovery actions are considered) is considered in measures reported in Table 4.7, because any action could restore full system capacity due to the experimental setting. The network effects of post-damage repair actions are studied through comparison of the resulting resilience measures by implementation (i.e. CC, P, R and P&R).

Table 4.7: Results of system health (small networks)

| Type | $v$ | $e$ | $\bar{d}$ | CC in $R^T$ | | | | CC in $R^{OD}$ | | | | CC in $R^{ARD}$ | | | |
|---|---|---|---|---|---|---|---|---|---|---|---|---|---|---|---|
| | | | | $\bar{R}$ | Max | Min | $s$ | $\bar{R}$ | Max | Min | $s$ | $\bar{R}$ | Max | Min | $s$ |
| 1 | 9 | 12 | 2.6 | 80.6 | 87.0 | 74.5 | 4.5 | 82.6 | 89.4 | 77.9 | 2.6 | 54.2 | 60.1 | 48.2 | 2.7 |
| 2 | 9 | 8 | 1.8 | 76.0 | 81.9 | 69.1 | 4.6 | 77.6 | 83.8 | 72.3 | 3.6 | 45.1 | 51.6 | 38.6 | 3.7 |
| 3 | 9 | 8 | 1.8 | 69.5 | 73.8 | 63.0 | 5.2 | 73.7 | 76.3 | 67.9 | 3.6 | 42.1 | 49.0 | 37.9 | 2.9 |
| 4 | 9 | 9 | 2 | 58.8 | 64.5 | 54.8 | 3.3 | 62.3 | 68.2 | 56.1 | 2.0 | 31.6 | 39.0 | 23.9 | 3.8 |
| 5 | 8 | 16 | 4 | 91.6 | 99.6 | 88.2 | 6.4 | 92.4 | 98.6 | 88.8 | 5.2 | 55.5 | 58.7 | 49.1 | 2.3 |
| 6 | 9 | 16 | 3.6 | 88.7 | 95.0 | 83.5 | 6.8 | 89.3 | 95.5 | 84.4 | 5.0 | 53.1 | 58.5 | 47.2 | 1.9 |
| 7 | 9 | 36 | 8 | 100 | 100 | 100 | 0.0 | 100 | 100 | 100 | 0.0 | 90.1 | 92.2 | 87.6 | 0.8 |
| 8 | 10 | 10 | 2 | 74.7 | 81.3 | 66.1 | 5.4 | 76.8 | 85.9 | 69.1 | 4.7 | 46.2 | 54.3 | 36.4 | 4.4 |
| 9 | 10 | 10 | 2 | 74.8 | 85.3 | 70.2 | 5.4 | 76.3 | 85.9 | 68.3 | 3.7 | 45.6 | 56.1 | 38.5 | 4.8 |
| 10 | 10 | 10 | 2 | 74.2 | 88.3 | 70.9 | 6.0 | 77.9 | 86.2 | 73.5 | 5.0 | 45.0 | 56.4 | 40.3 | 3.6 |
| 11 | 10 | 9 | 1.8 | 67.2 | 70.5 | 64.2 | 2.8 | 72.0 | 74.5 | 67.8 | 0.9 | 31.3 | 37.1 | 29.9 | 2.0 |

| 12 | 9 | 12 | 2.6 | 85.1 | 87.9 | 76.3 | 4.4 | 87.1 | 92.4 | 72.5 | 2.5 | 54.2 | 58.2 | 43.0 | 4.4 |
| 13 | 9 | 8 | 1.8 | 69.6 | 74.0 | 64.1 | 4.3 | 71.0 | 78.1 | 65.7 | 2.6 | 45.8 | 51.4 | 38.6 | 3.5 |
| 14 | 9 | 10 | 2.2 | 78.9 | 80.1 | 70.2 | 5.4 | 81.5 | 87.5 | 73.4 | 3.4 | 49.0 | 52.0 | 39.5 | 3.0 |
| 15 | 9 | 12 | 2.6 | 78.0 | 87.5 | 70.4 | 6.3 | 79.1 | 86.2 | 73.6 | 4.2 | 50.4 | 58.7 | 42.3 | 5.7 |
| 16 | 9 | 12 | 2.6 | 75.2 | 83.3 | 68.2 | 7.6 | 77.3 | 84.4 | 68.5 | 6.9 | 46.3 | 53.2 | 40.9 | 6.3 |
| 17 | 9 | 12 | 2.6 | 72.5 | 80.1 | 65.3 | 7.2 | 75.6 | 80.9 | 67.3 | 5.5 | 45.6 | 54.8 | 39.5 | 5.2 |

* 1 Grid, 2 Hub and Spoke, 3 Double Tree, 4 Ring Network, 5 Matching Pairs, 6 Complete grid network, 7 Complete network, 8 Central ring, 9 Double-U, 10 Converging tails, 11 Diverging tails, 12 Diamond Network,
13 Crossing paths networks, 14 single depot network, 15 Random network, 16 Scale Free, 17 Small world
* $\bar{R}$ -average resilience level, *Max*-Maximum resilience level, *Min*-Minimum resilience level, *s*-stand deviation of resilience

Table 4.8: Results of system health (100-node networks)

| Type | $\bar{d}$ | $D$ | $\hat{C}$ | $R^T$ | | | | $R^{OD}$ | | | | $R^{ARD}$ | | | |
|---|---|---|---|---|---|---|---|---|---|---|---|---|---|---|---|
| | | | | CC | P only | R only | P& R | CC | P only | R only | P& R | CC | P only | R only | P& R |
| 1 | 3.6 | 18 | 6.7 | 82.5 | 90.0 | 94.8 | 98.3 | 82.8 | 90.8 | 95.7 | 98.5 | 56.6 | 59.2 | 61.6 | 68.0 |
| 2 | 1.98 | 20 | 0.0 | 77.0 | 85.3 | 92.1 | 96.7 | 78.1 | 85.7 | 96.0 | 97.4 | 50.2 | 56.4 | 60.2 | 66.2 |
| 3 | 1.98 | 24 | 0.0 | 73.6 | 78.0 | 84.1 | 88.5 | 74.1 | 76.1 | 85.4 | 89.2 | 44.8 | 52.9 | 56.4 | 62.4 |
| 4 | 2 | 50 | 0.0 | 62.1 | 69.6 | 77.3 | 82.3 | 62.2 | 70.7 | 78.3 | 83.5 | 37.2 | 42.2 | 50.4 | 57.7 |
| 5 | 50 | 51 | 67.6 | 95.0 | 98.6 | 100 | 100 | 95.8 | 99.6 | 100 | 100 | 64.9 | 69.0 | 69.4 | 73.4 |
| 6 | 6.84 | 13 | 31.0 | 91.9 | 95.3 | 99.2 | 100 | 93.1 | 96.3 | 99.6 | 100 | 61.3 | 63.0 | 67.0 | 72.8 |
| 7 | 99 | 1 | 100 | 100 | 100 | 100 | 100 | 100 | 100 | 100 | 100 | 96.5 | 98.7 | 100 | 100 |
| 8 | 2 | 23 | 0.0 | 76.7 | 81.8 | 88.8 | 94.3 | 77.4 | 82.1 | 89.3 | 94.7 | 51.3 | 59.1 | 62.1 | 64.7 |
| 9 | 2 | 48 | 0.2 | 76.6 | 84.3 | 88.7 | 93.6 | 77.0 | 85.3 | 90.0 | 94.1 | 54.3 | 55.9 | 59.3 | 62.4 |
| 10 | 2 | 97 | 0.0 | 75.8 | 82.4 | 88.9 | 95.8 | 77.1 | 83.1 | 89.3 | 96.2 | 50.3 | 57.3 | 58.4 | 67.5 |
| 11 | 1.98 | 66 | 0.0 | 67.5 | 76.3 | 85.3 | 90.4 | 67.9 | 76.4 | 86.3 | 90.5 | 33.2 | 41.9 | 47.1 | 56.7 |
| 12 | 4 | 51 | 0.0 | 87.9 | 92.8 | 95.8 | 100 | 89.3 | 93.4 | 96.9 | 100 | 61.8 | 66.5 | 66.8 | 72.3 |
| 13 | 1.98 | 51 | 0.0 | 71.6 | 73.6 | 82.7 | 86.9 | 72.4 | 74.2 | 82.7 | 87.6 | 51.0 | 54.5 | 56.1 | 63.7 |
| 14 | 2.02 | 49 | 0.0 | 79.6 | 85.1 | 92.2 | 97.5 | 79.8 | 85.8 | 93.3 | 97.8 | 50.1 | 55.8 | 62.4 | 67.9 |
| 15 | 3.6 | 18 | 5.2 | 78.4 | 87.5 | 90.2 | 96.5 | 79.2 | 88.1 | 91.3 | 96.8 | 53.2 | 57.3 | 59.2 | 63.1 |
| 16 | 3.6 | 18 | 4.1 | 75.8 | 81.6 | 86.2 | 91.3 | 76.7 | 83.2 | 86.8 | 92.3 | 50.3 | 52.6 | 55.4 | 60.5 |
| 17 | 3.6 | 18 | 3.8 | 73.6 | 80.3 | 84.7 | 89.6 | 74.6 | 81.4 | 86.2 | 91.7 | 49.6 | 51.9 | 54.4 | 58.8 |

* 1 Grid, 2 Hub and Spoke, 3 Double Tree, 4 Ring Network, 5 Matching Pairs, 6 Complete grid network, 7 Complete network, 8 Central ring, 9 Double-U, 10 Converging tails, 11 Diverging tails, 12 Diamond Network, 13 Crossing paths networks, 14 single depot network, 15 Random network, 16 Scale Free, 17 Small world

*2 $\bar{d}$ - average degree, $D$ - diameter, and $\hat{c}$ - cyclicity.

Statistical analyses were conducted on the large networks to investigate the correlations between coping capacity with respect to $R^T$, $R^{OD}$ and $R^{ARD}$ of a topology and network structure as characterized by average degree $\bar{d}$ diameter $D$, and cyclicity $\hat{c}$. Results of correlation analyses are given in Table 4.9. The results indicate that resilience level has a relatively strong correlation with average degree. Cyclicity is also positively correlated with resilience, but the correlation is less significant as compared with average degree. Diameter is negatively, although weakly, correlated with resilience. All metrics ( $\bar{d}$, $D$, $\hat{c}$ ) are most strongly correlated with $R^{ARD}$ of the three resilience measures.

Table 4.9: Correlation of coping capacity of resilience and $\bar{d}$, $D$, and $\hat{c}$ in large network

|  | $R^T$ | $R^{OD}$ | $R^{ARD}$ |
|---|---|---|---|
| Average degree $(\bar{d})^T$ | 0.79 | 0.70 | 0.65 |
| Diameter ($D$) | -0.28 | -0.32 | -0.21 |
| Cyclicity ($\hat{c}$) | 0.83 | 0.73 | 0.71 |

The difference between resilience with only single-component damage and resilience with random damage is given in Table 4.10. The results indicate that throughput is most vulnerable to component level damage. Overall, damage that is concentrated in a small portion of the network is more damaging in terms of resiliency than when it is randomly spread about the network given the same total damage level.

Table 4.10: Difference between component health and overall system resilience

|  | $R^T$ | $R^{OD}$ | $R^{ARD}$ |
|---|---|---|---|
| CC | 7.23 | 6.18 | 4.12 |
| P | 6.25 | 7.52 | 3.17 |
| R | 5.74 | 4.96 | 2.41 |

| | | | |
|---|---|---|---|
| P&R | 3.85 | 3.44 | 2.32 |

Additionally, regression models with dependent variables $R^T$, $R^{OD}$ and $R^{ARD}$ and independent variables $\bar{d}$, $D$, and $\hat{C}$ were estimated. These models and measures of goodness-of-fit in terms of R-square and Significance F are provided in Table 4.11. The closer to 1.0 the R-square value, the better the fit. A Significance F of less than 0.05 indicates a good fit at a 95% confidence interval. It can be noted that with only 17 data points, the R-square values in some cases are poor; thus, only limited insights from the equations should be drawn. Experimentation with additional model forms, e.g. nonlinear forms, may produce betting fitting models. P-values, however, indicate with 95% confidence that all three graph theory metrics are significant in all equations. It is interesting to note that while the coefficient of $\hat{c}$ is always positive, the coefficients of $\bar{d}$ and $D$ vary between positive and negative values. In the case of $\bar{d}$, the coefficient is negative for all implementations of $R^T$ and $R^{OD}$, but is positive for all implementations of $R^{ARD}$. In the case of $D$, however, there is no discernible pattern.

Table 4.11: Estimated resilience regression equations

| Estimated regression equation | R-square | Significance F |
|---|---|---|
| $R^T (CC) = 64.63 - 0.16\,\bar{d} - 0.002\,D + 0.51\,\hat{C}$ | 0.70 | 0.005 |
| $R^T (P) = 73.13 - 0.26\,\bar{d} - 0.038\,D + 0.53\,\hat{C}$ | 0.56 | 0.011 |
| $R^T (R) = 78.14 - 0.26\,\bar{d} + 0.013\,D + 0.47\,\hat{C}$ | 0.55 | 0.013 |
| $R^T (P \& R) = 86.08 - 0.22\,\bar{d} + 0.031\,D + 0.35\,\hat{C}$ | 0.45 | 0.040 |
| $R^{OD} (CC) = 69.04 - 0.36\,\bar{d} + 0.02\,D + 0.65\,\hat{C}$ | 0.63 | 0.003 |
| $R^{OD} (P) = 72.9 - 0.31\,\bar{d} + 0.041\,D + 0.57\,\hat{C}$ | 0.58 | 0.008 |
| $R^{OD} (R) = 82.48 - 0.246\,\bar{d} + 0.029\,D + 0.42\,\hat{C}$ | 0.45 | 0.045 |

| | | |
|---|---|---|
| $R^{OD}(P\,\&\,R) = 89.7 - 0.21\,\bar{d} + \underline{\underline{0.028}}\,D + 0.31\,\hat{C}$ | 0.34 | 0.134 |
| $R^{ARD}(CC) = 46.68 + 0.19\,\bar{d} - 0.048\,D + 0.19\,\hat{C}$ | 0.75 | 0.001 |
| $R^{ARD}(P) = 49.96 + 0.26\,\bar{d} - \underline{\underline{0.025}}\,D + 0.12\,\hat{C}$ | 0.74 | 0.001 |
| $R^{ARD}(R) = 54.68 + 0.32\,\bar{d} - 0.04\,D + 0.058\,\hat{C}$ | 0.79 | 0.002 |
| $R^{ARD}(P\,\&\,R) = 59.2 + 0.32\,\bar{d} - \underline{\underline{0.005}}\,D + 0.05\,\hat{C}$ | 0.76 | 0.001 |

Note: double underline indicates that the parameter is statistically insignificant

## 4.6 *Analysis of Results*

Analysis of the results from the larger networks (with 100 nodes) given in the prior section provides several important insights. In general, *throughput*, *O-D connectivity* and *average reciprocal distance* resilience measures increase with average degree and greater cyclicity, but decrease with network diameter. Thus, the complete network has the highest values of resilience, while the ring network has the lowest. In all network topologies, improvements in all types of resilience are obtained from taking preparedness and/or recovery actions. The highest level is attained when both preparedness and recovery options are allowed. The improvement gains from recovery actions are more significant than from preparedness actions. The significance of these actions appears to be greatest for those networks with the lowest coping capacities. The overall ordering of the network topologies from most resilient to least resilient was found to be: complete, matching pairs, complete grid, diamond, grid, single depot, central ring, hub-and-spoke, double-u, converging tails, random, scale-free, small-world, crossing path, double tree, diverging tails and ring network. This ordering indicates a strong connection between resilience and average degree.

Generally, networks with higher coping capacity also have higher resilience level (accounting for the implementation of preparedness and recovery actions). Rankings under each category are similar, with change in ranking only for double tree and diamond networks for resilience with preparedness only. With only one exception for the hub-and-spoke network, resilience in terms of *O-D connectivity* is always higher than resilience in terms of throughput, which is always higher than resilience in terms of *average reciprocal distance*.

Other insights were gleaned from this analysis. For a comparable level of disaster-induced damage in networks with similar average degree, networks with critical arcs (i.e. arcs whose removal will cause the network to be disconnected) tend to be less resilient in terms of all three resilience measures considered herein. Such critical arcs are especially prevalent in double tree, diverging tail and crossing path networks. Greater percentage increase in resilience level was observed in such networks when preparedness and recovery actions were implemented than when similar actions were taken to rectify or mitigate damage in other network classes. That is, the benefits derived from taking mitigation and responsive actions are greatest for networks containing the greatest number of such critical arcs.

Networks with higher diameter are often sparser and contain less redundant connections. Consequently, they are more vulnerable and less resilient to disaster. For example, the double-U network with smaller diameter is more resilient than the diverging tails network. Given comparable average degree and diameter, networks with higher cyclicity tend to be more resilient. Cycles are by definition contain redundancy in that the removal of a single arc will not cause a loss in connectivity. This is exemplified by

comparing the grid and random networks, where grid networks have higher cyclicity and also notably greater resilience values.

The tested random, scale-free, small-world networks have the same average degree as the grid network, however, these networks tended to be less resilient than the grid network. This may be because scale-free and small world networks have greater connections between some nodes and fewer connections between other nodes as compared with the random network. Thus, some portions of these networks are highly redundant while others are more vulnerable to single link failure.

In considering the relationship between component health and system health, one can see that the resilience level of the ring and converging trail networks is most affected by degradation in the health of a system component. From the statistical analysis, it can be generally concluded that the average degree and cyclicity are better indicators of resiliency than diameter.

## 4.7 *Conclusions*

There are several general conclusions that can be drawn from the results of the numerical experiments. Specifically, the more redundancies built into the network, as indicated by average degree and cyclicity metrics, the greater the resilience level. Moreover, the more compact the network as indicated by a low diameter value, the more resilient the network. These insights have implications for transportation applications. For example, in designing and expanding transit systems, it is often the case that new lines are added that reach out into suburban areas. These expansions lead to less compact network designs, and thus lower resilience levels. As more riders rely on the new lines,

106

system resilience becomes increasingly important. Future additions to the network that not only have greater reach, but that help increase network compactness are worth considering.

Studying the differences in resilience of the various network topologies can provide a deeper understanding of how the addition or subtraction of specific links can affect system performance. This can have implications for transportation network planning, as well as disaster preparedness and response. In building evacuation, for example, the opening or closing of a doorway is represented by the existence or nonexistence of a link. Thus, understanding how network topology affects resilience can be useful in facility design decisions, as well.

The ability to compute such a resilience index allows decision makers to assess the potential impact of greater investment levels for recovery actions on facility resilience, as well as the magnitude of the benefits that can be derived from the application of security measures, including technology implementations and changes to the physical infrastructure.

In applications involving networks with ring or converging trail-like topologies for which the effects of component damage on system resilience are greatest, actions to reduce the possibility of component failure will be particularly beneficial. Alternatively, changes to the network topological structure may be helpful. Ring networks are common topologies for many urban roadway systems.

# Chapter 5: Conclusions and Extensions

## 5.1 *Conclusions*

This dissertation proposes models and solution algorithms for transportation network performance measurement, decision-making on pre-disaster preparedness and post-event recovery actions, and the analysis of the role of network topology in network resilience. It provides tools to support the creation of resilient intermodal freight transportation systems. In contrast to earlier works, it quantifies a network's resilience with consideration for the synergies between preparedness and recovery activities, and incorporates operational considerations of post-disaster recovery.

Three major operational concerns are addressed in the dissertation: resilience with preparedness options (RPO), resilience with Optimal Recovery Scheduling (RORS), and analysis of role of network topology in network resilience. Mathematical models associated with these problems are formulated in a stochastic environment using a multi-hazard approach, and solution algorithms are proposed..

The RPO problem is formulated as a two-stage stochastic integer program and solved using an integer L-shaped method. The RORS problem is a stochastic, time-dependent, nonlinear, integer program. An exact solution technique employing decomposition with branch-and-cut and a hybrid genetic algorithm are proposed for its solution. The solution to the model provides optimal allocation of a limited budget between preparedness, as well as recovery activities, and the planning and operations of

post-disaster recovery actions. Transportation management agencies can benefit from the proposed models to mitigate the impacts of potential disasters and related negative economic consequences. The proposed model and solution methodology were applied on illustrative example of a double-stack container network in United States.

In addition to the resilience function of throughput, O-D connectivity and average reciprocal distance were considered network resilience measures to investigate the role of network topology in network resilience. The integer L-shaped method is applied again for this purpose. The relationships between network resilience and average degree, diameter, and cyclicity are also investigated. Furthermore, this dissertation assesses the impact of damage at the component level on overall system health and recovery capability. The ranking of networks with respect to resilience level and insights related to network topology's role in resilience are provided.

This dissertation assumes that the total budget available for disaster preparedness and/or recovery actions to be fixed. For some emergency events, the budget may increase after disaster. This is particularly true in long-term recovery from large-scale disasters. The models could directly incorporate a separate added fund to be used for post-disaster recovery only. Both RPO and RORS do not account for demand uncertainty. It is also assumed that demand is inelastic to the event, and thus, the pre-disaster demand for shipments (e.g. in tonnage) is assumed to remain post-disaster. Finally, early arrival of shipments (ahead of schedule and thus before time Tmax) will not result in improved resilience.

*5.2 <u>Extensions</u>*

In addition to addressing limitations of the proposed models and solution methods due to assumptions discussed in the previous subsection, a number of extensions to this network resilience study may lead to additional insights. Some perspective extensions are summarized next.

The integer L-shaped method can solve only small problem instances to optimality. Moreover, its efficiency deteriorates when the problem instances increase. A quicker and more efficient solution method is desired for larger problem instances, involving larger networks, more disaster scenarios, or more preparedness and recovery options. Heuristics may be required for large problem instances.

In RPO, resilience is formulated based on the maximum post-disaster throughput that can be accommodated. There are tradeoffs between the allowed recovery time, budget, and resilience level. Given a specific resilience level and a fixed time window, transportation agencies may also seek a recovery plan with least cost. For this consideration, the problem can be reformulated with an objective of minimizing the required budget needed to attain a given resilience level in a given amount of time.

RORS did not consider the role of preparedness in resilience measurement or its role in enhancing post-disaster recovery. Future work might extend the RORS model for scheduling recovery activities considering the synergies between preparedness and recovery. Such a study would likely require a multi-stage, stochastic, time-dependent nonlinear integer program. The new problem will be much more difficult to solve; thus, the proposed integer L-shaped method and D-BAC cannot be apply directly. Another

promising direction to extend RORS is to prioritize chosen O-D pairs. Such prioritization could support emergency response post-disasters.

Although the proposed model is built on the rail-based transportation network, it can also be applied for networks involving other transportation modes, e.g. road and air transportation. The proposed models should be modified to take into account the operational characteristics of these other modes.

# References

1. Albert R, Jeong H, and Barabasi, AL. (1999). Diameter of the World-wide Web. Nature 401:130-131.

2. Altay N and Green WG (2006). OR/MS research in disaster operations management. Eur J Oper Res; 175(1): 475–493.

3. Aronson JE (1989). A survey of dynamic network flows. Annals of Operations Research (20): 1-66.

4. Barabási AL and Albert R (1999). Emergence of scaling in random networks. Science 286:509-12

5. Barbarosoğlu G, Özdamar L and Çevik A (2002). An interactive approach for hierarchical analysis of helicopter logistics in disaster relief operations. European Journal of Operational Research. 140 (1):118-133.

6. Benders JF (1962). Partitioning procedures for solving mixed-variables programming problems. Numerische Mathematik. 4: 238-252.

7. Berkes F and Folke C (1998). Linking social and ecological systems: management practices and social mechanisms for building resilience. Cambridge University Press. Cambridge. UK.

8. Boccaletti S, Latora V, Moreno Y, Chavez M and Hwang D (2006). Complex Networks: Structure and Dynamics. Physics Reports 424: 175-308.

9. Bondy JA and Murty USR. (2008), Graph Theory, Springer.

10. Brown GG and Vassiliou A (1993). Optimizing disaster relief: Real-Time operational and tactical decision support. Naval Research Logistics. (40): 1-23.

11. Bruneau M, Chang S, Eguchi RT, Lee G, O'Rourke T, Reinhorn A, Shinozuka M, Tierney K, Wallace W and Von Winterfelt D (2003). A framework to

quantitatively assess and enhance the seismic resilience of communities. Earthquake Spectra. 19(4): 733–752.

12. Cai X, Sha D and Wong CK (2001). Time-varying minimum cost flow problems. European Journal of Operational Research 131(2): 352-374

13. Carbajal JA, Ergun O, Keskinocak P, Siddhanthi A and Villarreal M (2009). Debris management operations. Humanitarian Logistics Conference, Atlanta. Georgia.

14. Carnahan JV, Davis WJ, Shahin MY, Keane PL and Wu MI (1987). Optimal maintenance decisions for pavement management. Journal of Transportation Engineering 113(5): 554-572

15. Cappanera P, Scaparra MP (2011). Optimal allocation of protective resources in shortest path networks.Transportation Science. 45: 64-80.

16. Chang C, Tung YK and Yang JC (1994). Monte Carlo Simulation for correlated variables with marginal distributions. Journal of Hydraulic Engineering. 120(3): 313-331.

17. Chang H, Lafrenz M, Jung IW, Figliozzi M, Platman D, and Pederson C (2010). Potential impacts of climate change on flood-induced travel disruption: a case study of Portland in Oregon, USA. Annals of the Association of American Geographers. 100(4): 938–952.

18. Chatterjee A (2003). An Overview of Security Issues Involving Marine Container Transportation and Ports. Presented at 82nd Annual Meeting of the Transportation Research Board. Washington, D.C.

19. Chen L and Miller-Hooks E. Optimal team deployment in urban search and rescue. In review.

20. Chen L and Miller-Hooks E (2012). Resilience: an indicator of recovery capability in intermodal freight transport. Transportation Science.

21. Chen YW and Tzeng GH (1999). A fuzzy multi-objective model for reconstructing post-earthquake road-network by genetic Algorithm. International Journal of Fuzzy Systems 1(2): 85-95

22. Childress S and Durango-Cohen P (2005). On parallel machine replacement problems with general replacement cost functions and stochastic deterioration. Naval Research Logistics. 52(5):409-419.

23. Daryl B (1998). Disaster recovery response to tropical storm Alberto. In: Spennemann D H R and Look D W, editors. Disaster Management Programs for Historic Sites. 133-138.

24. Duncan JW and Steven H S (1998). Collective dynamics of 'small-world' networks, Nature 393: 440-442.

25. Durango-Cohen P and Sarutipand P (2009). Maintenance optimization for transportation systems with demand responsiveness. Transportation Research Part C: Emerging Technologies. 17(4):337-348.

26. Faturechi R and Miller-Hooks E (forthcoming). A Mathematical framework for quantifying and optimizing protective actions for civil infrastructure systems. Computer-Aided Civil and Infrastructure Engineering Systems.

27. Fan Y and Liu C (2010). Solving stochastic transportation network protection problems using the progressive hedging-based method. Networks and Spatial Economics. 10(2): 193-208.

28. Feng C and Weng C (2005). A bi-level programming model for allocating private and emergency vehicle flows in seismic disaster areas. Proceedings of the Eastern Asia Society for Transportation Studies. 1408-1423.

29. FEMA (2007). Public Assistance Debris Management Guide. FEMA-325

30. FEMA. Guidance for Earthquake Mitigation Projects. URS Project No. 15702304.00100, Prepared for the Federal Emergency Management Agency

Washington DC; 2006.

31. Fetter G and Rakes TR (2011). A self-balancing CUSUM approach for the efficient allocation of resources during post-disaster debris disposal operations. Operations Management Research (4): 51-60.

32. Fiedrich F, Gehbauer F and Rickers U (2000). Optimized resource allocation for emergency response after earthquake disasters. Safety Science (35): 41-57.

33. Fleischer LK (2000). Approximating fractional multicommodity flows independent of the number of commodities. SIAM Journal on Discrete Mathematics (13):505-520.

34. Floyd R.W. (1962): Algorithm 97, Shortest Path, Communication of ACM 5, 345.

35. Ford LR and Fulkerson DR (1958). Constructing maximal dynamic flows from static flows. Operation Research (6): 419-433.

36. Fortuny-Amat J and McCarl B(1981). A representation and economic interpretation of a two-level programming problem. Journal of the Operational Research Society 32 (9):783–792.

37. Frantz TL, Cataldo M and Carley KM (2010). Robustness of centrality measures under uncertainty: Examining the role of network topology. Computational and Mathematical Organization Theory, 15(4), 303-328.

38. Ganesh A, Massoulié L and Towsley D (2005), The effect of network topology on the spread of epidemics IEEE INFOCOM.

39. Gooding PA, Hurst A, Johnson J and Tarrier N (2012). Psychological resilience in young and older adults. International Journal of Geriatric Psychiatry 27(3): 262-270.

40. Gunderson LH and Holling CS (2002). Understanding transformations in human and natural systems. Island Press. Washington. D.C. USA.

41. Hagget, P and Chorley RJ (1967). Models, paradigms and the new geography. In Models in Geography: 19-41.

42. Halpern J (1979). A generalized dynamic flows problem. Networks. 9:133-167.

43. Havidán R, Enrico LQ and Russell RD (2006). Handbook of disaster research. Handbooks of Sociology and Social Research. Springer.

44. Holling CS (1973). Resilience and stability of ecological systems. Annual Review of Ecology and Systematics 4: 1-23.

45. Holmgren AJ, Jenelius E and Westin J (2007). Evaluating strategies for defending electric power networks against antagonistic attacks. IEEE Transactions on Power Systems. 22(1):76-84.

46. Hoppe B and Tardos E (1994). Polynomial time algorithms for some evacuation problems. Proceedings of the fifth annual ACM-SIAM symposium on discrete algorithms. 433-441.

47. Huang M, Smilowitz KR and Balcik B (2013). A continuous approximation approach for assessment routing in disaster relief. Transportation Research Part B. V.50: 21-40

48. Huang YX, Fan Y and Cheu RL (2007). Optimal Allocation of Multiple Emergency Service Resources for Critical Transportation Infrastructure Protection. Transportation Research Record. 2022: 1-8.

49. Ip WH and Wang D (2009). Resilience Evaluation Approach of Transportation Networks. CSO (2). 618-622.

50. Jeffery T, Du W, Kolk S. Storm Surge (2011). Flood Risk Modeling and Actuarial Analytics. CoreLogic.

51. Jonsbraten T, Wets R and Woodruff D (1998). A class of stochastic programs with decision dependent random elements. Annals of Operations Research. 82: 83-106.

52. Juhl G (1993). FEMA develops prototype disaster planning and responses system. American City and County. 108(3): 30-38.

53. Kansky KJ (1963). Structure of transport networks: Relationships between network geometry and regional characteristics, University of Chicago, Department of Geography, research paper #84.

54. Knott R (1988). Vehicle scheduling for emergency relief management: a knowledge-based approach. Disasters 12 (4):285-293.

55. Kondaveti R and Ganz R (2009). Decision support system for resource allocation in disaster management. 31st Annual International Conference of the IEEE EMBS; Minneapolis Minnesota. 3425-3428.

56. Madanat S and Ben-Akiva M (1994). Optimal inspection and repair policies for infrastructure facilities. Transportation Science 28(1):55-61.

57. Miller-Hooks E and Patterson SS (2004). On solving quickest time problems in time-dependent and dynamic networks. Journal of Mathematical Modeling and Algorithms 3(1):39-71.

58. Miller-Hooks E, Zhang XD and Faturechi R (2012). Measuring and maximizing resilience of freight transportation networks. Computers and Operations Research 39(7):1633-1643.

59. Murray-Tuite PM (2006). A comparison of transportation network resilience under simulated system optimum and user equilibrium conditions. Proceedings of the 2006 Winter Simulation Conference: 1398-1405.

60. Nair R, Avetisyan H and Miller Hooks E. (2010). Resilience of Ports. Terminals and other intermodal components. Transportation Research Record (2166): 54-65.

61. Laporte G and Louveaux F V (1993). The integer L-shaped method for stochastic integer problems with complete recourse. Operations Research Letters. 13: 133-142.

62. Laporte G, Louveaux F V (1998). Solving stochastic routing problems with the integer L-shaped method. Crainic TG, Laporte G, editors. Fleet Management and Logistics. 59-167.

63. Listes O (2007). A generic stochastic model for supply-and-return network design. Computers & Operations Research. 34: 417–442.

64. Liu C, Fan Y, and Ordóñez F (2009). A two-stage stochastic programming model for transportation network protection. Computers & Operations Research. 36(5): 1582–1590.

65. Miller-Hooks E, Chen L, Nair R and Mahmassani H (2009). Security and mobility of intermodal freight networks: A simulation-assignment evaluation framework. Transportation Research Record. 2317: 109-117.

66. Morlok EK and Chang DJ (2004). Measuring capacity flexibility of a transportation system. Transportation Research Part A. 38: 405–420.

67. Murray-Tuite PM (2006). A Comparison of Transportation Network Resilience under Simulated System Optimum and User Equilibrium Conditions. Proceedings of the 2006 Winter Simulation Conference; Monterey, CA. 1398-1405.

68. Nair R, Avetisyan H and Miller Hooks E (2010). Resilience of Ports, Terminals and Other Intermodal Components. Transportation Research Record. 2166: 54-65.

69. Ogier RG (1988). Minimum-delay routing in continuous-time dynamic networks with Piecewise-constant capacities. Networks 18(4): 303-318

70. Orda A and Rom R (1991). Minimum weight paths in time-dependent networks. Networks 21 (3): 295-320.

71. Özdamar L, Ekinci E and Kucukyazici B (2004). Emergency logistics planning in natural disasters. Annals of Operations Research (129):217-245.

72. Peeta S, Salman FS, Gunnec D and Viswanath K (2010). Pre-disaster investment decisions for strengthening a highway network. Computers & OR. 37(10): 1708-1719.

73. Perna A, Jost C, Valverde S, Gautrais J, Theraulaz G and Kuntz P (2008). The topological fortress of termites. Lect Notes Comput Sci 5151:165–73.

74. Rathi AK. Church RL and Solanki RS (1992). Allocating resources to support a multicommodity flow with time windows. Logistics and Transportation Review 28 (2):167-188

75. Rawls CG and Turnquist MA (2010). Pre-positioning of emergency supplies for disaster response. Transp Res B. 44: 521–534.

76. Rockafellar RT and Wets R J-B (1991). Scenarios and policy aggregation in optimization under uncertainty. Mathematics of Operations Research. 16: 119-147.

77. Rose A (2004). Defining and measuring economic resilience to earthquakes. Disaster Prevention and Management. 13(4): 307-314.

78. Sen S and Sherali HD (2006). Decomposition with branch-and-cut approaches for two-stage stochastic mixed-integer programming. Mathematical Programming 106(2):203-223.

79. Sheu JB (2006). A novel dynamic resource allocation model for demand-responsive city logistics distribution operations. Transportation Research Part E. Logistics and Transportation Review (42)445-472.

80. Srinivasan K (2002). Transportation network vulnerability assessment: A Quantitative Framework. Security Papers, Southeastern Transportation Center. 60-79.

81. Sun Y, Turnquist MA, and Nozick LK (2006). Estimating Freight Transportation System Capacity, Flexibility, and Degraded-Condition Performance. Journal of

the Transportation Research Board. 1966: 80-87.

82. Ta C, Goodchild A and Pitera K (2009). Structuring a definition of resilience for the freight transportation system. Transportation Research Record. 2097: 19-25.

83. Tamura T, Sugimoto H and Kamimae T (1994). Application of genetic algorithms to determining priority of urban road improvement. Japan Society of Civil Engineers 482(22): 37-46.

84. Research and Innovative Technology Administration (RITA) (2010). Freight Transportation: Global Highlights 2010. U.S. Department of Transportation (USDOT), Bureau of Transportation Statistics (BTS). Washington, DC.

85. Rosoff H, John R (2009). Decision Analysis by Proxy for the Rational Terrorist. 30th Annual Meeting of the Society for Judgment and Decision Making (SJDM), Poster, Refereed Abstract, Boston, MA, CREATE.

86. Van Slyke R and Wets R. J-B (1969). L-shaped linear programs with application to optimal control and stochastic programming. SIAM Journal on Applied Mathematics. 17(4): 638-663.

87. Wallace SW and Ziemba W T (2005). Applications of stochastic programming. SIAM.

88. Watts DJ and  Strogatz SH (1998). Collective dynamics of 'small-world' networks". Nature 393 (6684): 440–442.

89. Warshall S. (1962): A theorem on Boolean Matrices, Journal of ACM 9, 11-12.

90. Williams G, Batho S and Russell L (2000). Responding to urban crisis: the emergency planning response to the bombing of Manchester City Centre. Cities. 17(4): 293-304.

91. Willis HH, Morral AR, Kelly TK, Medby JJ (2005). Estimating terrorism risk. RAND Corporation, Report from Center for Terrorism Risk Management Policy.

66.

92. Wollmer RD (1980). Two stage linear programming under uncertainty with 0–1 integer first stage variables. Mathematical Programming. 19(1): 279-288.

93. Yan S and Shih Y (2009). Optimal scheduling of emergency roadway repair and subsequent relief distribution. Compute Operation Research (36):2049-2065.

94. Yi W and Ozdamar L (2007). A dynamic logistics coordination model for evacuation and support in disaster response activities. European Journal of Operational Research. 179 (3): 1177-1193.

95. Zhao X. M. and Gao Z. Y. (2007). Topological effects on the performance of transportation networks. Chinese Physics Letters 24 283

96. Zhang L, Huang Z, Wen Y, and Jin M (2009). The Framework for Calculating the Measure of Resilience for Intermodal Transportation Systems. State Study 220, Reprot No. FHWA/MS-DOT-RD-10-220 A, final report submitted to Mississippi Department of Transportation.

97. Zhu J, Liu D, Huang J and Han J (2010). Determining storage locations and capacities for emergency response. The Ninth International Symposium on Operations Research and Its Applications (ISORA'10). 262–269.